2000

Structural and paleomagnetic study of thrust rotation of a Late Cretaceous sill Gibson Reservoir Bob Marshall Wilderness Montana

Brian M. Priest
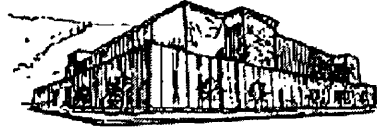*The University of Montana*

STRUCTURAL AND PALEOMAGNETIC STUDY OF THRUST ROTATION OF A

LATE CRETACEOUS SILL, GIBSON RESERVOIR, BOB MARSHALL

WILDERNESS, MONTANA

by

Brian M. Priest

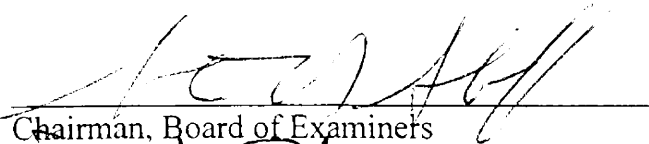Bachelors of Science, University of California, Santa Barbara, 1997

Presented in partial fulfillment of the requirements for the degree of
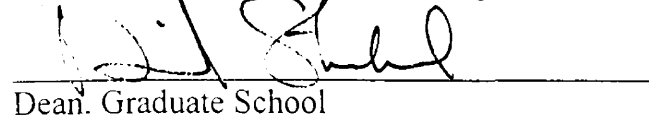
Master of Science

THE UNIVERSITY OF MONTANA

2000

Approved by

_____

Chairman, Board of Examiners

_____

Dean, Graduate School

12-4-00

_____

Date

UMI Number: EP37941

UMI

Dissertation Publishing

UMI EP37941

ProQuest

STRUCTURAL AND PALEOMAGNETIC STUDY OF THRUST ROTATION OF A LATE CRETACEOUS SILL, GIBSON RESERVOIR, BOB MARSHALL WILDERNESS, MONTANA

Director: Sheriff, Steven D.

The fold and thrust belt of northwestern Montana has been the subject of many structural and paleomagnetic studies, which indicate both counterclockwise and clockwise rotations of thrust sheets. To further delineate the boundaries of diverging rotations and the nature of emplacement of thrust sheets, structural and paleomagnetic data were collected from the footwall of the Lewis-Eldorado-Hoadley (LEH) thrust plate. This thesis is a test for rotation about a nearby vertical axis accompanying thrust emplacement in the northern Rocky Mountains based on structural and paleomagnetic analysis. The area of interest was mapped for geologic relations; bedding attitudes, simple folds thought to be associated with thrusting, and fold plunges. Research shows a trachyandesite sill and adjacent sedimentary units in the area are folded with a slight vergence to the east and plunge ~17° NNW. The sill yields a $^{40}Ar/^{39}Ar$ biotite cooling age of 58.8 +/- 1.5 Ma, but is interpreted to have a crystallization age of 75.9 +/- 1.2 Ma (prethrusting) from stratigraphic, petrographic, and structural constraints. Fifty-six oriented hand samples were collected in the field and at least one core drilled from each sample. A paleomagnetic investigation yielded a stratigraphic mean direction of Dec = 200.0° and Inc = -62.3°, with a virtual geomagnetic pole located at 75.5°N, 166.2°E. A fold test failed at the 95% confidence level when stratigraphically corrected, but progressive tilt correction of the sill suggests a positive fold test at the 95% confidence level at 80% of unfolded. Yet a statistical analysis yielded the highest precision and smallest α_{95} at 70% of unfolding of the sill. This may indicate the Late Cretaceous sill intruded into partially folded strata in the footwall of the LEH plate as thrusting continued to the east, and that deformation of the Montana disturbed belt began before 76 Ma. Reference directions from the Late Cretaceous to Eocene are undistinguishable at the 95% confidence level. A comparison of the observed direction to the expected direction for the Late Cretaceous yields a 38° +/- 13.2° clockwise rotation about a nearby vertical axis.

ACKNOWLEDGEMENTS

TABLE OF CONTENTS

LIST OF TABLES

LIST OF FIGURES

Introduction

Rotation about a nearby vertical axis in western Montana and southern Canada was described by Symons and Timmins (1992), from a paleomagnetic investigation of the Middle Proterozoic Aldridge Formation and the Moyie sills of British Columbia. They found that the Purcell anticlinorium in the Lewis-Eldorado-Hoadley (LEH) thrust plate rotated 37° +/- 12° in a clockwise manner (Figure 1). Yet, Elston *et al.* (2000) measured both clockwise and counter-clockwise rotations, usually below 15°, of the Middle Proterozoic Belt-Purcell Supergroup within the United States and southern Canada. However, the results by Symons and Timmins (1992) might be the most important study for the overall sense of rotation of the LEH thrust plate in western Montana and southern Canada. Other paleomagnetic studies have also shown significant rotations of thrust sheets within the Rocky Mountain front from Montana to Wyoming. A paleomagnetic study by Brunt (1997) showed clockwise rotation of the Late Cretaceous Kootenai Formation at Ford Creek and a study by Eldredge and Van der Voo (1988) showed clockwise rotations between 23° to 54° and some minor counter-clockwise rotations within the McCarthy and Helena salients of western Montana. A study within the Wyoming salient by Grubbs and Van der Voo (1976) shows 30° of clockwise rotation in the southern portion of the salient. But, Grubbs and Van der Voo (1976) also showed 60° of counter-clockwise rotation within the northern portion of the Wyoming salient. Also, Eldredge and Van der Voo (1988) in the Lower Cretaceous Kootenai Formation and Jolly and Sheriff (1992) in the Two-Medicine Formation have both measured counter-clockwise rotations between 25° to 30° within the northern Helena salient of western

Montana (Figure 1). Brunt (1997) measured probable counter-clockwise rotations of the Kootenai Formation in southern study sites at Marias Pass (Figure 1). The studies by Grubbs and Van der Voo (1976), Jolly and Sheriff (1992), Eldredge and Van der Voo (1988), and Brunt (1997) are located along the eastern edge of the Rocky Mountain front of the western United States. Their results are inconsistent from the model of an overall clockwise rotation of the LEH plate, probably due to shear against basement rock of the North American craton.

The Rocky Mountains of western Montana are the result of millions of years of shortening followed by post middle Eocene normal and transverse faults (Mudge, 1970). This shortening of the crust produced a regional feature that can be divided into the hanging-wall, known as the Lewis-Eldorado-Hoadley (LEH) thrust plate, and the footwall, labeled the Montana disturbed belt along the Rocky Mountain front (Figure 1). In the early to middle 20th century, structural and stratigraphic studies showed an imbrication of west-dipping thrust sheets with associated folds and relatively younger normal and transverse faults (Willis, 1904; Stebinger, 1917, 1918; Clapp, 1932; Deiss, 1943a, b; Mudge, 1965, 1966a, b, c, 1967, 1968, 1970; McGill *et al.*, 1967; Viele *et al.*, 1965; Mudge *et al.*, 1968). These early studies provided varying theories as to the formation of the Rocky Mountains, such as the theory of large scale gravitation sliding (Wisser 1957; Rubey and Hubbert 1959; Eardley 1963, 1968; Roberts 1968; Mudge 1970). Throughout the 1960's and 1970's the theory of plate tectonics became an accepted explanation of mountain building. Within the past couple of decades geophysical techniques have been applied to the western Rocky Mountains of the United States and Canada to better understand the structure and history.

2
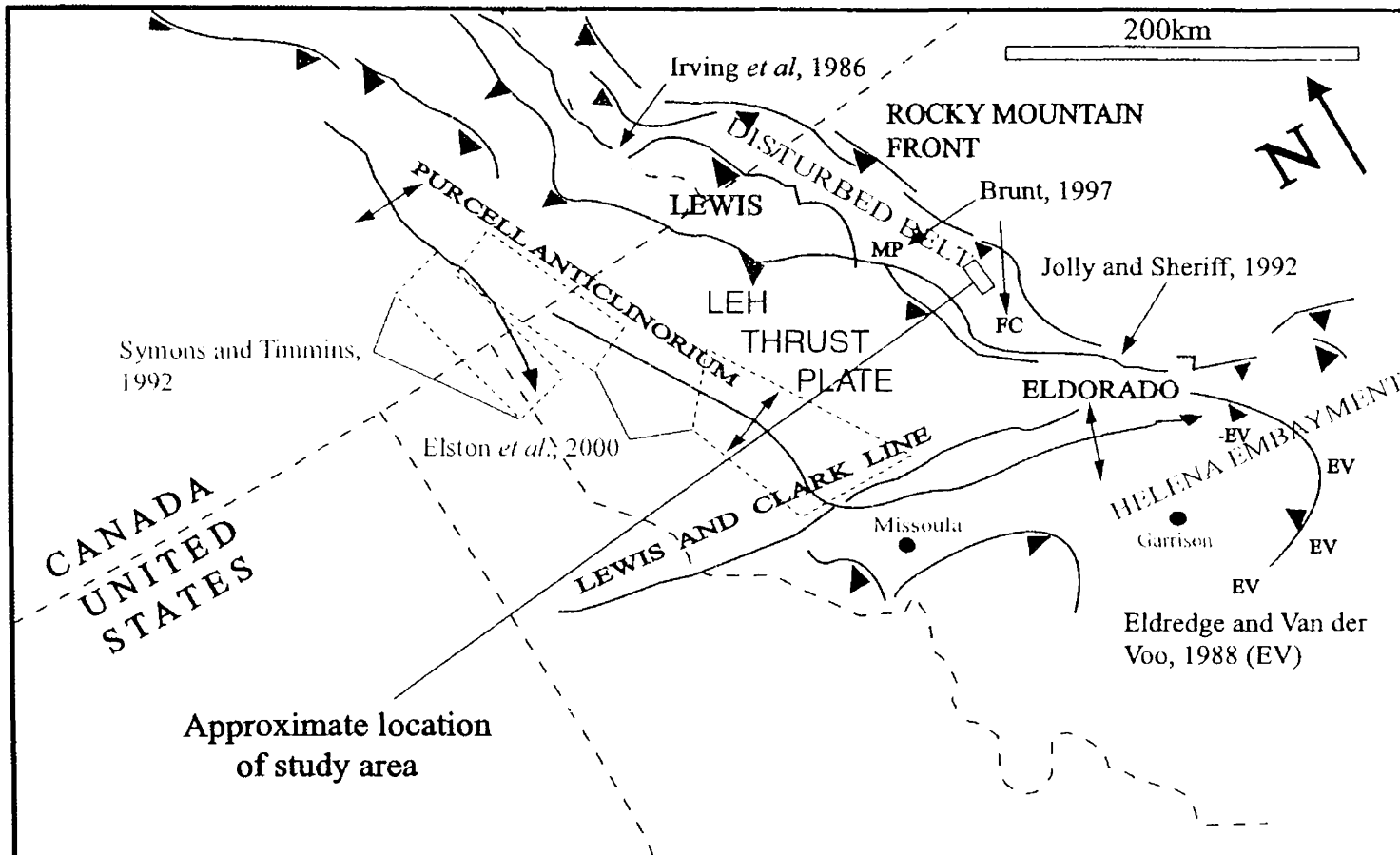
Figure 1. Regional relationship between study area and five other studies. Clockwise rotations measured at locations of Irving *et al.*(1986), Eldredge and Van der Voo (1988) (EV), Symons andTimmins (1992), and Brunt (1997) (FC). Counterclockwise rotations measured at locations of Jolly and Sheriff (1992), and also Eldredge and Van der Voo (1988) (-EV), and Brunt (1997) (MP).
(Figure modified from Brunt, 1997)

A recent model by Sears (1994) and Price and Sears (2000) suggests a clockwise rotation about a nearby vertical axis close to Helena, Montana, of the Mesoproterozoic Belt/Purcell rocks. Sears (1994) and Price and Sears (2000) developed this model by considering ten balanced cross sections from southern Canada to northern Montana (Price and Mountjoy, 1970; Monger et al., 1985; Price, 1981; Price and Fermor, 1985; Fermor and Moffat, 1992; Burton et al., 1994; Harris, 1985; Lidke and Wallace, 1994; Sears, 1988; Sears and Buckley, 1994) and by restoring thrust sheets that include the Belt-Purcell rocks and the adjacent foreland thrust and fold belt. The creation of a balanced palinspastic map shows Belt-Purcell rocks and Mesozoic rocks experiencing 30° of clockwise rotation about a nearby vertical axis near Helena, Montana. Southern Alberta contains thrust sheets experiencing linear displacements greater than 250 km, with decreasing displacement southward to less than 20 km in the Little Belt Mountains of west-central Montana.

Structural and paleomagnetic studies of the emplacement of thrust sheets have helped constrain the timing, amount, and type of deformation within western Montana and southern Canada. However, paleomagnetic studies show no simple picture regarding the sense of rotation along the Montana disturbed belt and front ranges. Therefore, the objective of my study is to quantify the amount that a Late Cretaceous sill rotated about a nearby vertical axis during Paleocene thrusting within the Sawtooth Ranges of the Montana disturbed belt (Figures 2 & 3).

This study entails a structural interpretation to determine the amount of deformation the sill experienced and to provide structural information for the paleomagnetic investigation. Structural goals include mapping the sill and sedimentary units and

4

sufficiently measuring units for attitude control. The structural and paleomagnetic considerations should lead to the timing, amount, and type of rotation the sill experienced.

Regional Geology

Western Montana and southern Alberta are dominated by a large-scale structure known as the Lewis-Eldorado-Hoadley (LEH) thrust pate (Figures 1 & 2). The LEH thrust plate is the result of shortening toward the northeast that first folded, then thrusted and folded during the Late Cretaceous to Eocene, displacing the Mesoproterozoic Belt/Purcell basin to the west over the adjacent foreland to the east (Mudge, 1970; Hoffman et al., 1976). The leading edge of the interleaved LEH thrust faults defines the trace between the hanging wall containing the Mesoproterozoic Belt rocks and the footwall containing Proterozoic and Mesozoic rocks. The Proterozoic and Mesozoic rocks of the footwall are imbricated into many thrust sheets, nine of which contain the sill. These imbricated thrust sheets make up the Montana disturbed belt (Figures 2 and 3) and are subdivided into the Sawtooth Ranges to the east and the Lewis and Clark Ranges to the west (Mudge, 1970).

The site of interest lies within the western Sawtooth Ranges between the Dry thrust fault to the east and the Elk normal fault to the west and parallels the eastern bank of the North Fork of the Sun River (Figures 2 and 3). At the 12 km^2 study site, moderately to steeply dipping sedimentary units enclose a trachyandesite sill that makes up a north-
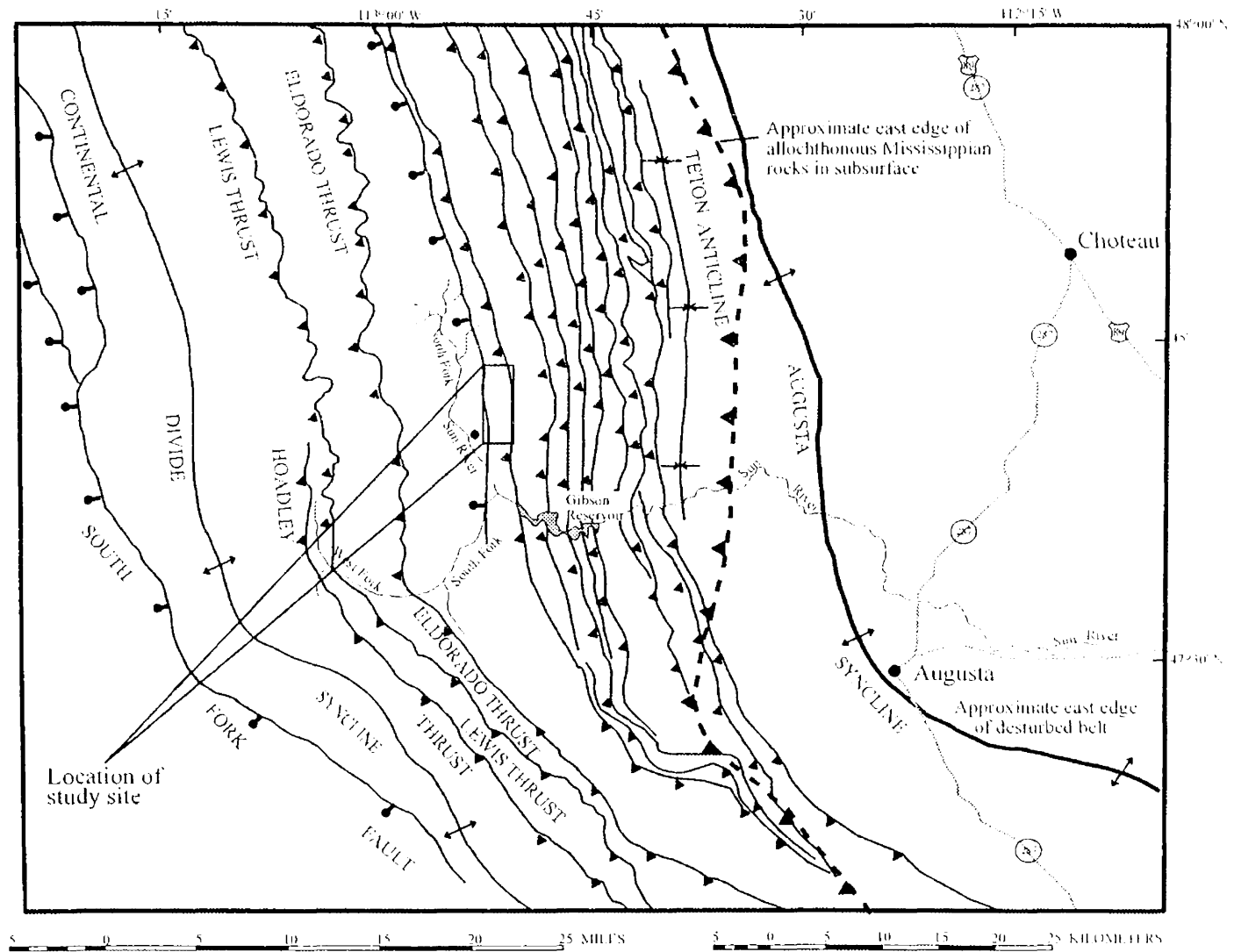
Figure 2. Structrual map of major features of the southern portion
of the Montana disturbed belt. Map modified from Mudge et al., 1982.

south trending ridge with approximately 300 to 450 meters of relief. The sedimentary units that crop out in the area are the early Cretaceous Kootenai Formation and three members of the mid-Cretaceous Blackleaf Formation; Flood Shale, Taft Hill, and Vaughn (Mudge, 1967; Mudge and Earhart, 1983).

This site was chosen because the Late Cretaceous trachyandesite sill intrudes into the Cretaceous Kootenai and Blackleaf Formations and shown by Mudge (1967) to be folded with the adjacent sedimentary units (Figure 3). Also, the site lies between the study sites of Symons and Timmons (1992) and Brunt (1997) to the north and Eldredge and Van der Voo (1988), Jolly and Sheriff (1992), and Brunt (1997) to the south (Figure 1). This study will ultimately add and fill a gap in the paleomagnetic data between previous studies, the most important being the site localities of Brunt (1997) because they are the closest to the proposed site and currently give the best constraint of rotation in the area.

Field Methods

Mudge (1967) mapped an area that includes the study site, at the 1:24,000 scale and showed excellent structural and stratigraphic relationships. He mapped a folded sill within the Blackleaf Formation that obliquely crosscuts the Flood Shale, Taft Hill, and Vaughn members. The map that Mudge produced became the foundation for the paleomagnetic investigation of the sill, but to ensure accurate paleomagnetic results the study site was mapped for greater structural control adjacent to the sill. Mapping at the

Figure 3. Geologic map of southern portion the Montana distrubed belt.
Rectangle outlines field site. Gibson Reservoir outlined for reference.
(map modified from Mudge and Earhart, 1983)
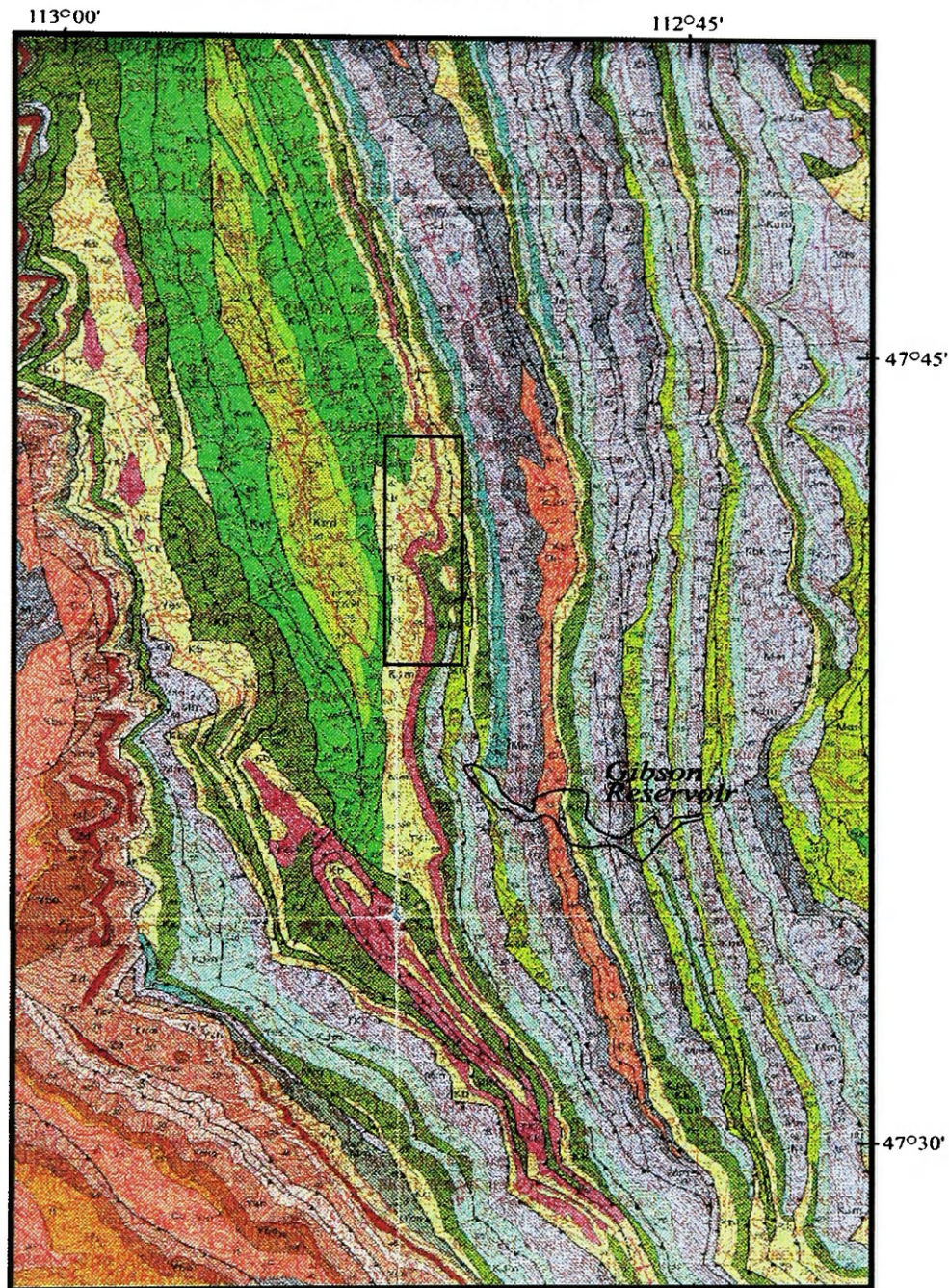
SCALE
1:125,000

TKt	TRACHYANDESITE (PALEOCENE OR UPPER CRETACEOUS)
Ksm	ST. MARY RIVER FORMATION (UPPER CRETACEOUS)
Kh	HORSETHIEF SANDSTONE, HORSETHIEF-BEARPAW TRANSITION UNIT, AND THE BEARPAW SHALE (UPPER CRETACEOUS)
	TWO MEDICINE FORMATION (UPPER CRETACEOUS)
Ktm	Sedimentary facies
Ktv	Volcanic and sedimentary facies
Kvt	VIRGELLE SANDSTONE AND TELEGRAPH CREEK FORMATION (UPPER CRETACEOUS)
Km	MARIAS RIVER SHALE (UPPER CRETACEOUS)
Kbk	BLACKLEAF AND KOOTENAI FORMATIONS, UNDIVIDED (LOWER CRETACEOUS)
Kb	BLACKLEAF FOMATION (LOWER CRETACEOUS)
Kk	KOOTENAI FORMATION (LOWER CRETACEOUS)
Kmp	MOUNT PABLO FORMATION (LOWER CRETACEOUS)
KJm	LOWER CRETACEOUS MOUNT PABLO FOMATION AND JURASSIC MORRISON FORMATION AND SLLIS GROUP, UNDIVIDED

Je	ELLIS GROUP (UPPE AND MIDDLE JURASSIC)
Mm	MADISON GROUP (UPPER AND LOWER MISSISSIPPIAN)
Du	THRE FORKD, JEFFERSON, AND MAYWOOD FORMATIONS, UNDIVIDED (UPPER AND MIDDLE DEVONIAN)
Cu	CAMBRIAN ROCKS
Zd	DIORITE (PROTEROZOIC Z)
Ym	GARNET RANGE FORMATION (POTEROZOIC Y)
	MCNAMARA FOMATION (PROTEROZOIC Y)
Yba	BONNER QUARTZITE (PROTEROZOIC Y)
Yb	MOUNT SHEILDS, SHEPARD, SNOWSLIP, AND HELENA, FORMATIONS, UNDIVIDED (PROTEROZOIC Y)
Yma	MOUNT SHEILDS FORMATION (PROTEROZOIC Y)
Ysh	SHEPARD FORMATION (PROTEROZOIC Y_
Tsn	SNOWSLIP (PROTEROZOIC Y)
Ybe	HELENA, EMPIRE, AND SPOKANE FORMATIONS, UNDIVIDED (PROTEROZOIC Y)
Yh	HELENA FORMATION (PROTEROZOIC Y)
Yes	EMPIRE AND SPOKANE FORMATIONS (PROTEROZOIC Y)
Ye	EMPIRE FORMATION (PROTEROZOIC Y)
Ys	SPOKANE FORMATION (PROTEROZOIC Y)

8

1:24.000 scale provided the necessary detail to accurately identify the structure and to locate sampling sites along the sill.

The locality of the study site is within the Bob Marshall Wilderness, thus oriented hand samples were collected instead of standard oriented drill cores to minimize aesthetic damage. The measurement of bedding attitudes and the orientation of hand samples were performed using a Brunton compass. Hand samples are from locations along a 3 km trend of relatively fresh, exposed sections of the sill and away from fractures or joints. From Mudge (1967) the site has one main sill and two to three very thin sills. The thinner sills are assumed to have intruded at the same time, but my sampling focused on the main sill that is 120 to 180 meters thick. To average out the effects of a nondipole field and random walking of the geomagnetic pole, stratigraphic sampling of the sill should yield a time averaged paleopole (average of site-mean virtual geomagnetic paleopole (VGPs)) which average paleosecular variation to a constant value.

I collected a total of 56 samples at fourteen sites along the sills of Sheep Reef, within the Bob Marshall Wilderness (Figure 4). A site represents a single outcrop that includes one to six hand samples from which standard cores were drilled in the laboratory. Sites 6-14 and 17-20 are located along the main sill and sites 16 and 18 are located along adjacent thinner sills to the east. Six sites are located on the western limb of the anticline, two sites are on the eastern limb of the anticline (or western limb of the syncline), and six sites are on the eastern limb of the syncline. The size of hand samples range from 10 to 15cm in diameter, large enough for one or more 2.5 cm by 3.8 cm cores to be drilled in the laboratory.
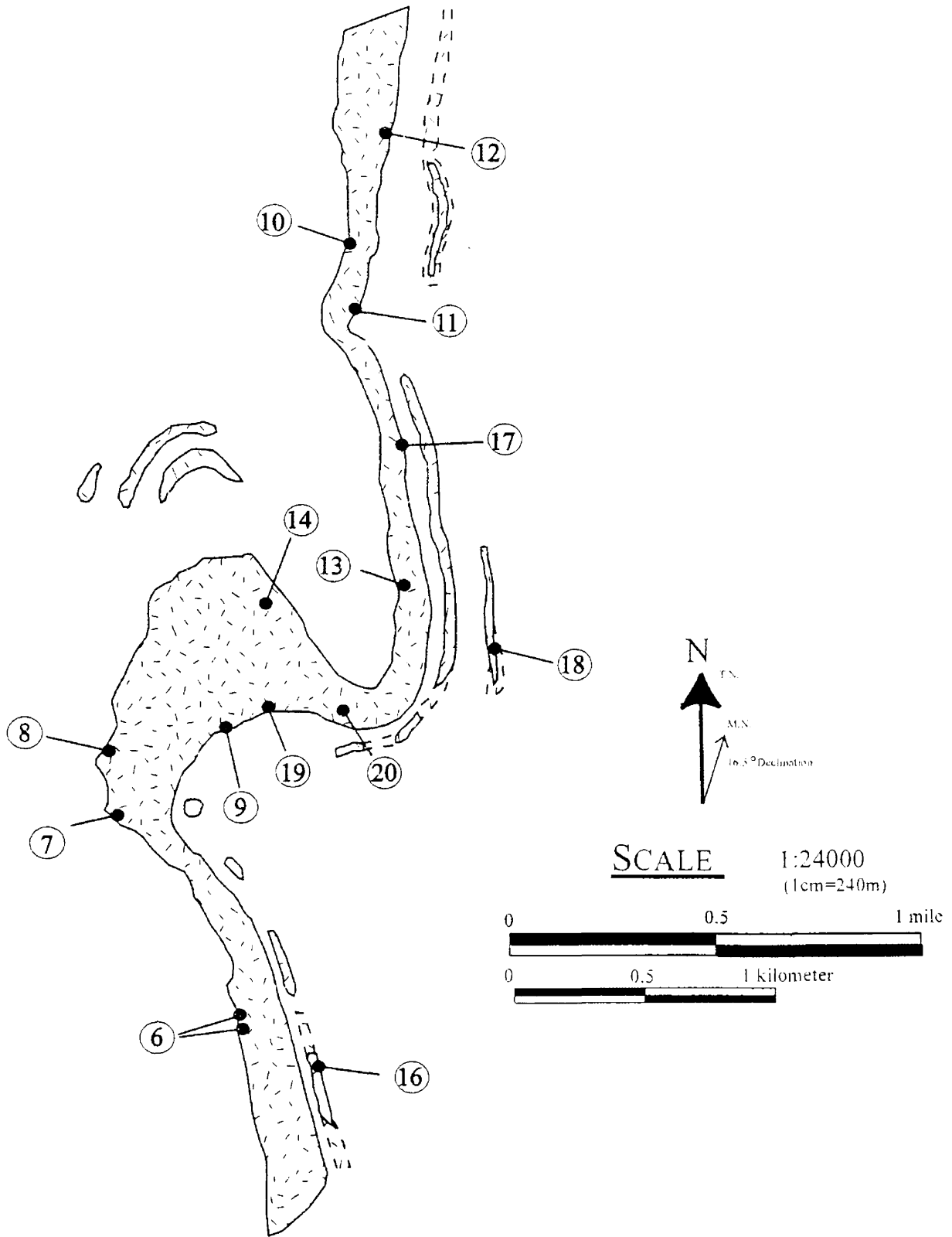
Figure 4. Paleomagnetic site locations in the trachyandesite sill.

Approximately 250 to 350 pounds of rocks were packed nearly thirteen miles out of the wilderness by the United States Forest Service. My thanks to Patti Johnston of the USFS in Choteau, MT for orchestrating the use of horses in packing out my rocks.

Laboratory Techniques

Progressive alternating field (AF) cleaning techniques were applied to evaluate the natural remanent magnetization (NRM) of each specimen. Magnetization was measured with a Schonstedt SSM-2A spinner magnetometer with NRM intensities ranging from 1×10^{-3} to 3×10^{-6} A/m. Specimens typically received 10 to 20 steps of AF cleaning from 2.5 to 102.5 mT, using a Molspin two-axis tumbling demagnetizer capable of inductions up to 102.5 mT. Cleaning levels averaging between 16.5 to 30.0 mT removed any viscous remanent magnetization (VRM) that obscured the primary directions. The uncleaned, NRM directions showed no coherent directions either between or within sites and does not parallel the present day magnetic field (Figure 5).

After reducing intensities to a few percent of the original magnetization, the characteristic remanent directions (ChRM), or the primary NRM component, were identified for each specimen using standard orthogonal vector diagrams (Zijderveld, 1967) and principal component analysis (Kirschvink, 1980). Cleaning techniques isolated single component characteristic remanent magnetization directions for 43 of the 56 specimens collected, 38 were used for the final analysis (Figures 5 and 6). A secondary magnetic component is recognizable in 15 of the 43 specimens using standard orthogonal

11

NRM
N = 43
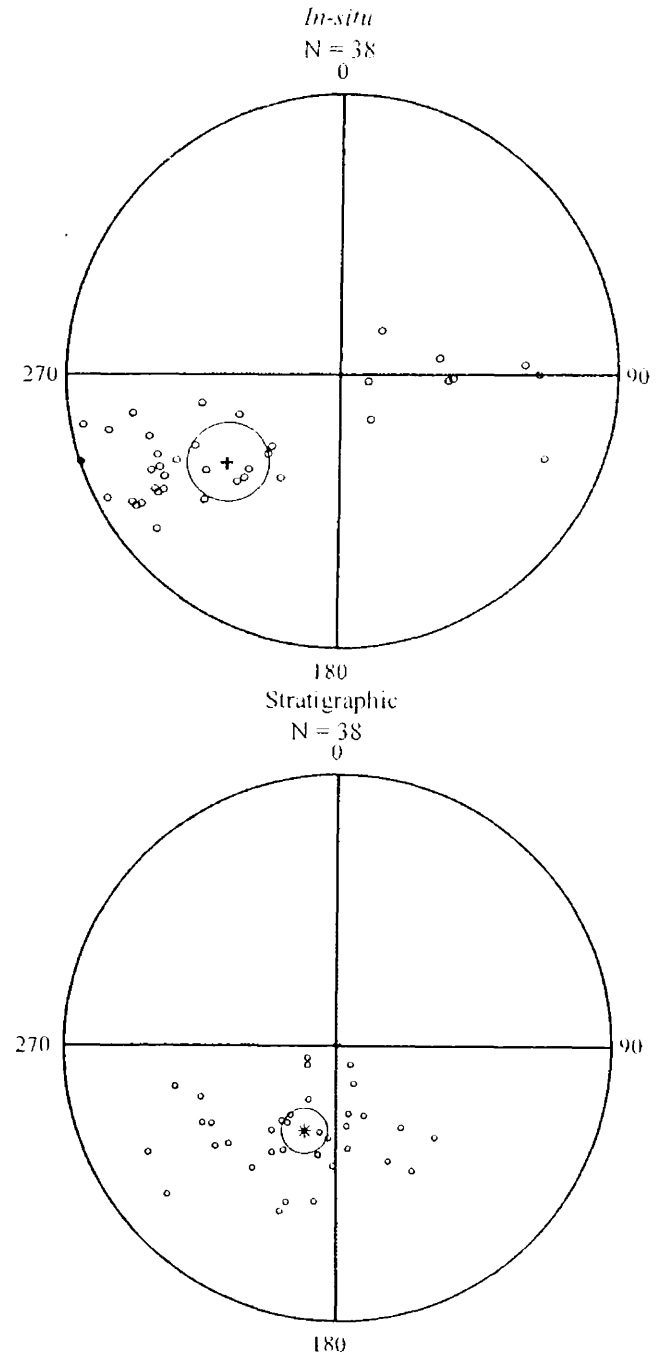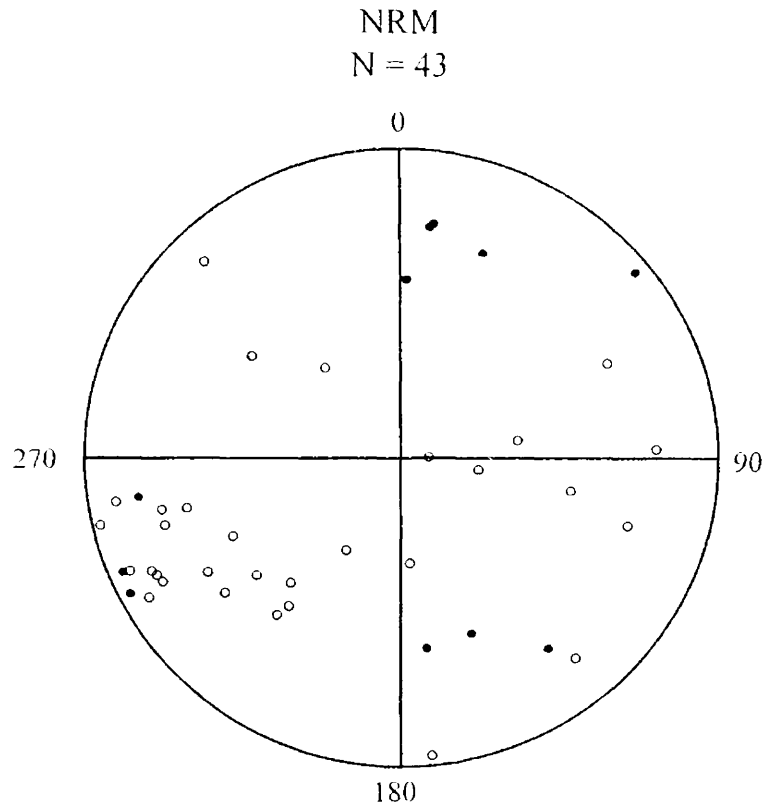
Figure 5. Equal-area projections of NRM and ChRM directions for *in-situ* and stratigraphic coordinates with averaged direction and α_{95} radius of confidence. Open circles indicate reversed polarity, closed circles indicate normal polarity.
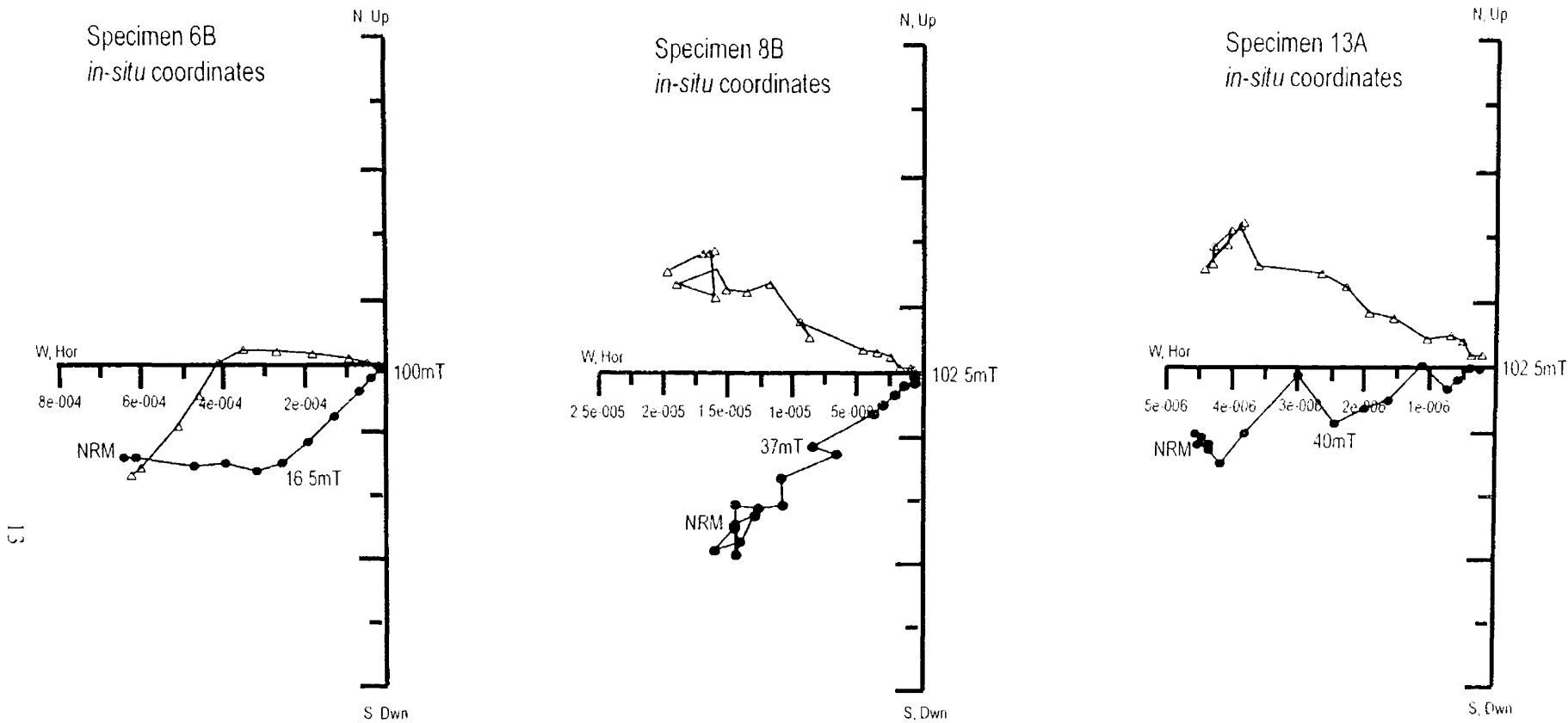
Figure 6. Vector endpoint diagram of typical specimens during alternating field (AF) demagnetization. Closed circles indicate declination, open triangles indicate inclination.
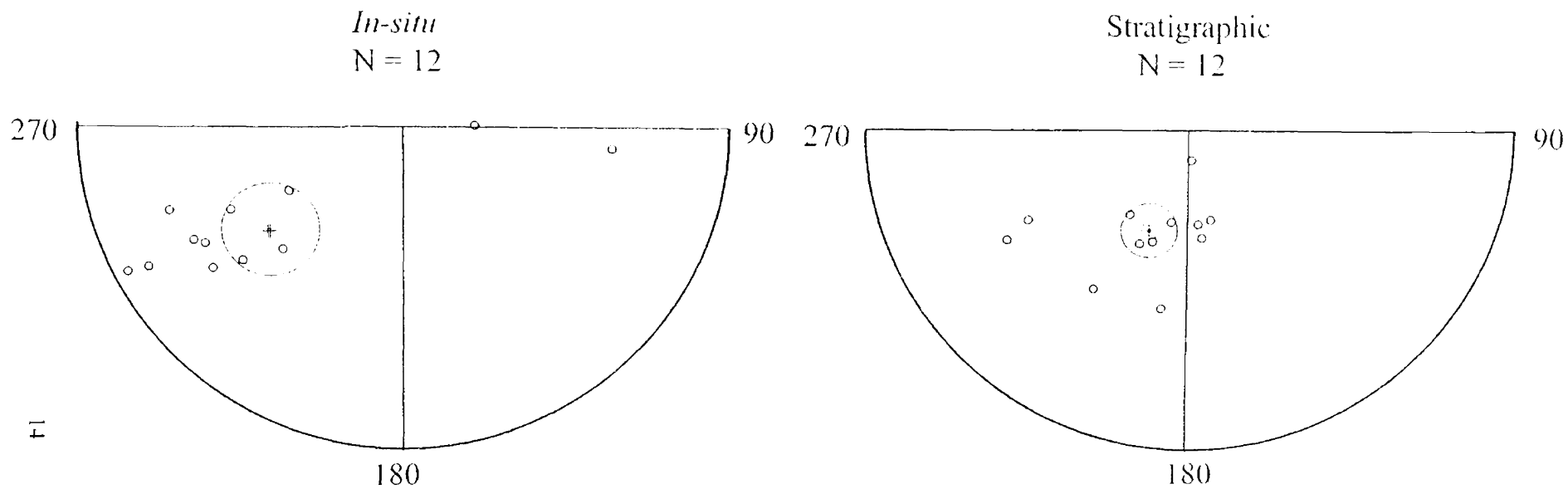
Figure 7. Equal-area projection of site-mean directions
for *in-situ* and stratigraphic coordinates. Open circles indicate
reversed polarity.

vector diagrams (Zijderveld, 1967). The secondary magnetic component did not show any coherent directions for the 15 specimens.

Mean directions with associated statistical data were computed using the methods of Fisher (1953) for 13 of the 14 sites with single component final magnetizations. Twelve of the original 14 sites have reliable site mean directions; all are reversed in polarity (Figure 7). Two sites were rejected from the final statistical analysis for the following reasons. Site 12 has a mean direction with an angular distance from the mean greater than 140°; approximately eight times the angular dispersion inherent in paleosecular variation at the sampling paleolatitude (McElhinny and Merrill, 1975). Site 18 did not yield a site mean direction because magnetization intensities for specimens were below the limit of measurement for the magnetometer. Since site 18 is located on one of the thinner sills, the anomalous behavior could be attributed to local weathering factors (Figure 4).

Tilt Correction

Conventional tilt correction in paleomagnetic studies assumes tilt takes place about the line of strike of bedding. But, if the tilt was produced by rotation about an inclined axis, the conventional tilt correction introduces a "declination anomaly" or error into the paleomagnetic data (MacDonald, 1980). This anomaly increases scatter in paleomagnetic declinations and interpretation of the paleomagnetic data becomes difficult. The geologic map and corresponding cross-sections produced from this study (Figures 8 & 9) show an anticline and syncline with fold axis plunges between 9° and 29° to the north-northwest

Figure 8. Geologic Map of Field Site, North Fork of the Sun River, Bob Marshall Wilderness, Montana

N
T.N.
M.N.
16.5° Declination

SCALE
1:24000
(1cm=240m)

LEGEND

Qal	Culluvium deposit
Kbv	Vaughan Member
Kbt	BLACKLEAF FORMATION — Taft Hill Member
Kbf	Flood Shale Member
	(unconformity)
Kk	KOOTENAI FORMATION
Ki	Non Stratigraphic Unit Late Cretaceous to Ealy Paleocene sill; alkaline in composition

Exposed   Covered   Talos

Unit contact

Folds: Anticline

Syncline

Strike and Dip:

inclined   overturned
35   40
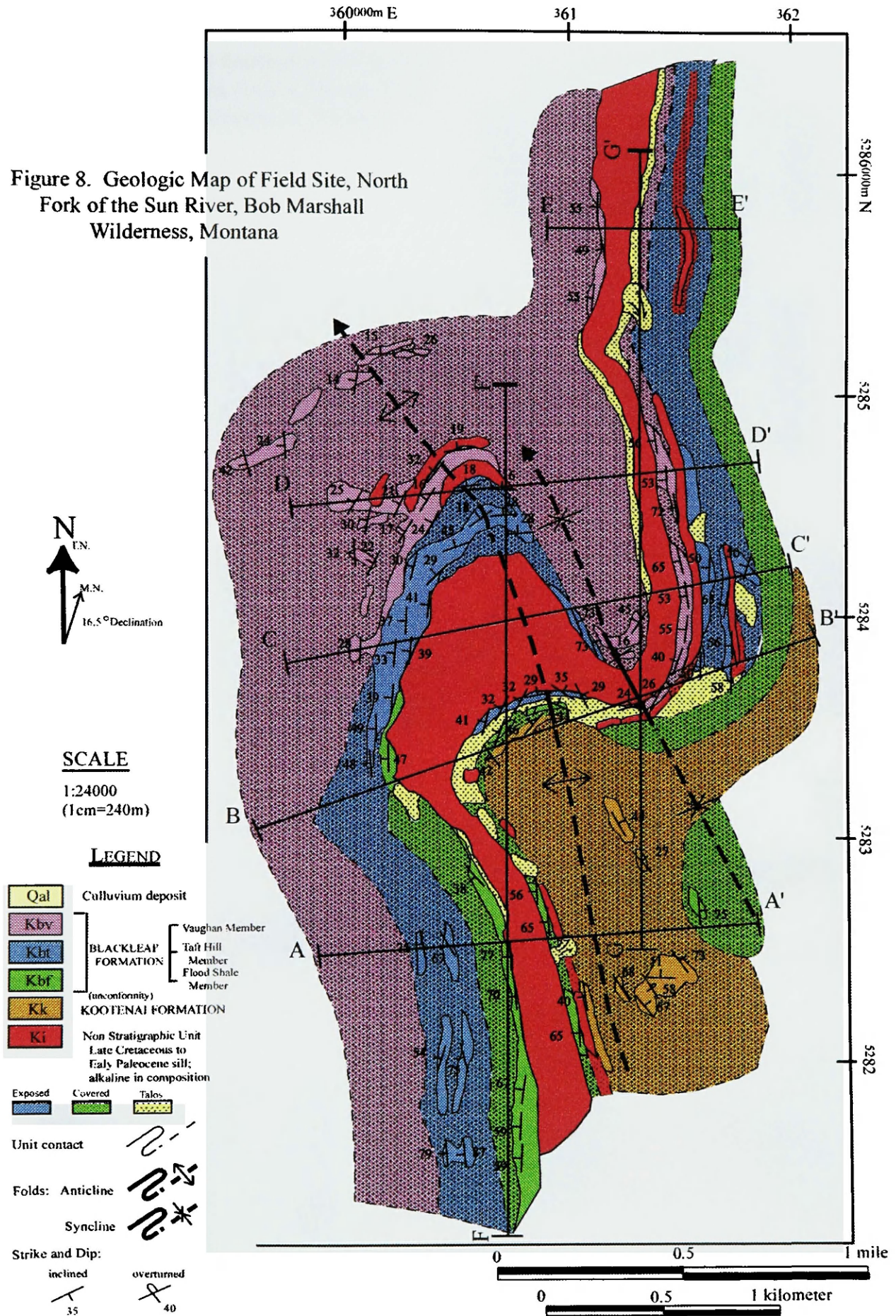
Figure 9. East-West Geologic Cross Sections of Sheep Reef, North Fork of the Sun River, Bob Marshall Wilderness, Montana

SCALE

1:24000

(1cm=240m)

LEGEND

Kbv	Vaughan Member
Kbt	BLACKLEAF FORMATION — Taft Hill Member
Kbf	Flood Shale Member
	(unconformity)
Kk	KOOTENAI FORMATION
Ki	Non Stratigraphic Unit Late Cretaceous sill, alkaline in composition

17
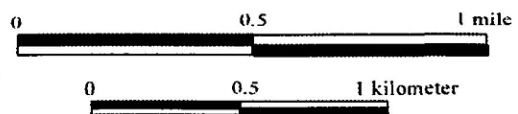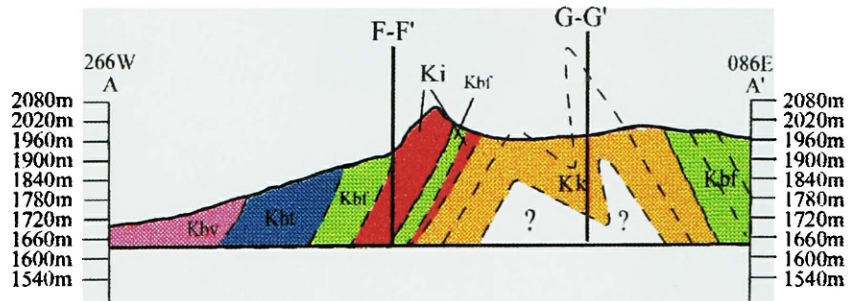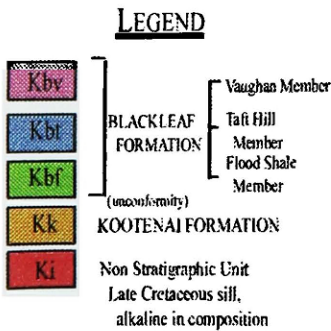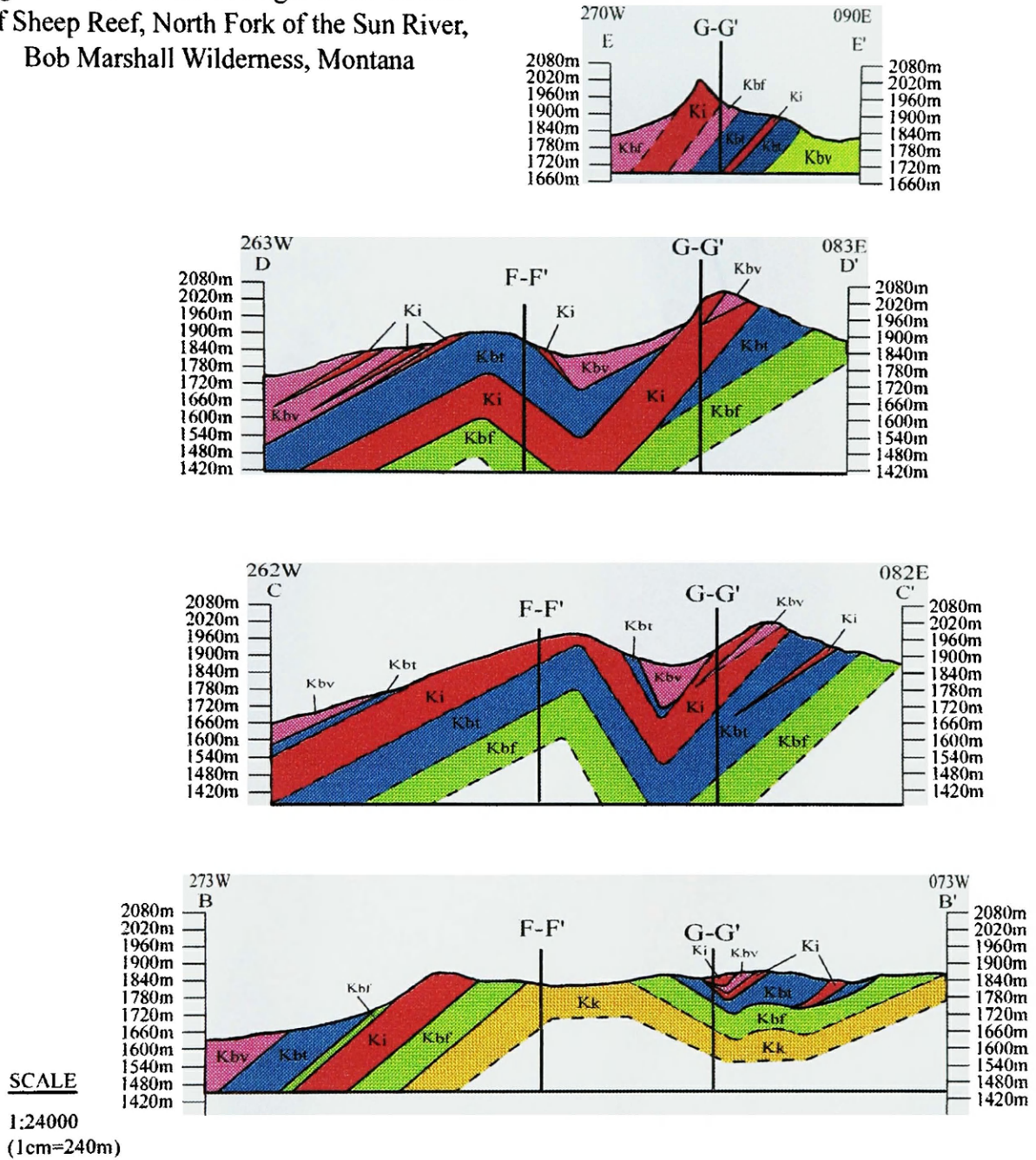
Figure 10. North-South Geologic Cross Sections of Sheep Reef, North
Fork of the Sun River, Bob Marshall Wilderness, Montana

SCALE   1:24000
(1cm=240m)

0   0.5   1 mile

0   0.5   1 kilometer

18
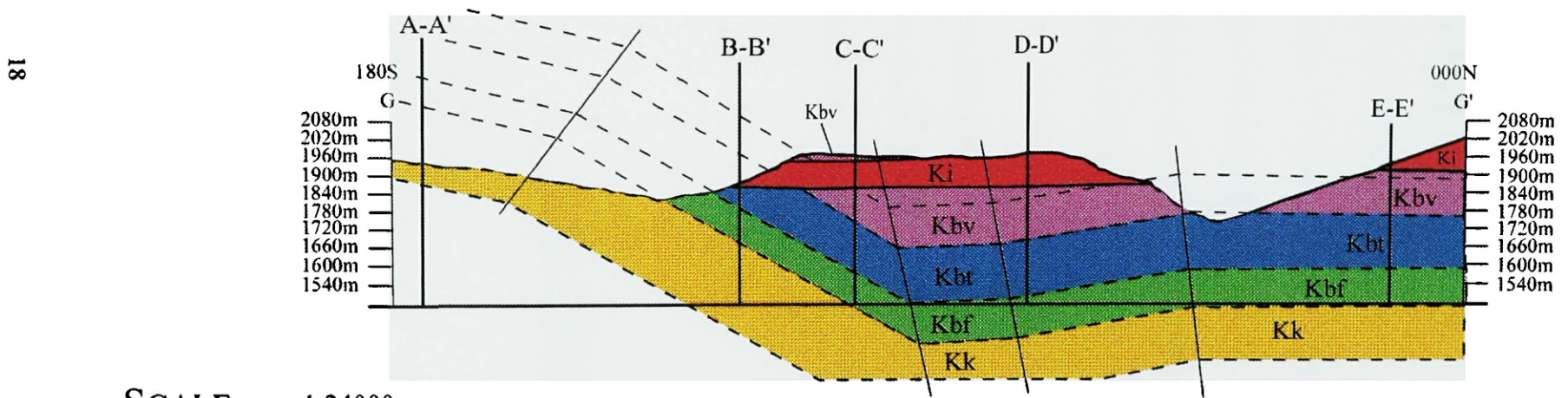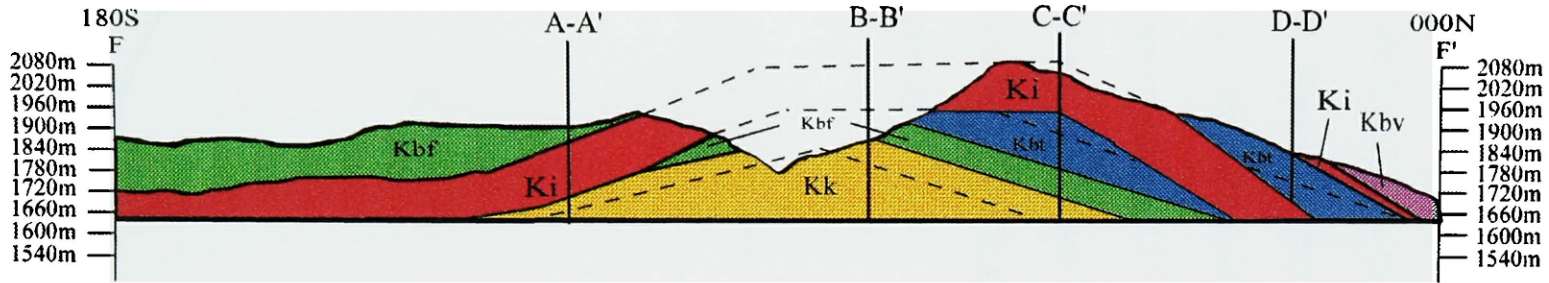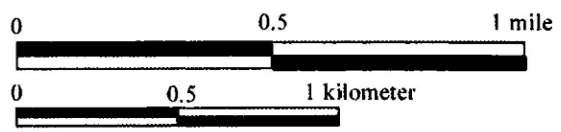
(Figure 10 & 11). Chan (1988) provides examples from three sites in the Northern

Apennines and shows at the three sites, Gubbio (Lowrie and Alvarez, 1977), Rocca

Leonella (Chan *et al.*, 1985), and Moria (Alvarez and Lowrie, 1978), that a rotation axis

plunge of nearly 10° can produce declination anomalies between 11° to 16°. Since strata

in the study site has a fold plunge greater than 10° to the northwest, a procedure must be

followed that accurately restores bedding to horizontal (Figure 11).

Before tilt correcting, identifying the types of bedding restoration to horizontal must

be established. Three possible restorations are 1) to flatten bedding by the amount of

stratigraphic dip without correcting for the fold plunge, 2) tilt correct about an inclined

axis, or 3) restore plunge of the fold axis to horizontal, then flatten bedding by the

amount of the new stratigraphic dip. I used the third method because a common strike

line is needed to tilt correct bedding on either limb without changing the internal structure

of the plunging fold.
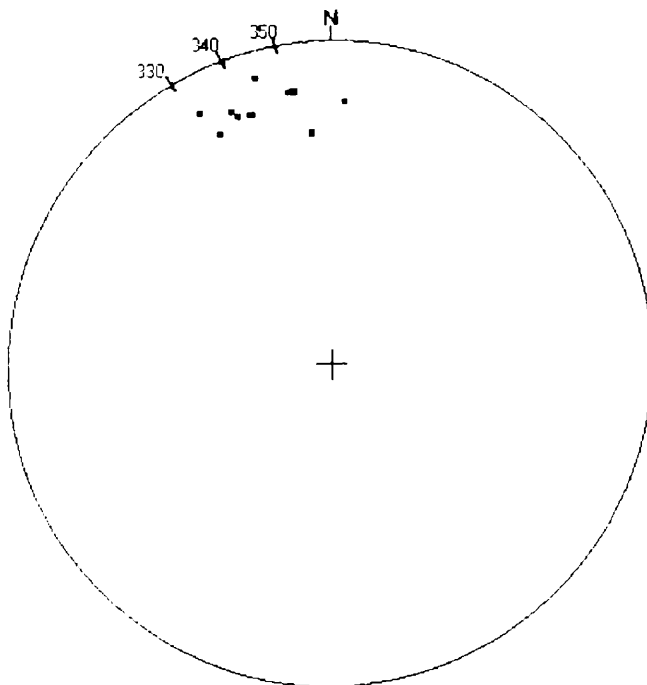
Figure 11. Equal-area projection of fold axis directions for paleomagnetic sites.

A two step tilt correcting method was applied to each paleomagnetic site. The first

step entailed locating bedding attitudes on each fold limb for the associated

paleomagnetic site. Once located, bedding was restored by the amount of plunge creating

a new strike and dip (Table 1). The restoration of plunge not only created new bedding

attitudes but also created new paleomagnetic directions. After the plunge corrected

directions and attitudes had been identified, the traditional tilt correction was applied to

the paleomagnetic data. For future discussion, *in-situ* coordinates indicate non-corrected

data and stratigraphic coordinates indicate plunge and tilt corrected data.

	TABLE 1. TILT CORRECTIONS						
Site	FA	BA	FBA	GDec	GInc	SDec	SInc
	plunge/trend	strike/dip	strike/dip	degrees	degrees	degrees	degrees
6-D10-99	16 / 352	176 / 77W	172 / 76W	240.9	-11.9	189.2	-65.6
7-C8-99	22 / 334	177 / 47W	155 / 42W	241.3	-27.8	213.7	-64.0
8-C8-99	22 / 334	177 / 47W	155 / 42W	232.8	-28.0	203.1	-58.3
9-D7-99	20 / 003	207 / 41W	182 / 37W	224.1	-45.5	188.5	-42.5
10-E4-99	20 / 342	184 / 53W	168 / 48W	239.0	-29.6	197.0	-59.9
11-E4-99	20 / 342	184 / 53W	168 / 48W	243.6	-41.3	173.5	-12.1
12-E3-99	19 / 339	174 / 55W	160 / 52W	357.9	42.6	328.0	25.6
13-E6-99	09 / 345	169 / 65W	165 / 65W	250.3	-24.7	173.0	-81.9
14-D6-99	09 / 345	342 / 75E	344 / 74E	88.6	-71.7	238.0	-34.7
16-D10-99	13 / 332	168 / 40W	152 / 38W	241.7	-5.2	240.0	-43.0
17-E6-99	17 / 338	170 / 56W	158 / 54W	230.6	-35.8	166.4	-66.0
19-D7-00	29 / 355	254 / 29NW	170 / 05W	239.4	-57.3	210.4	-41.9
20-E7-00	16 / 351	335 / 73E	344 / 60E	96.4	-36.0	172.2	-61.9

Table of two component structural correction to each site. FA is the unique fold
axis associated with each site. BA is the associated bedding attitude for each
site. FBA is the bedding attitude after correcting for the fold plunge. GDec and
GInc are the associated *in-situ* declination and inclination for each
paleomagnetic site-mean direction. SDec and SInc are the stratigraphic
declination and inclination for each paleomagnetic site-mean direction.

Fold Test

The purpose of determining a method for tilt correction is to provide for an accurate fold test of the paleomagnetic data. The fold test evaluates the paleomagnetic stability that can provide information about the timing of characteristic remanent magnetization (ChRM) acquisition. Butler (1991) states that if

"...a ChRM was acquired prior to folding, directions of ChRM from

sites on opposing limbs of a fold are dispersed when plotted in

geographic coordinates (in situ) but converge when the structural

correction is made ("restoring" the beds to horizontal). The ChRM

direction are said to 'pass the fold test'".

McFadden and Jones (1981) suggest a fold test that determines "whether the mean direction of a group of sites from one limb of a fold may be distinguished statistically from the mean direction of a group of sites from another limb." Since the sill is folded into three limbs, McFadden and Jones (1981) provide an adequate fold test for multiple limbs suitable for this study. For this fold test, the hypothesis of a common true mean direction for the three limbs may be rejected if the observed value of f exceeds the critical value of the F distribution at the required significance level. The observed value f is defined as:

$$\frac{(N-m)}{(m-1)} * \frac{(\Sigma R_i - R^2/\Sigma R_i)}{2(N - \Sigma R_i)} = f \sim F \, [2(m-1), 2(N-m)]$$

N = the number of sites.
m = number of limbs.
i = 1 to m.
Ri is the length of the vector resultants from each limb.
R is the length of the resultant vector of all the site mean directions.
F [2(m-1), 2(N-m)] is the degrees of freedom for the F distribution.

21

Results

My structural investigation resulted in a 12 km² geologic map with approximately 20% exposure of sedimentary units and 90% exposure of the sill (Figure 8). The best exposures of sedimentary units are located in contact with the sill and decrease in exposure further away from the sill. The ridge-forming sill is the dominant feature in the area with 300-450 meters of relief. The sedimentary units and sill are folded into an anticline and syncline with axial trends toward the northwest, plunging at an average of 17° (Figures 8, 9, and 10).

East-west cross-sections show moderately to steeply dipping units with an overall vergence to the east (Figure 9). Cross-sections also show that the sill cuts obliquely across stratigraphic units from the Kootenai Formation to the Vaughn member of the Blackleaf Formation (Figures 9 & 10). This either indicates the sill did not intrude as a horizontal sheet, the sedimentary units were not horizontal at the time of intrusion, or the sill intruded as a discordant sheet into folded or non-folded strata.

Table 2 summarizes the results of the paleomagnetic investigation of the Late Cretaceous sill. The paleomagnetic reference pole for the Late Cretaceous is at 82.2°N, 209.9°E, α_{95} = 6.8° (Gunderson and Sheriff, 1991). For the Paleocene, the reference pole is at 81.5°N, 192.6°E, α_{95} = 3.2° (Diehl *et al.*, 1983), and the Eocene pole is at 82.8°N, 170.4°E, α_{95} = 3.0° (Diehl *et al.*, 1983). The 12 sites (38 specimens) with reliable site-mean directions from this study provide an average paleomagnetic direction in *in-situ* coordinates of, Dec = 232.4°, Inc = -46.6°, α_{95} = 13.4° and in stratigraphic coordinates of, Dec = 200.0°, Inc = -62.3°, α_{95} = 7.6°. These two averaged directions are different at

Site	Slat (N)	Slong (W)	N/No	GDec	GInc	SDec	SInc	α_{95}	k	CSD	R	Plat	Plong
6-D10-99	47°41'	112°51'15"	4/5	240.9	-11.9	189.2	-65.6	15.08	38.09	13.12	3.92	-83.8	153.1
7-C8-99	47°41'15"	112°52'	2/2	241.3	-27.8	213.7	-64.0	5.04	2458.56	1.63	2.00	-67.0	149.6
8-C8-99	47°41'15"	112°52'	2/2	232.8	-28.0	203.1	-58.3	33.05	59.21	10.52	1.98	-71.5	·76.0
9-D7-99	47°41'	112°52'	1/1	224.1	-45.5	188.5	-42.5	-	-	-	1.00	-	-
10-E4-99	47°42'30"	112°51'	5/6	239.0	-29.6	197.0	-59.9	21.21	13.96	21.75	4.17	-76.0	-179.3
11-E4-99	47°42'30"	112°51'	1/2	243.6	-41.3	173.5	-66.0	-	-	-	1.00	-	-
12-E3-99	47°42'30"	112°51'	4/5	357.9	42.6	328.0	25.6	68.64	2.77	49.93	2.92	46.6	115.9
13-E6-99	47°42'	112°51'	5/6	250.3	-24.7	173.0	-81.9	9.47	66.22	9.94	4.94	-63.3	62.9
14-D6-99	47°42'	112°51'15"	5/5	88.6	-71.7	238.0	-34.7	14.71	28.02	15.31	4.86	-35.4	167.3
16-D10-99	47°41'	112°51'15"	1/6	241.7	-5.2	240.0	-43.0	-	-	-	1.00	-	-
17-E6-99	47°42'15"	112°51'	4/6	230.6	-35.8	166.4	-66.0	25.59	13.86	21.34	3.78	-80.3	-13.9
18-F7-99	47°42'	112°51'	0/2	-	-	-	-	-	-	-	-	-	-
19-D7-00	47°42'	112°51'15"	4/4	239.4	-57.3	210.4	-41.9	13.71	45.85	11.95	3.93	-56.4	-169.2
20-E7-00	47°42'	112°51'	4/4	96.4	-36.0	172.2	-61.9	21.91	18.55	18.84	3.84	-82.9	-59.7

Paleomagnetic data for all sites. Sites 6-14 and 17-20 are hand-sampled from various locations along the main sill; sites 16 and 18 are locations along thinner sills parallel to the main sill; Slat and Slong are the present day site latitude and longitude; N/No are the number of specimens used / number of specimens collected. GDec and GInc are the *in-situ* declination and inclination; SDec and SInc are the structurally corrected site mean directions; α_{95} is radius of 95% confidence cone in degrees; k is Fisher's (1953) precision parameter; CSD is the circle standard deviation; R is the resultant vector; Plat and Plong are VGP latitude and longitude.

TABLE 3. PALEOMAGNETIC FIELD AREA AND REFERENCE MEANS

Observed Coordinates	N	Dec_o	Inc_o	A_{95}	K	CSD	VGP Lat (°N)	Long (°E)	dp (degrees)	dm (degrees)
Geographic	38	232.4	-46.6	13.4	4.0	41.2	45.1	343.9	11.1	17.2
10% Unfolding	38	219.0	-41.7	11.9	4.8	37.6	51.1	359.3	8.9	14.6
20% Unfolding	38	218.6	-44.9	10.6	5.8	34.1	53.2	358.4	8.5	13.4
30% Unfolding	38	218.5	-46.9	9.5	7.0	31.0	54.4	356.5	7.9	12.3
40% Unfolding	38	217.7	-49.5	8.4	8.7	27.7	56.4	354.6	7.4	11.1
50% Unfolding	38	215.7	-52.6	7.4	10.8	24.8	59.6	352.6	7.1	10.2
60% Unfolding	38	214.1	-54.6	6.8	12.8	22.7	61.8	351.1	6.7	9.5
70% Unfolding	38	212.1	-56.4	6.3	14.4	21.4	64.2	349.8	6.6	9.2
80% Unfolding	38	207.6	-58.8	6.6	13.4	22.2	68.5	349.4	7.3	9.8
90% Unfolding	38	206.7	-59.5	6.5	13.7	22.0	69.6	348.3	7.3	9.8
Stratigraphic	38	200.0	-62.3	7.6	10.4	25.3	75.5	346.2	9.2	11.3

Expected Coordinates		Dec_x	Inc_x	Lat (°N)	Long (°E)	A_{95}	K			
Present day (IGRF, 1995)	-	2.7	73.0	79.0	254.9	-	-	-	-	-
Eocene, (Diehl et al.,1983)	-	349.3	66.4	82.8	170.4	3.0	16.1	-	-	-
Paleocene, (Diehl et al, 1983)	-	348.7	68.7	81.5	192.6	3.2	29.2	-	-	-
L. K. (Gunderson and Sheriff, 1991)	-	352.0	69.8	82.2	209.9	6.8	18.4	-	-	-

N is number of sites; Dec_o and Inc_o are declination and inclination of field area in degrees; A_{95} is radius of 95% confidence cone in degrees; K is Fisher (1953) precision parameter; CSD is the circular standard deviation; VGP, virtual geomagnetic pole; dp and dm are principal semiaxes of 95% confidence interval about a pole. Calculated VGPs flipped to northern hemisphere. Dec_x and Inc_x are expected directions and Lat (°N) and Long (°E) are paleomagnetic pole positions for the Late Cretaceous to Eocene.

the 95% confidence level, are distinct from the present day magnetic direction, Dec = 357.2°, Inc = 72.8° (IGRF, 1995), and different from the Late Cretaceous through Eocene reference directions (Table 3 and Figure 12).

Table 4 is a summary of the fold test with the required statistics for the 12 reliable sites from all three fold limbs. The fold test is an important step in determining the relative age of the ChRM, to validate paleomagnetic stability and to rule out possible recent remagnetizations. The observed value f, from McFadden and Jones (1981), calculated at the 95% confidence level for *in-situ* coordinates is 45.07 and for stratigraphic coordinates is 8.20. The critical value of the F distribution at the 95% confidence level is 2.53, concluding that the hypothesis of a common true mean for both the *in-situ* and stratigraphic coordinates may be rejected.

TABLE 4. FOLD TEST FOR GEOGRAPHIC AND STRATIGRAPHIC COORDINATES
(Mcfadden & Jones, 1981; eq. #8)

	In-situ	Stratigraphic
N	38	38
N_E	9	9
N_{W1}	14	14
N_{W2}	15	15
R	28.77	34.43
R_E	8.28	7.93
R_{W1}	13.05	13.46
R_{W2}	14.28	14.19
d.f.={4,70}		
f =	45.07	8.20

F = 2.53 @ 95% confidence level

Fold test analysis. *In-situ* are uncorrected coordinates of the sill; Stratigraphic is the fold-corrected coordinates of the sill; N is the number of specimens from the 12 reliable sites; N_E is the number of specimens from the east dipping limb of the anticline; N_{W1} is the number of specimens from the west dipping limb of the anticline; N_{W2} is the number of specimens from the west dipping limb of the syncline; R, R_E, R_{W1}, and R_{W2} are the resultant vectors from paleomagnetic directions; d.f. is the degrees of freedom for the F distribution; f is the observed value calculated from equation #8 from McFadden & Jones (1981).

Both the *in-situ* and stratigraphic coordinates failed the fold test and the reason appears to be an over correction when stratigraphically corrected (Figure 12). Three explanations are possible: 1) the associated bedding attitude for each paleomagnetic site
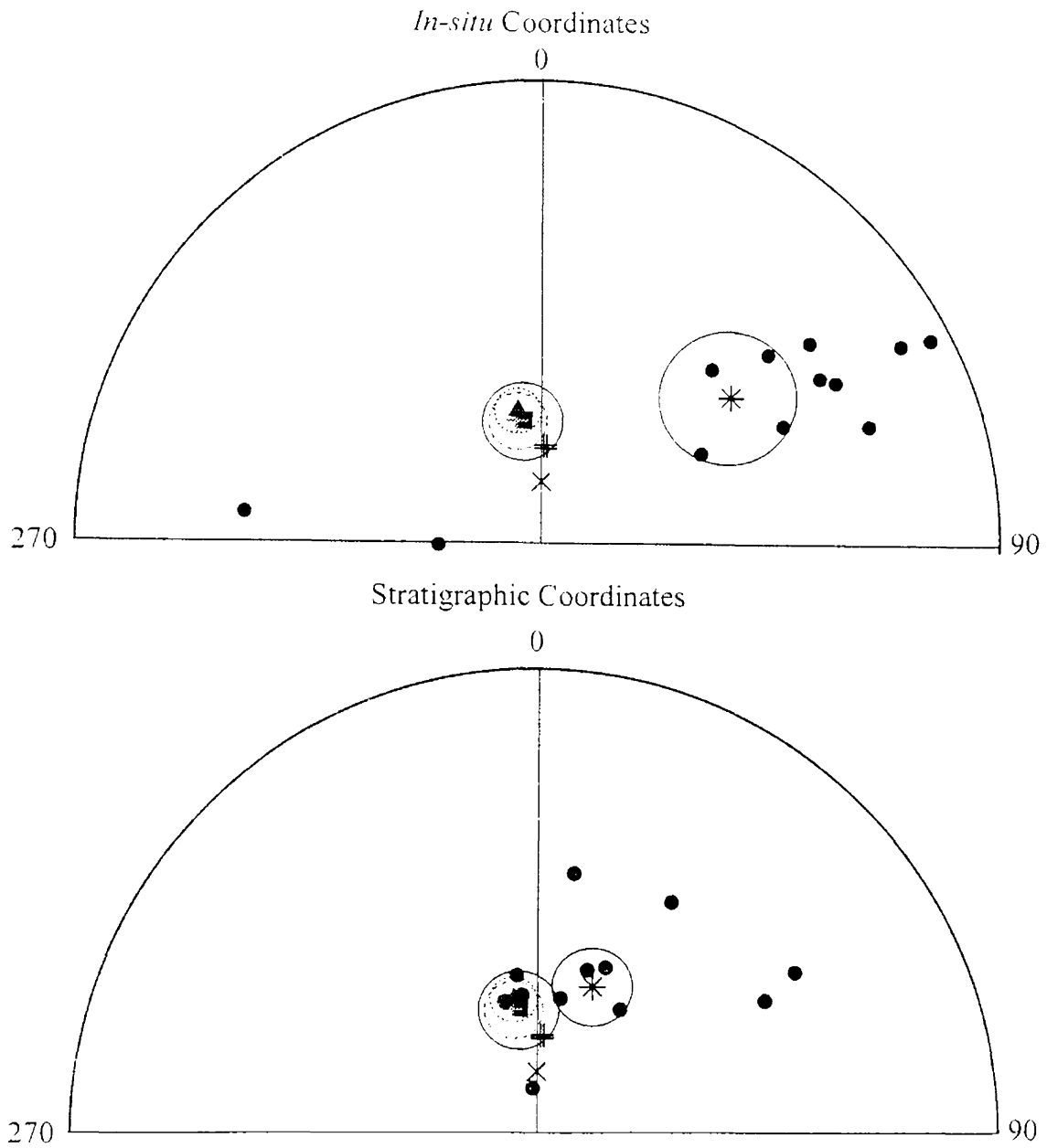
Figure 12. Equal-area projection of 12 site mean directions. Reverse polarities are flipped to normal polarity. Upper projection shows direction before correcting for local folding. Lower projection shows direction after correcting for local folding. Square is the Late Cretaceous reference directions from Gunderson *et al.*, 1991. Cross is the Paleocene reference directions from Diehl *et al.*, 1983. Triangle is the Eocene reference directions from Diehl *et al.*, 1983. Circles are the a95 radius of confidence. X is the spin axis of the Earth, ✚ is the present magnetic field direction, (IGRF, 1995).

25

is incorrect, 2) the sill intruded into partially deformed sedimentary rocks, and/or 3) there is unrecorded penetrative strain associated with the sill. Explanation two seems to be the most likely cause for the over correction but all three might contribute to some degree.

The first reason addressed for the over-correction is the lack of structural control of sedimentary units for each paleomagnetic site. I do not think this is likely as I collected numerous bedding attitudes measured close to the sill (Figure 8). Figures 9 and 10 show that reasonable cross-sections can be produced from the structural measurements. The fold axis from the anticline and syncline are well constrained as seen in Figure 11. Sites 10-13 has somewhat sparse control but are still sufficient for a representative tilt correction of the area.

The second reason is the likelihood that the sill intruded into partially folded sedimentary rocks. After structurally correcting the sill and recognizing a possible over-correction of paleomagnetic directions, I decided to tilt correct in 10% increments of total unfolding for the associated attitudes for each site. Table 5 summarizes the site-mean directions for the paleomagnetic results at each percentage step and Figure 13 graphically displays each unfolding percent compared to kappa (precision parameter) and α_{95}. The statistical results of the step-wise unfolding produced the smallest α_{95} value of 6.3° with the highest precision parameter k = 14.4 at 70% unfolding. Table 3 summarizes the average of the site-mean directions for each unfolding percentage with the appropriate Fisher (1953) statistics.

TABLE 5. PALEOMAGNETIC RESULTS FROM THE TRACHYANDESITE SILL, SHEEP REEF AREA, MONTANA

				Unfolding									
				90%		80%		70%		60%		50%	
Site	Slat (N)	Slong (W)	N/No	Dec	Inc	Dec	Inc	Dec	Inc	Dec	Inc	Dec	Inc
6-D10-99	47°41'	112°51'15"	4/5	203.5	-62.4	214.1	-57.9	221.7	-52.4	227.1	-46.4	231.0	-40.0
7-C8-99	47°41'15"	112°52'	2/2	217.6	-60.3	220.6	-56.6	222.9	-52.7	224.8	-48.8	226.3	-44.8
8-C8-99	47°41'15"	112°52'	2/2	207.2	-55.1	210.5	-51.7	213.3	-48.2	215.5	-44.5	217.4	-40.9
9-D7-99	47°41'	112°52'	1/1	191.8	-42.0	195.0	-41.2	198.1	-40.3	201.1	-39.2	203.8	-37.9
10-E4-99	47°42'30"	112°51'	5/6	203.7	-57.3	209.2	-54.3	213.8	-51.0	217.5	-47.5	220.6	-43.7
11-E4-99	47°42'30"	112°51'	1/2	183.9	-65.1	193.2	-63.4	201.2	-61.1	207.8	-58.2	213.2	-55.0
12-E3-99	47°42'30"	112°51'	4/5	330.5	26.6	333.1	27.3	335.8	27.8	338.6	28.1	341.4	28.1
13-E6-99	47°42'	112°51'	5/6	208.3	-78.9	225.0	-73.8	233.2	-67.9	237.8	-61.8	240.7	-55.5
14-D6-99	47°42'	112°51'15"	5/5	236.3	-41.8	233.9	-48.8	230.3	-55.7	224.8	-62.3	215.9	-68.5
16-D10-99	47°41'	112°51'15"	1/6	240.1	-39.2	240.2	-35.4	240.2	-31.6	240.3	-27.8	240.4	-24.0
17-E6-99	47°42'15"	112°51'	4/6	177.8	-64.7	187.7	-62.4	195.8	-59.4	202.2	-55.8	207.3	-51.9
18-F7-99	47°42'	112°51'	0/2	-	-	-	-	-	-	-	-	-	-
19-D7-00	47°42'	112°51'15"	4/4	210.7	-41.6	211.0	-41.3	211.4	-40.9	211.7	-40.6	212.0	-40.3
20-E7-00	47°42'	112°51'	4/4	160.9	-62.2	149.8	-61.3	139.9	-59.3	131.5	-56.4	124.6	-52.9

				Unfolding							
				40%		30%		20%		10%	
Site	Slat (N)	Slong (W)	N/No	Dec	Inc	Dec	Inc	Dec	Inc	Dec	Inc
6-D10-99	47°41'	112°51'15"	4/5	233.8	-33.4	235.8	-26.6	237.2	-19.8	238.1	-12.8
7-C8-99	47°41'15"	112°52'	2/2	227.5	-40.8	228.5	-36.8	229.3	-32.8	230.0	-28.7
8-C8-99	47°41'15"	112°52'	2/2	218.9	-37.2	220.2	-33.4	221.3	-29.5	222.1	-25.7
9-D7-99	47°41'	112°52'	1/1	206.4	-36.4	208.8	-34.8	211.0	-33.1	213.0	-31.3
10-E4-99	47°42'30"	112°51'	5/6	223.1	-39.8	225.2	-35.8	226.9	-31.8	228.3	-27.6
11-E4-99	47°42'30"	112°51'	1/2	217.6	-51.5	221.1	-47.7	223.9	-43.8	226.3	-39.8
12-E3-99	47°42'30"	112°51'	4/5	344.2	27.8	346.9	27.3	344.5	26.6	352.0	25.6
13-E6-99	47°42'	112°51'	5/6	242.6	-49.2	244.0	-42.8	245.0	-36.4	245.7	-30.0
14-D6-99	47°42'	112°51'15"	5/5	200.3	-73.7	174.3	-76.7	143.5	-76.0	121.3	-72.1
16-D10-99	47°41'	112°51'15"	1/6	240.4	-20.2	240.5	-16.4	240.5	-12.6	240.5	-8.8
17-E6-99	47°42'15"	112°51'	4/6	211.3	-47.7	214.5	-43.3	217.0	-38.7	219.0	-34.0
18-F7-99	47°42'	112°51'	0/2	-	-	-	-	-	-	-	-
19-D7-00	47°42'	112°51'15"	4/4	212.3	-40.0	212.6	-39.6	212.9	-39.3	213.2	-38.9
20-E7-00	47°42'	112°51'	4/4	119.3	-49.0	115.0	-44.8	111.7	-40.3	109.0	-35.6

Paleomagnetic data for all sites. Sites 6-14 and 17-20 are hand-sampled from various locations along the main sill; sites 16 and 18 are locations along thinner sills parallel to the main sill; Slat and Slong are the present day site latitude and longitude; N/No are the number of specimens used / number of specimens collected. Unfolding percentages are the percent amount that was tilt corrected to obtain the site mean directions.

Figure 13. Percent Unfolding vs Kappa and Radius of 95% confidence
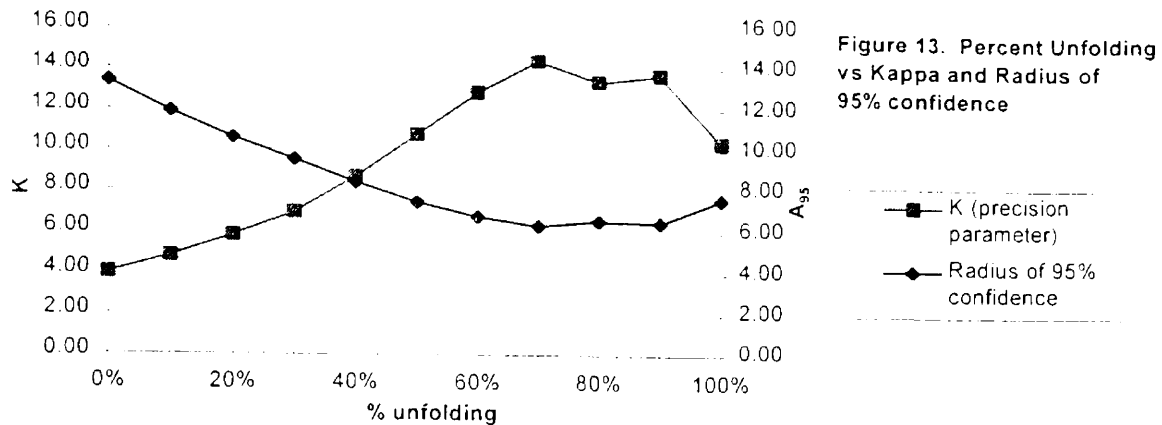
A fold test was calculated for each unfolding percent for the same reasons as with *in-situ* and stratigraphic coordinates. The fold test results (Table 6) indicate 80% of unfolding to be the most significant with an observed value of $f = 1.28$ compared to the critical value $F = 2.53$ at the 95% confidence level. But the fold test for 70% of unfolding produced an observed value of $f = 3.43$ suggesting that at the 95% confidence level the hypothesis of a common true mean direction may be rejected, even though the largest precision, k, and smallest α_{95} are associated with 70% unfolding.

TABLE 6. STATISTICAL SUMMARY AND FOLD TEST FOR PERCENT TILT CORRECTION

	Unfolding								
	90%	80%	70%	60%	50%	40%	30%	20%	10%
N	38	38	38	38	38	38	38	38	38
R	35.30	35.23	35.43	35.12	34.56	33.72	32.69	31.62	30.28
K	13.72	13.38	14.39	12.83	10.75	8.65	6.97	5.80	4.79
A_{95}	6.51	6.60	6.34	6.75	7.43	8.39	9.50	10.58	11.90
CSD	21.95	22.23	21.42	22.71	24.83	27.74	30.99	34.05	37.57
N_E	9	9	9	9	9	9	9	9	9
N_{W1}	14	14	14	14	14	14	14	14	14
N_{W2}	15	15	15	15	15	15	15	15	15
R_E	7.89	7.93	7.98	8.02	8.06	8.12	8.15	8.19	8.22
R_{W1}	13.54	13.27	13.65	13.66	13.66	13.62	13.57	13.49	13.39
R_{W2}	14.21	14.22	14.23	14.23	14.24	14.21	14.20	14.23	14.23
d.f.={4,70}									
$f =$	2.49	1.28	3.43	6.63	11.65	18.45	25.95	33.78	41.55

$F = 2.53$ @ 95% confidence level

Statistical summary and fold test analysis for each unfolding step from paleomagnetic data of the trachyandesite sill. In-situ are uncorrected coordinates of the sill; Stratigraphic is the fold corrected coordinates of the sill; N is the number specimens from the reliable 12 sites; NE is the number of specimens from the east dipping limb of the anticline; NW1 is the number if specimens from the west dipping limb of the anticline; NW2 is the number of specimens from the west dipping limb of the syncline; R, RE, RW1, and RW2 are the resultant vectors from paleomagnetic directions; d.f. is the degrees of freedom for the F distribution; f is the observed value calculated from equation #8 from McFadden & Jones (1981).

The statistical calculations and fold test, based on the paleomagnetic data, suggest that the sill intruded into sedimentary rocks that had already been folded 20% to 30%. Structural cross-sections (Figures 9 & 10) support the same conclusion that the sill intruded into partially folded sedimentary units. These cross sections show that the sill cuts across the hinges of both the anticline and syncline indicating the sill, assumed to be horizontal, intruded into non-horizontal strata.

The third reason addressed for the over correction is any unrecorded penetrative strain associated with the sill, such as cleavage within the sill or sedimentary units acquired during folding. Stamatakos and Kodama (1991) investigated how penetrative strain affects remanence in sedimentary rocks by examining the relationship between the strain geometry and the magnetizations in the Mississippian Mauch Chunk Formation. Their structural results from a first-order anticline fold of the Mauch Chunk Formation in the Appalachian Valley indicate bedding-parallel shear associated with folding. They found that this type of strain skewed their paleomagnetic results by shallowing remanent inclinations on the south dipping limb and steepening remanent inclinations on the north-dipping limb. This gave apparent synfolding geometry from a prefolding magnetization of the Mauch Chunk Formation.

An application of the study by Stamatakos and Kodama (1991) requires some type of penetrative strain either on the mesoscopic or microscopic scale, as was seen in their study. If strain, such as cleavage or bedding-parallel shear has been recognized, then an analysis of how it effects the paleomagnetic remanent directions can be measured. In the case of this study, penetrative strain on the mesoscopic scale was not recognized nor measured within the sill and sedimentary units. Eight thin sections from various locations

of the sill were analyzed with a petrographic microscope for any occurrence of penetrative strain. Foliation was not recognized in any of the thin sections and the plagioclase feldspar grains retained good albite twining. As a result, I assume that no penetrative strain has affected magnetization of the sill.

Thrust Sheet Rotation and Timing

To test the hypothesis that significant rotation around a nearby vertical axis of the thrust sheet occurred, the 12 reliable sites were combined by averaging their site-mean directions. The observed tilt corrected average is Dec = 200.0°, Inc = -62.3°, α_{95} = 7.6° and the paleomagnetic pole derived from the averaging the 12 VGPs is -75.5°S, 166.2°E. The paleomagnetic reference directions from the Late Cretaceous to Eocene (Gunderson and Sheriff 1991; Diehl *et al.*, 1983) are summarized in Table 3 and are undistinguishable at the 95% confidence level. By the methods of Beck (1980) the average rotational amount from the expected direction for the *in-situ* mean direction is 60.5° referenced to the Late Cretaceous, 64.4° referenced to the Paleocene, and 64.0° referenced to the Eocene direction (Table 7 and Figure 12). For stratigraphically corrected paleomagnetic mean directions the average rotational amount is 27.9° referenced to the Late Cretaceous, 31.9° and 31.5° referenced to the Paleocene and Eocene, respectively (Figure 12). Given the likelihood that the sill intruded into partially folded strata, rotational amounts were calculated for 50%, 60%, 70%, 80%, and 90% of unfolding (Table 7 and Figure 14).

Age determination of the sill is an important step for constraining the time of deformation along the Rocky Mountain fold and thrust belt. Sears *et al.* (2000) provide a

^{40}Ar/^{39}Ar biotite age of 58.8 +/- 1.5 Ma for the same sill 5 km south from this study site. Their sample, from the center of a 200-meter thick section of the sill (Mudge and Earhart, 1983), is partially chloritized and sericitized. They argue that the age of their sill is a re-set cooling age caused by burial and exhumation of the sill in the footwall. Sears et al. (2000) also sampled a sill of nearly the same stratigraphic setting as the study sill intruding into formations from the Albian through Campanian within the Garrison depression that is caught up in the LEH plate (Gwinn, 1961; Gwinn and Mutch, 1965; Webb, 1999). A biotite ^{40}Ar/^{39}Ar analysis of the sill within the Garrison depression yielded an age of 75.9 +/- 1.2 Ma and is interpreted to be the age of crystallization and intrusion. Sears et al. (2000) concluded both sills are of the same complex based on their petrology, geochemistry, and stratigraphic and structural setting and that they intruded the foreland basin around 76 Ma, before the movement of the LEH plate.

Results from stratigraphic studies further constrain the relative initiation of deformation of the Montana disturbed belt. Campanian (74.5 – 84 Ma) volcanic-rich formations (Adel Mountains, Belly River, Horsethief Sandstone, Two Medicine, and the Elkhorn Mountains) that have stratigraphic continuity across the foreland basin are the youngest deposits prior to the emplacement of the LEH plate (Viele and Harris, 1965; Mudge and Earhart, 1983; Schmidt, 1987; Rogers et al., 1993). The youngest rocks cut by the LEH plate that overlie the Two Medicine and Belly River formations are the basal St Mary River Formation (~74 Ma) which stretches from southwestern Alberta to central-western Montana (Price and Mountjoy, 1970; Mudge et al., 1982).

Conclusions presented by Sears et al. (2000) based on balanced and restored cross-sections, age data of sills, thermal constraints, and ambient geothermal gradient suggest

Table 7. Study Site VGP with Observed Directions and Degrees From Expected Directions

	VGP		Observed Direction		Degrees From Expected Direction		
	Lat N	Long E	Dec	Inc	*Late Cretaceous*	*Paleocene*	*Eocene*
Geographic	45.1	343.9	52.4	46.6	60.5 +/- 18.0	64.4 +/- 16.8	64.0 +/- 16.2
50% Unfolding	59.6	352.6	35.7	52.6	43.6 +/- 13.3	47.5 +/- 11.7	47.2 +/- 10.8
60% Unfolding	61.8	351.1	34.1	54.6	42.1 +/- 13.0	46.0 +/- 11.3	45.6 +/- 10.4
70% Unfolding	64.2	349.8	32.1	56.4	40.1 +/- 12.9	44.0 +/- 11.1	43.6 +/- 10.3
80% Unfolding	68.5	349.4	27.6	58.8	35.6 +/- 13.6	39.5 +/- 12.0	39.2 +/- 11.2
90% Unfolding	69.6	348.3	26.7	59.5	34.6 +/- 13.7	38.6 +/- 12.1	38.2 +/- 11.3
Stratigraphic	75.5	346.2	20.0	62.3	27.9 +/- 15.9	31.9 +/- 14.5	31.5 +/- 13.9

(positive # implies clockwise rotation)

The calculated VGP and observed directions are flipped to the northern hemisphere.
Gunderson and Sheiff (1991) provide the reference direction for the Late Cretaceous;
Diehl *et al*. (1983) provide the reference directions for Paleocene and Eocene. The
rotational amount calculated from Beck (1980) with Demarest (1983) corrections.

90% unfolding
0

270

80% unfolding
0

70% unfolding
0

90

60% unfolding
0

270

50% unfolding
0

90
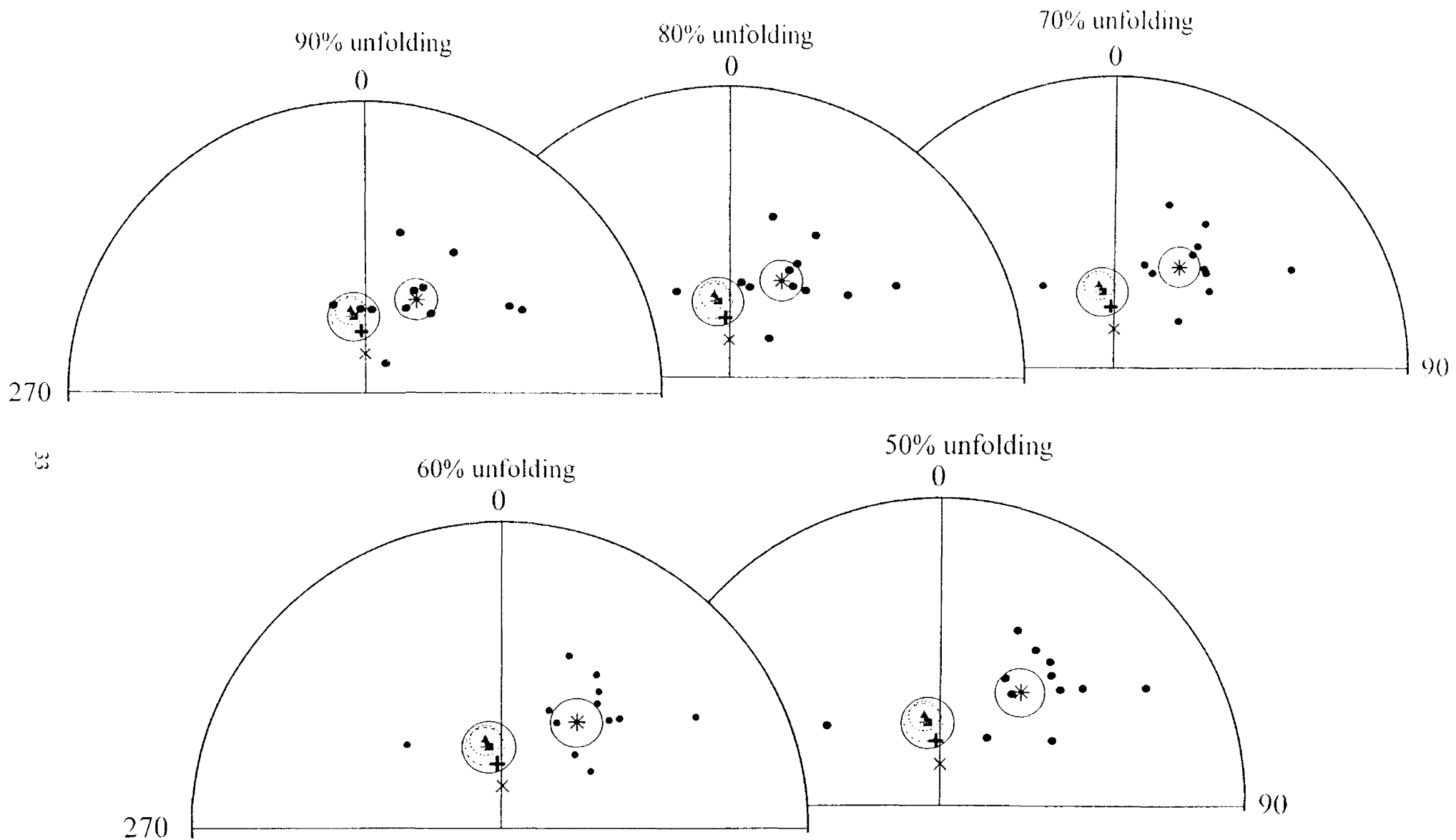
Figure 14. Equal-area projection of paleomagnetic mean directions from 90% to 50% unfolding. Field area directions are flipped to normal polarity. (✳) shows the mean direction with α_{95} circle of confidence.Square is the Late Cretaceous reference paleopole from Gunderson *et al.*, 1991. Cross is the Paleocene reference paleopole from Diehl *et al.*, 1983. Triangle is the Eocene refernce paleopole from Diehl *et al.*, 1983. Circles are the α_{95} radius of confidence. X is the spin axis of the Earth. ✚ is the present magnetic field direction (IGRF, 1995).

deformation in the footwall from the over-riding Lewis-Eldorado-Hoadley (LEH) plate

ceased by 58 Ma. Also, Mudge *et al.* (1982) show 58 Ma porphyritic dikes crosscutting

faults that outline the edge of the LEH thrust plate. This is important to show the

cessation of deformation in the footwall because the age of the sill (58.8 +/- 1.5 Ma)

presented by Sears *et al.* (2000) contradicts the amount of deformation the sill

experienced. For arguments sake, if the age of emplacement, cooling, and acquisition of

magnetization of the sill from this study is 58.8 +/- 1.5 Ma (Sears *et al.*, 2000) then the

sill would have experienced at least 70% of folding within a 1 to 2 million year time

span. The thrust sheet would have also experienced a clockwise rotation about a nearby

vertical axis at rates of 18° to 35° per million years. This seems highly unlikely.

Average thrust emplacement rates can be predicted by taking the amount of linear

displacement of the thrust sheet and dividing by the age constraint of the thrust event.

Price and Sears (2000) predict a linear displacement up to 100 km of the LEH thrust plate

near the Sun River Canyon area. Hoffman *et al.* (1976) predict an age constraint for

thrusting from 72 to 56 Ma by K-Ar dating of potash bentonite from Mesozoic

sedimentary rocks in the disturbed belt of Montana that was buried by the overriding

thrust sheets. From these studies, a predicted emplacement rate of thrust sheets near the

study area is ~6 km per million years with average rotation rates between 2° to 3° per

million years.

The combination of unprobable deformation rates along with stratigraphic

constraints and the age argument by Sears *et al.* (2000), suggest a more likely argument

that the sill is around 76 Ma and thrusting and folding of the footwall from the over

riding LEH plate began near 74 Ma and ceased by 58 Ma. But, the paleomagnetic and

structural evidence from this study indicate that the sill intruded into strata that had been folded up to 25%. This would indicate that the footwall, or at least this particular thrust sheet, began folding prior to 76 Ma and that thrusting might not have initiated until 74 Ma.

The magnetic polarity time scale provides another means of dating the age of the sill. Figure 15 presents the time scale from 50 Ma to 83 Ma (Cande and Kent, 1995) and shows Sears *et al.* (2000) interpreted age of the sill (75.9 +/- 1.2 Ma) in the middle of a large normal interval (73.619 Ma to 79.075 Ma). Yet all my specimens are of reversed polarity. Reversed polarities become more frequent toward the age of the sill actually given by the biotite $^{40}Ar/^{39}Ar$ analysis (58.8 +/- 1.5 Ma). This indicates that the sill
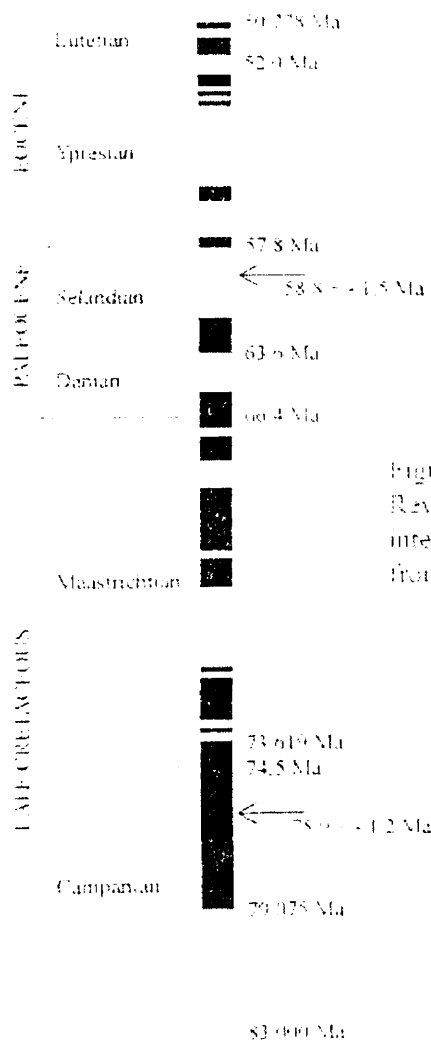
Figure 15. Polarity time scale. Normal polarity shown in black. Reversed polarity shown in white. Arrows with date indicate interpreted sill age (75.9 Ma) and actual age (58.8 Ma). Time scale from Cande and Kent, 1995.

acquired magnetization at a younger time than the predicted age of around 76 Ma and intruded at time when the magnetic field was briefly reversed.

If the sill intruded around 76 Ma then the sill would need to be above the Curie temperature of magnetite (570 °C) for nearly 2

35

million years until the next reversal interval appeared (73.374 Ma to 73.619 Ma) and then cool below 570 °C for the sill to acquire magnetization. Evidence suggests that the sill at the time of intrusion, either around 76 Ma or 59 Ma, was never buried more than 1.5 km (McMannis, 1965 and Mudge, 1972b) and thus cooled in 250 to 750 years (Jaeger, 1957). So, acquisition of magnetization was likely instantaneous in geologic time and the age of the sill is younger than the interpreted age of around 76 Ma. Nonetheless, the sill records much of the deformation of the thrust sheet and is rotated in a clockwise manner.

The "larger picture" from this study ties in with the study from Symons and Timmins (1992), which described a clockwise sense of rotation of the LEH plate in western Montana and southern Canada. Other paleomagnetic studies by Grubbs and Van der Voo (1976), Jolly and Sheriff (1992), Eldredge and Van der Voo (1988), and Brunt (1997) show discrepancies with this model of clockwise rotation. But, Eldredge and Van der Voo (1988) relate these results to a buttressing effect that might not translate into the interior of the Helena salient from their study and perhaps does not translate into the interior of the fold and thrust belt of western Montana. All the paleomagnetic results came about from previous studies that show the complex structural and stratigraphic relationships along western Montana and southern Canada.

The model by Sears (1994) and Price and Sears (2000) agrees with Symons and Timmins (1992) clockwise rotation results. But Sears (1994) and Price and Sears (2000) base their conclusions on a palinspastic map from balanced regional structural sections of the fold and thrust belt (Price and Mountjoy, 1970; Monger et al., 1985; Price, 1981; Price and Fermor, 1985; Fermor and Moffat, 1992; Burton et al., 1994; Harris, 1985; Lidke and Wallace, 1994; Sears, 1988; Sears and Buckley, 1994). Sears (1994) and Price

and Sears (2000) argue for a 30° clockwise rotation about a vertical axis near Helena, Montana.

Data from my study shows the thrust sheet that the sill occupies rotated in a clockwise manner about a nearby vertical axis an average of 38° +/- 13.2° compared to the Late Cretaceous paleopole and 42° +/- 11.5° compared to the Paleocene paleopole. This result agrees with the Symons and Timmins (1992), Sears (1994), and Price and Sears (2000) model of an overall clockwise rotation. The result from this study also agrees with findings from Irving *et al.* (1986), Eldredge and Van der Voo (1988), and Brunt (1997) (Figure 1). But contrasts the results from studies by Jolly and Sheriff (1992), Eldredge and Van der Voo (1988), and Brunt's (1997) counterclockwise rotation near Marias Pass.

To help determine if the sill intruded into partially folded strata, future paleomagnetic investigations similar to this one need to be performed for the same sill where it resides within at least nine or more thrust sheets further west in the footwall of the Montana disturbed belt (Mudge and Earhart, 1983). Another future study that would help define the type of rotation of the LEH plate would be a paleomagnetic investigation of the dikes and sills in the Garrison depression (Gwinn, 1961; Gwinn and Mutch, 1965; Webb, 1999).

References

Alvarez, W., and Lowrie, W., 1978, Upper Cretaceous paleomagnetic stratigraphy at Moria (Umbrian Apennines Italy): Verification of the Gubbio section, *Geophys. J. R. Astron. Soc.*, *55*, p. 1-17.

Beck, M.E., 1980, Paleomagnetic record of plate-margin tectonic processes along the western edge of North America, *Journal of GeophysicalResearch*, *v. 85, no. B12*, p. 7115-7131.

Brunt, K.M., 1997, Paleomagnetic investigation of the Lower Cretaceous Kootenai Formation, western Montana. Thesis (M.S.), University of Montana.

Burton, B.R. et al., 1994, Deep drilling result and new interpretations of the Lombard thrust, southwestern Montana; *in* Belt Symposium III, Proceedings, Whitefish, Montana; *Montana Bureau of Mines and Geology Special Publication.*

Butler, R.F., 1991, Chapter 5: Paleomagnetic Stability, Field Tests of Paleomagnetic Stability; *in* Paleomagnetism: Magnetic Domains to Geologic Terranes. p. 123.

Cande, S.C. and Kent, D.V., 1995, Revised calibration of the geomagnetic polarity time scale for the Late Cretaceous and Cenozoic, *Journal of Geophysical Research*, 100, p. 6093-6095.

Chan, L.S., Montanari, A., and Alvarez, W., 1985, Magnetic stratigraphy of the Scaglia Rossa: Implications for syndepositional tectonics of the Umbria-Marches Basin, *Riv. Ital. Paleontol. Stratig.*, *91*, p. 219-258.

Chan, L.S., 1988, Apparent Tectonic Rotations, Declination Anomaly Equations, and Declination Anomaly Charts: *Journal of Geophysical Research, v. 93, no. B10*, p. 12,151-12,12,158.

Clapp, C.H., 1932, Geology of a portion of the Rocky Mountains of northwestern Montana: *Montana Bur. Mines and Geology Mem. 4*, 30p.

Deiss, C.F., 1943a, Stratigraphy and structure of southwest Saypo quadrangle, *Montana: Geol. Soc. America Bull., v. 54, no. 2*, p. 205-262.

Deiss, C.F., 1943b, Structure of central part of Sawtooth Range, Montana: Geol. Soc. America Bull., v. 54, no. 8, p. 1123-1167.

Demarest, H.H. Jr., 1983, Error analysis for the determination of tectonic rotation from paleomagnetic data, *Journal of Geophysical Research, v. 88, no. B5*, p. 4321-4328.

Diehl, J.F., Beck, M.E., Beske-Diehl, S., Jacobson, D., and Hearn, B.C., 1983, Paleomagnetism of the Late Cretaceous-early Tertiary north-central Montana alkalic province. *J. Geophys. Res.*, *88*, p. 10,593-10,609.

Eardley, A.J., 1963, Relation of uplifts to thrusts in Rocky Mountains, *in* Backbone of the Americas: *Am. Assoc. Petroleum Geologists Mem.* *2*, p. 209-219.

Eardley, A.J., 1968, Major structures of the Rocky Mountains of Colorado and Utah, *in* A coast to coast tectonic study of the United States: *Univ. Missouri research Jour.* *1* *(V.H. McNutt-Geology Dept. Colloquium Ser. 1)*, p. 79-99.

Eldredge, S. and Van der Voo, R., 1988, Paleomagnetic study of thrust sheet rotations in the Helena and Wyoming salients of the northern Rocky Mountains, *Geol. Soc. Am. Memoir*, *171*, p. 319-332.

Elston, D.P., Enkin, R.J., Baker, J., Kisilevsky, D.K., 2000, Tightening the Belt: Paleomagnetic constraints on the Deposition and Deformation of the Middle Proterozoic Belt-Purcell Supergroup, U.S. and Canada. GeoCanada 2000, poster.

Fermor, P.R. and Moffat, I.W., 1992, Chapter 3: Tectonics and structure of the Western Canadian foreland basin; in MacQueen, R.W. and Leckie, D.A. (editors), Foreland basins and fold belts; Tulsa, Oklahoma, *American Association of Petroleum Geologists Memoir 55*, p. 81-105.

Fisher, R.A., 1953, Dispersion on a sphere, *Royal Society of London Proceedings*, *217*, p. 295-305.

Grubbs, K.L. and Van der Voo, R., 1976, Structural deformation of the Idaho-Wyoming overthrust belt (U.S.A.), as determined by Triassic paleomagnetism: *Tectonophysics*, *v. 33*, p. 321-336.

Gunderson, J.A., and Sheriff, S.D., 1991, A New Late Cretaceous Paleomagnetic Pole form the Adel Mountains, West Central Montana, *J. Geophys. Res.*, *96*, p. 317-326.

Gwinn, V.E., 1961, Geology of the Drummond area, central-western Montana: *Montana Bureau of Mines and Geology, Geologic Map 4*.

Gwinn, V.E., and Mutch, T.A., 1965, Intertongued Upper Cretaceous volcanic and nonvolcanic rocks, central-western Montana: *Geol. Soc. America. Bull.*, *v.76*, p. 1125-1144.

Harris, D.W., 1985, Crustal structure of northwestern Montana; unpublished M.S., University of Montana, p. 63.

Hoffman, J., Hower, J., Aronson, J.L., 1976, Radiometric dating of time of thrusting in the disturbed belt of Montana: *Geology, 4, 1*, p. 16-20.

Irving, E., Wynne, P.J., Evens, M.E., and Gough, W., 1986, Anomalous paleomagnetism of the Crowsnest Formation of the Rocky Mountains, *Canadian Journal of Earth Science, v. 23*, p. 591-598.

Jaeger, J.C., 1957, The temperature in the neighborhood of a cooling intrusive sheet, *American Journal of Sciences, 255, 4*, p. 306-318.

Jolly, A.D. and Sheriff, S.D., 1992, Paleomagnetic study of thrust-sheet motion along the Rocky Mountain front in Montana, *Geol. Soc. Am. Bull., 104*, p.779-785.

Kirschvink, J.L., 1980, The least-squares line and plane and the analysis of paleomagnetic data, *Royal Astronomical Society Geophysical Journal, 62*, p. 699-718.

Lidke, D.J. and Wallace, C.A., 1994, Structure section across south-central Belt terrane, west-central Montana; *in* Belt Symposium III, Proceedings, Whitefish, Montana; *Montana Bureau of Mines and Geology Special Publication*.

Lowrie, W. and Alvarez, W., 1977, Late Cretaceous geomagnetic polarity sequence: detailed rock and paleomagnetic studies of the Scaglia Rossa limestone at Gubbio, Italy, *Geophys. J. R. Astron. Soc., 51*, p. 561-581.

MacDonald, W.D., 1980, Net Tectonic Rotation, Apparent Tectonic Rotation, and the Structural Tilt Correction in Paleomagnetic Studies: *Journal of Geophysical Research, v. 85. no. B7*, p. 3659-3669.

McElhinny, M.W., and Merrill, R.T., 1975, Geomagnetic variation over the past 5 m.y., *Rev. Geophys., 13*, p. 687-708.

McFadden, P.L., and Jones, D.L., 1981, The fold test in paleomagnetism, *Geophys. J. Res. Astr. Soc., 67*, p.53-58.

McGill, G.E., and Sommers, D.A., 1967, Stratigraphy and correlation of the Precambrian Belt Supergroup of the southern Lewis and Clark Range, Montana: *Geol. Soc. America Bull., v. 78, no. 3*, p. 343-351.

McMannis, W.J., 1965, Resume of depositional and structural history of western Montana: *AAPG Bull., v. 49*, p. 1801-1823.

Monger, J.W.H., et al., 1985, Centennial Continent/Ocean Transect #7, B-2 Juan de Fuca Plate to Alberta Plains; *in* Speed, R., Decade of North American Geology Continent/Ocean Transects; *Geological Society of America, v. B-2, 2 sheets*, p. 21.

Mudge, M.R., 1965, Bedrock geologic map of the Sawtooth Ridge quadrangle, Teton and Lewis and Clark Counties, Montana: *U.S. Geol. Survey Geol. Quad. Map GQ-381*.

Mudge, M.R., 1966a, Geologic map of the Patricks Basin quadrangle, Teton and Lewis and Clark Counties, Montana: *U.S. Geol. Quad. Map GQ-453*.

Mudge, M.R., 1966b, Geologic map of the Pretty Prairie quadrangle, Teton and Lewis and Clark Counties, Montana: *U.S. Geol. Quad. Map GQ-454*.

Mudge, M.R., 1966c, Geologic map of the Glenn Creek quadrangle, Teton and Lewis and Clark Counties, Montana: *U.S. Geol. Quad. Map GQ-499*.

Mudge, M.R., 1967, Geologic map of the Arsenic Peak quadrangle, Teton and Lewis and Clark Counties, Montana: *U.S. Geol. Survey Geol. Quad. Map GQ-597*.

Mudge, M.R., 1968, Bedrock geologic map of the Castle Reef quadrangle, Teton and Lewis and Clark Counties, Montana: *U.S. Geol. Quad. Map GQ-711*.

Mudge, M.R., Erickson, R.L., and Kleinkopf, Dean, 1968, Reconnaissance geology, geophysics, and geochemistry of the southeastern part of the Lewis and Clark Range, Montana: *U.S. Geol. Survey Bull., 1252-E*, 35p.

Mudge, M.R., 1970, Origin of the Disturbed Belt in Northwestern Montana: *Geol. Soc. Of America Bull., v. 81*, p. 377-392.

Mudge, M.R., Earhart, R.L., Whipple, J.W., and Harrison, J.E, 1982, Geologic and structure map of the Choteau 1 x 2 degree Quadrangle, western Montana: *U.S. Geol. Survey MI Map I-1300*, scale 1:250,000.

Mudge, M.R. and Earhart, R.L., 1983, Bedrock geologic map of part of the northern disturbed belt, Lewis and Clark, Teton, Pondera, Glacier, Flathead, Cascade, and Powell Counties, Montana: U.S. Geol. Survey, Miscellaneous Investigations Map I-1375, 1:125,000.

Price R.A., 1981, The Cordilleran foreland thrust and fold belt in the southern Canadian Rocky Mountains; *in* McClay, K.R. and Price, N.J. (editors), Thrust and nappe tectonics; *The geological Society of London, v. Special Publication Number 9*, p. 427-448.

Price, R.A., and Mountjoy, E.W., 1970, Geologic structure of the Canadian Rocky Mountains between Bow and Athabasca Rivers: A progress report, in Wheeler, J.O., ed., Structure of the southern Canadian Cordillera: *Geological Association of Canada, Special Publication 6*, p. 7-25.

Price, R.A. and Fermor, P.R., 1985, Structure of the Cordilleran foreland thrust and fold belt west of Calgary, Alberta; *Geological survey of Canada Paper 84-14*.

Price, R.A., and Sears, J.W., 2000, A preliminary palinspastic map of the Mesoproterozoic Belt-Purcell Supergroup, Canada and USA: Implications for the tectonic setting and structural evolution of the Purcell anticlinorium and the Sullivan deposit, *in* Lydon, J.W., ed., The Sullivan deposit and its geological environment, *Canadian Association of Geologists, Special Paper*.

Roberts, R.J., 1968, Tectonic framework of the Great Basin, *in* A coast to coast tectonic study of the United States: *University Missouri Research Journal 1 (V.H. McNutt-Geology Dept. Colloquium Ser. 1)*, p. 101-119.

Rogers, R.R., Swisher, C.C., III, and Horner, J.R., 1993, 40Ar/39Ar age and correlation of the nonmarine Two Medicine Formation (Upper Cretaceous), northwestern Montana, U.S.A.: *Canadian Journal of Earth Science, v. 30*, p. 1066-1075.

Rubey, W.W., and Hubbert, M.K., 1959, Overthrust belt in geosynclinal area of western Wyoming in light of fluid-pressure hypothesis, [Pt.] 2 *of* Role of fluid pressure in mechanics of overthrust faulting: *Geol. Soc. America Bull., v. 70, no. 2*, p. 167-205.

Schmidt, R.G., 1978, Rocks and mineral resources of the Wolf Creek area, Lewis and Clark and Cascade Counties, Montana: *U.S. Geological Survey Bull. 1441*, p. 91.

Sears, J.W., 1988, Two major thrust slabs in the west-central Montana Cordillera, *Geol. Soc. Am., 171*, p. 165-170.

Sears, J.W., 1994, Thrust rotation of the Belt basin, Canada and United States: *Northwest Geology, v. 23*, p. 81-92.

Sears, J.W. and Buckley, S.N., 1994, Cross section of the Rocky Mountain thrust belt from Choteau to Plains, Montana; Implication for the eastern margin of the Belt Basin; *in* Belt Symposium III, Proceedings, Whitefish, Montana; *Montana Bureau of Mines and Geology Special Publication*.

Sears, J.W., Hendrix, M.S., Waddell, A., Webb, B., Nixon, B., King, T., Roberts, E., and Lerman, R., 2000, Structural and stratigraphic evolution of the Rocky Mountain foreland basin in central-western Montana. *in* Roberts, Sheila, and Winston, Don, eds., Geologic field trips, Western Montana and adjacent areas: Rocky Mountain Section of the Geological Society of America, University of Montana, p.131-155.

Stamatakos, J. and Kodama, K.P., 1991, Flexural flow folding and the paleomagnetic fold test: an example of strain reorientation of remanence in the Mauch Chunk Formation, *Tectonics, v. 10, no. 4*, p. 807-818.

Stebinger, E., 1917, Anticlines in the Blackfeet Indian Reservation. Montana: *U.S. Geol. Survey Bull. 641-J*, p. 281-305.

Stebinger, E., 1918, Oil and gas geology of the Birch Creek-Sun River area, Northwestern Montana: *U.S. Geol. Survey Bull. 691-E*, p. 149-184.

Symons, D.T.A., and Timmins, E.A., 1992, Geotectonics of the cratonic margin from paleomagnetism of the middle Proterozoic Aldridge (Prichard) Formation and Moyie Sills of British Columbia and Montana, in: Bartholomew, M.J., Hyndman, D.W., Mogk, D.W., and Mason, R.; eds., Basement tectonics 8: Characterization and comparison of Precambrian through Mesozoic continental margins (Butte, Montana, 1988), p. 373-384.

Viele, G.W., and Harris, F.G., 3d, 1965, Montana Group stratigraphy, Leis and Clark County, Montana: *Am. Assoc. Petroleum Geologists Bull., v. 49, no. 4*, p. 379-417.

Webb, B., 1999, Detailed Mapping of the Garrison and Luke Mountain Quadrangle Powell County, Montana. Thesis (B.S.), University of Montana. pgs 33.

Wisser, E.H., 1957, Deformation in the Cordilleran region of western United States, *in* Hartman, H.L., *Chairman*, Behavior of materials in the earth's crust: *Colorado School Mines Quart., v. 52, no. 3*, p. 54-73.

Zijderveld, J.D.A., 1967, A.C. demagnetization of rocks: Analysis of results, *in* Collinson, D.W., Creer, K.M., and Runcorn, S.K., eds., *Methods in paleomagnetism: New York, Elsevier*, p. 254-286.

APPENDIX A.

PALEOMAGNETIC DATA

Site summary with specimen NRM and ChRM directions and intensities. Site statistical summary with R = resultant vector; k = Fisher (1953) precision parameter; α_{95} = radius of 95% confidence; σ_{63} = circular standard deviation; Dec. = site stratigraphic declination; Inc. = site stratigraphic inclination; VGP = virtual geomagnetic pole.
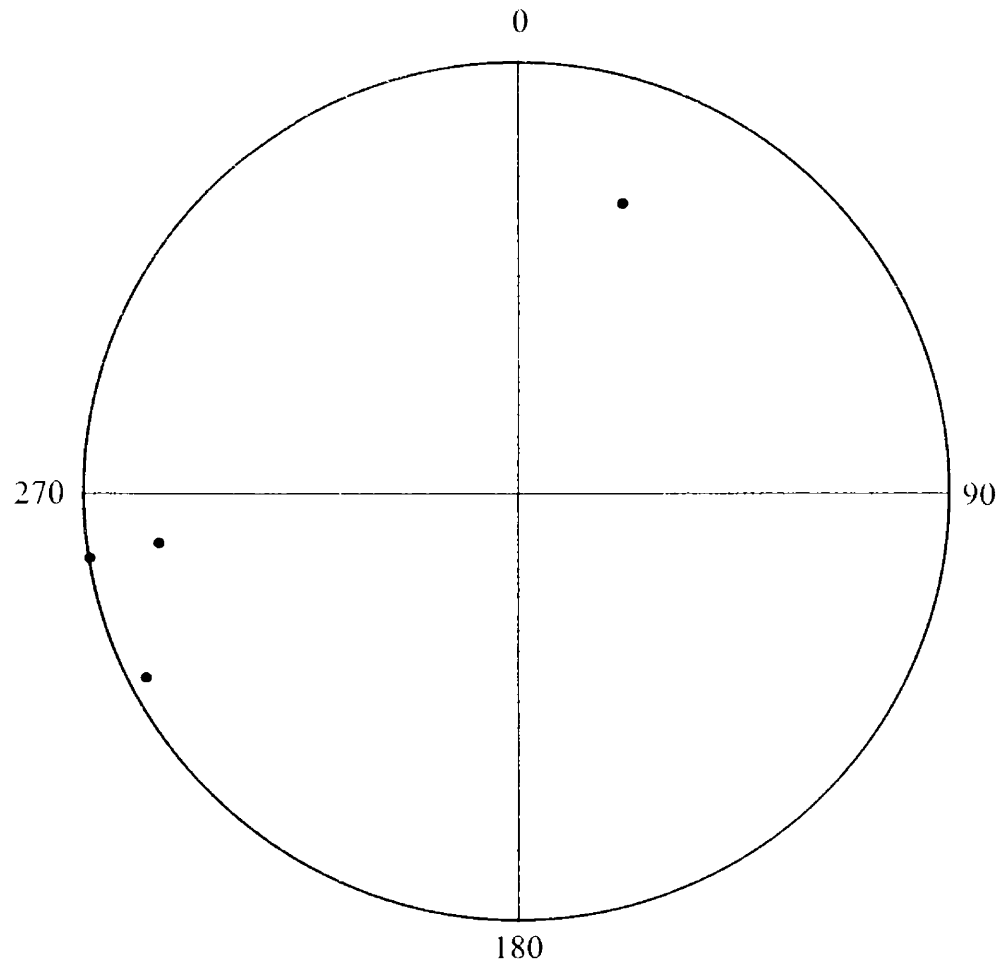
Site: 6-D10-99
Lith: Trachyandesite Sill   Samples: 4/5

| Specimens | J_o | NRM | | ChRM Stratigraphic | | |
		Dec.	Inc.	J_o	Dec.	Inc.
6A	1.90E-04	20.4	29.0	1.36E-04	181.9	-52.4
6B	6.67E-04	261.7	16.9	3.47E-04	185.4	-62.4
6C	-	-	-	-	-	-
6D	8.35E-04	260.9	0.0	2.80E-04	236.6	-79.7
6E	8.91E-04	243.3	3.7	4.43E-04	185.8	-62.5

R   3.9212
k   38.0866
α_{95} 15.08
s_{63} 13.12
Dec.   189.2
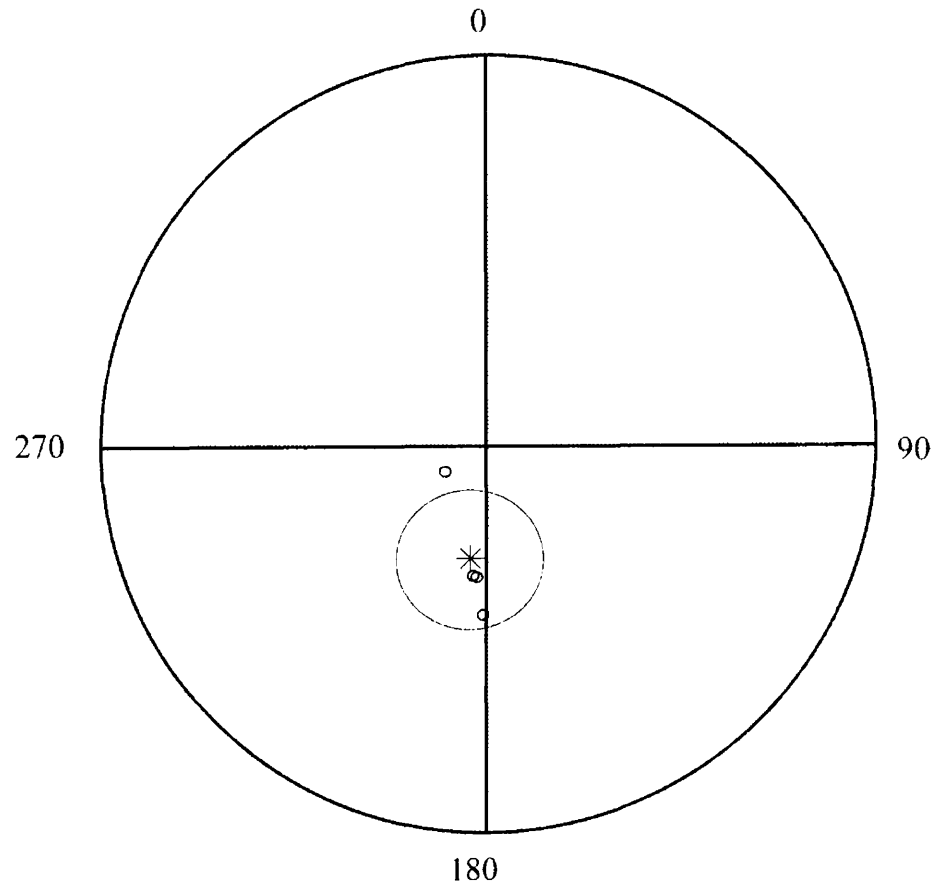Inc.   -65.6
VGP   -83.8/153.1

6-D10-99
NRM
equal-area

6-D10-99
geographic coordinates
equal-area

6-D10-99
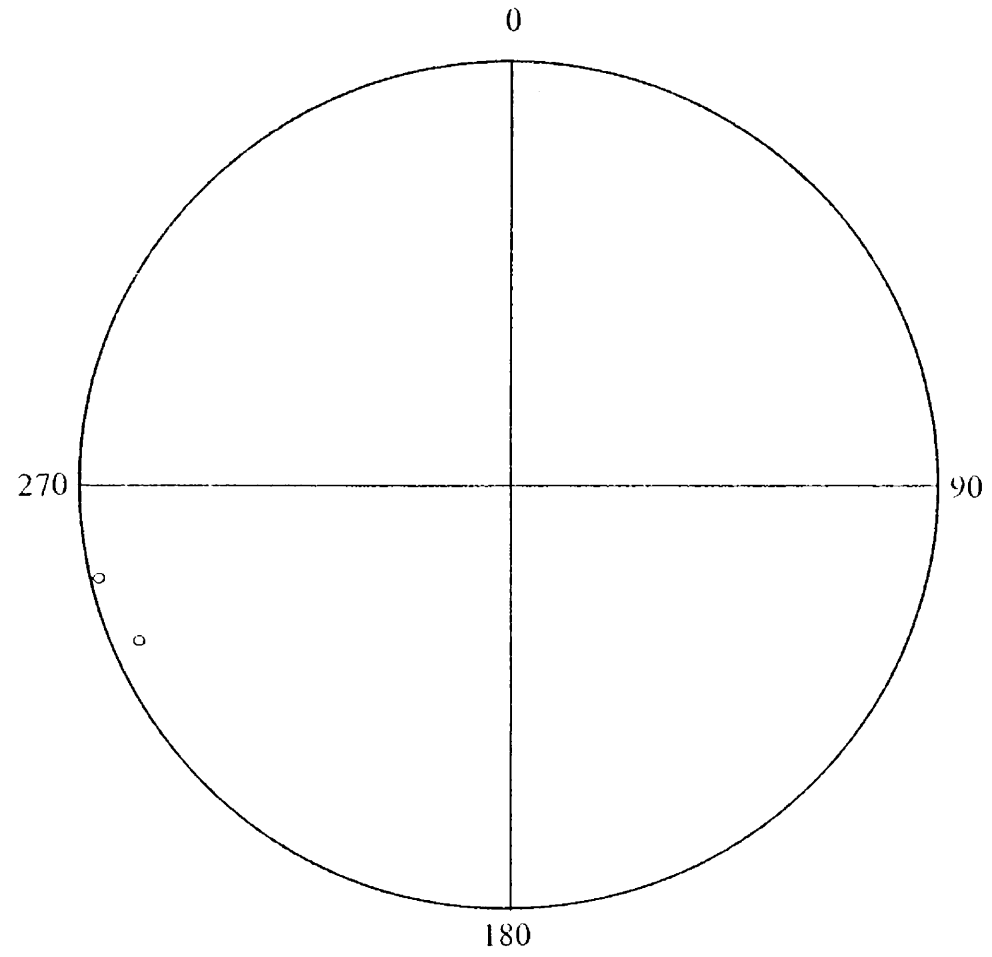stratigraphic coordinates
equal-area

47
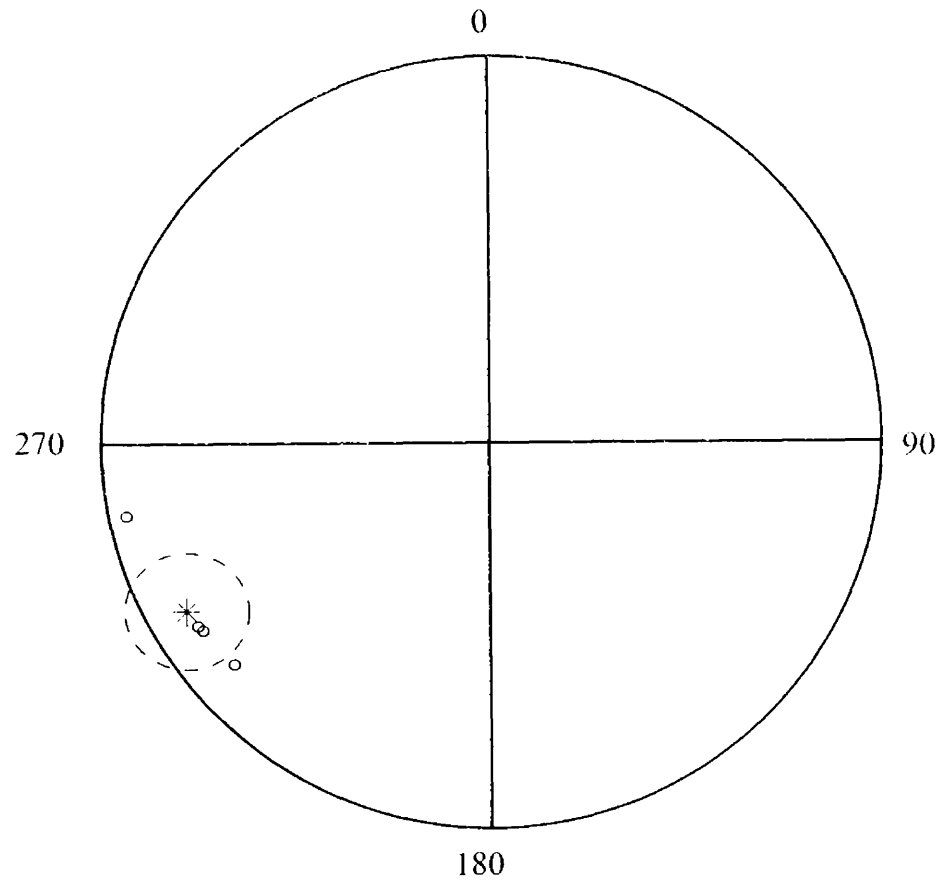
Site: 7-C8-99
Lith: Trachyandesite Sill   Samples: 2/2

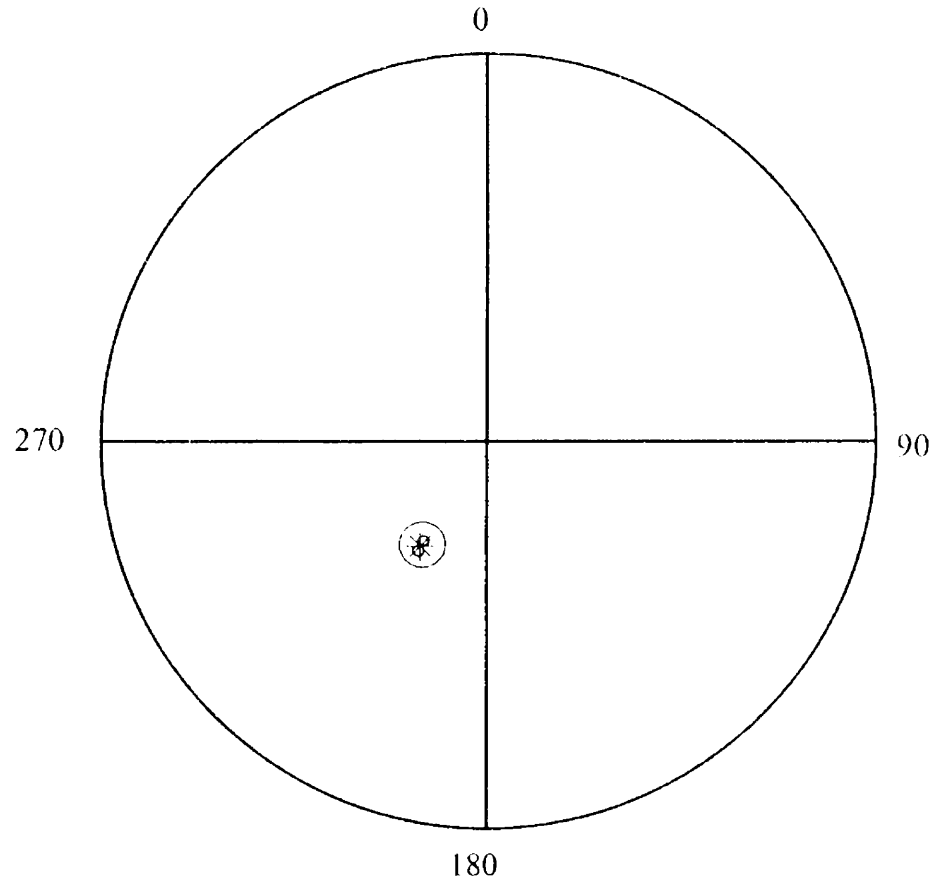|		NRM		ChRM Stratigraphic		
Specimens	J_o	Dec.	Inc.	J_o	Dec.	Inc.
7A	2.14E-04	257.3	-2.0	1.66E-04	212.6	-62.9
7B	1.15E-03	247.3	-7.1	3.33E-04	214.8	-65.0

R   1.9996
k   2458.56
α_{95} 5.04
s_{63} 1.63
Dec.   213.7
Inc.   -64.0
VGP   -67.0/149.6

7-C8-99
NRM
equal-area

0

270

90

180

7-C8-99
geographic coordinates
equal-area
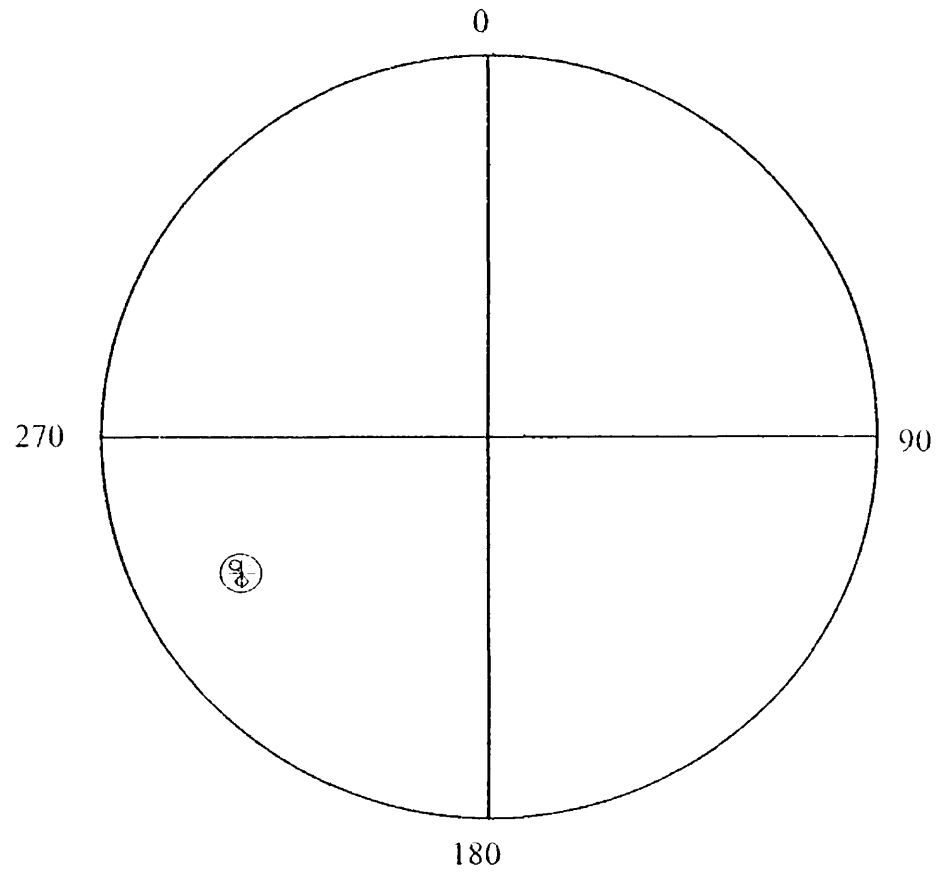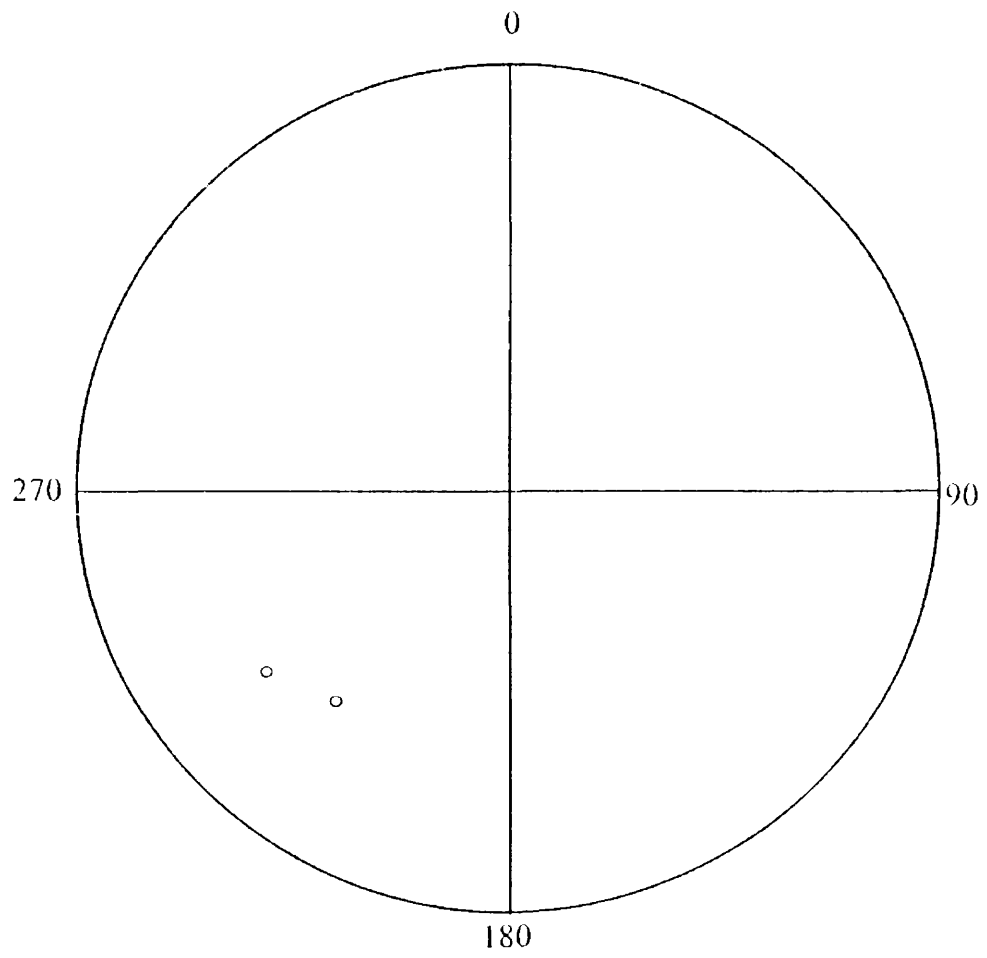
7-C8-99
stratigraphic coordinates
equal-area

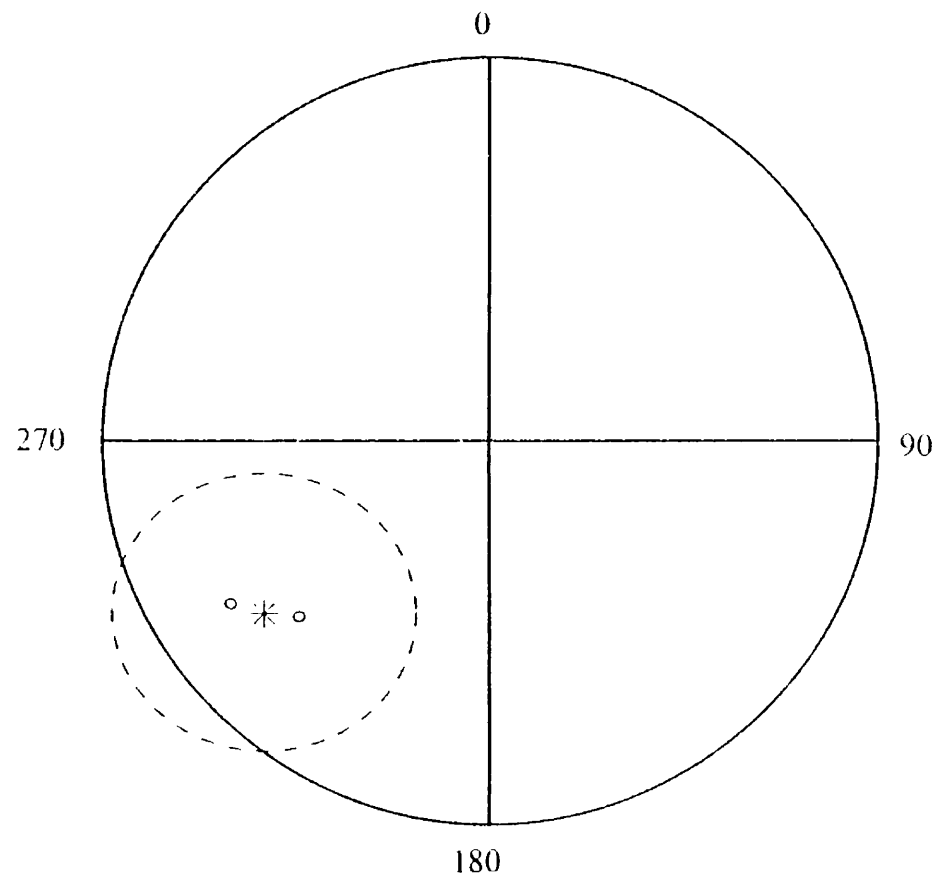Site: 8-C8-99
Lith: Trachyandesite Sill   Samples: 2/2

| Specimens | J_o | NRM | | ChRM Stratigraphic | | |
		Dec.	Inc.	J_o	Dec.	Inc.
8A	1.50E-05	218.9	-35.7	8.12E-06	189.4	-57.0
8B	1.86E-05	233.1	-29.6	9.50E-06	217.3	-58.1

R   1.9831
k   59.2060
α_{95} 33.05
s_{63} 10.52
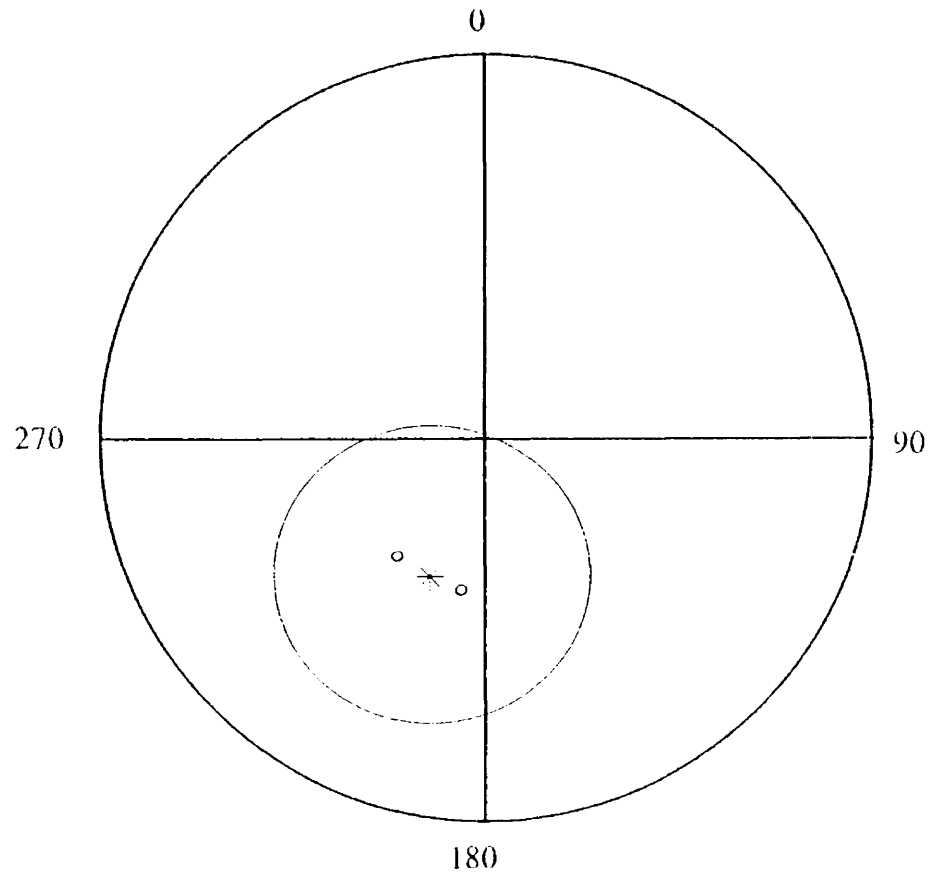Dec.   203.1
Inc.   -58.3
VGP   -71.2/176.0

8-C8-99
NRM
equal-area

8-C'8-99
geographic coordinates
equal-area

8-C8-99
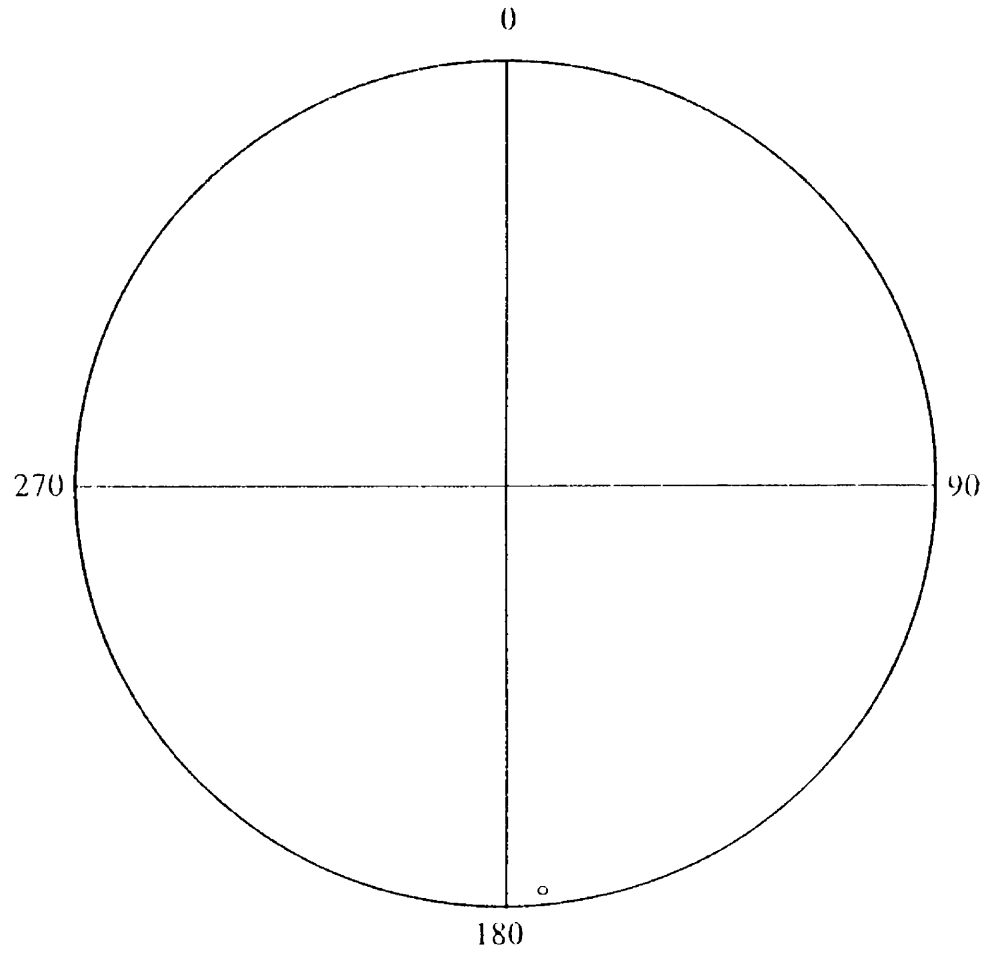stratigraphic coordinates
equal-area

55

Site: 9-D7-99
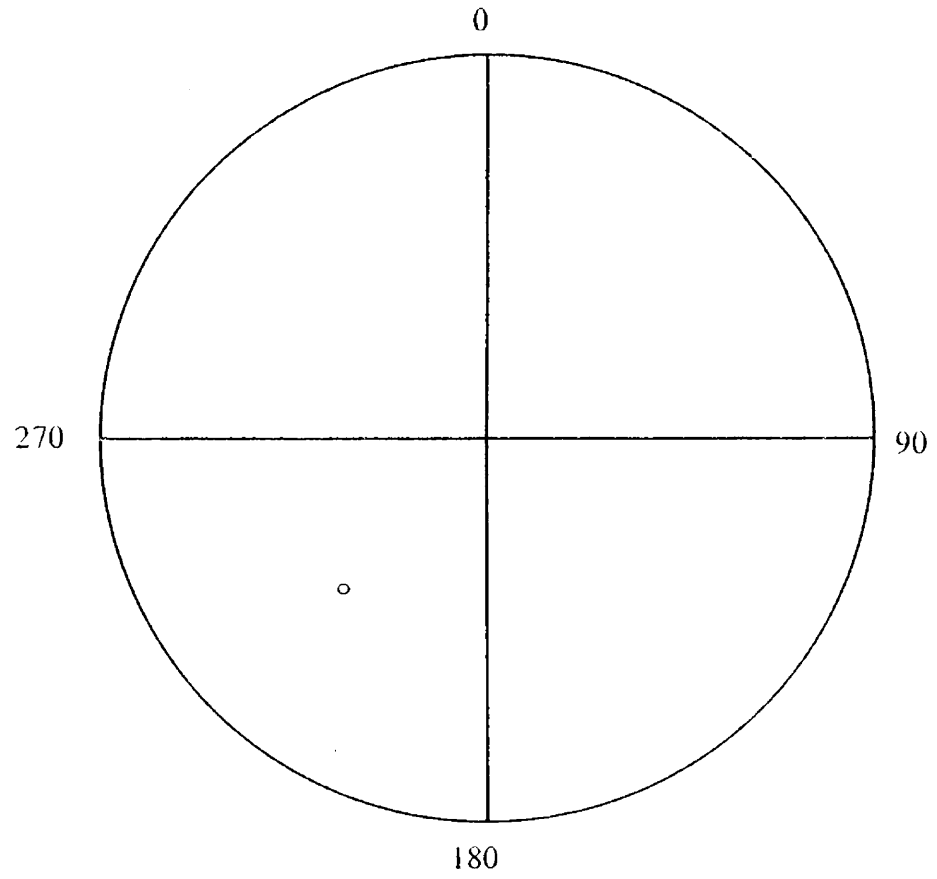Lith: Trachyandesite Sill   Samples: 1/1

| Specimens | J_0 | NRM | | ChRM Stratigraphic | | |
		Dec.	Inc.	J_0	Dec.	Inc.
9A	4.50E-06	175.0	-4.5	7.10E-07	188.5	-42.5

R   1.00
k   -
α_{95} -
S_{63} -
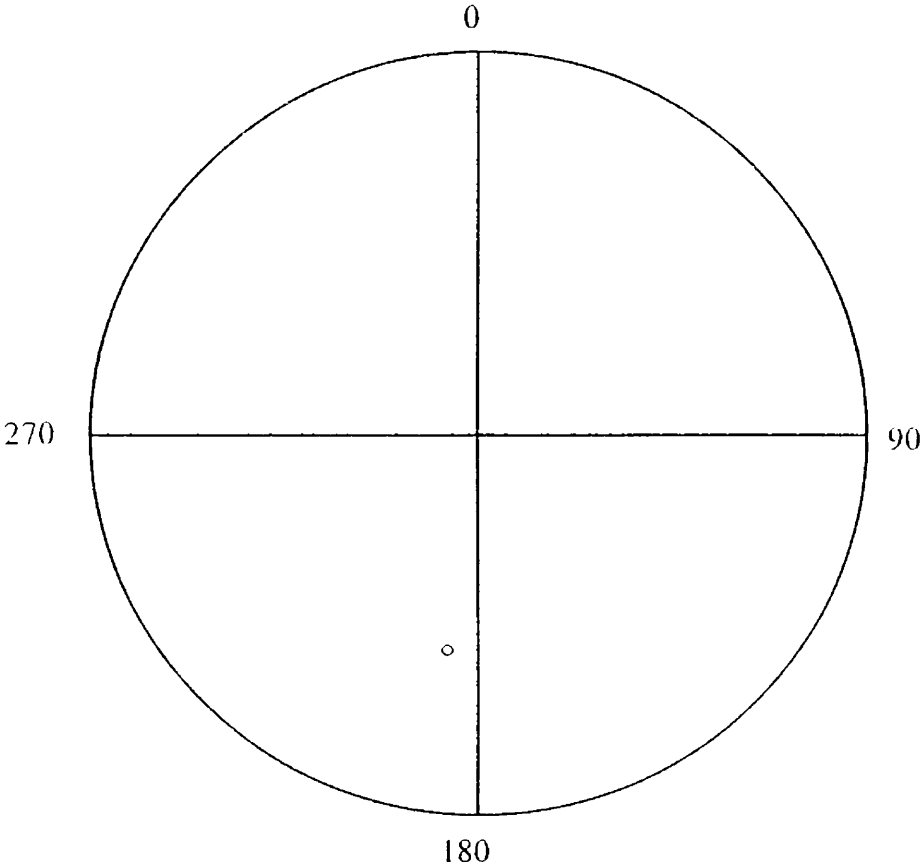Dec.   188.5
Inc.   -42.5
VGP   -66.0/-132.1

9-D7-99
NRM
equal-area

0

270

90

180

9-D7-99
geographic coordinates
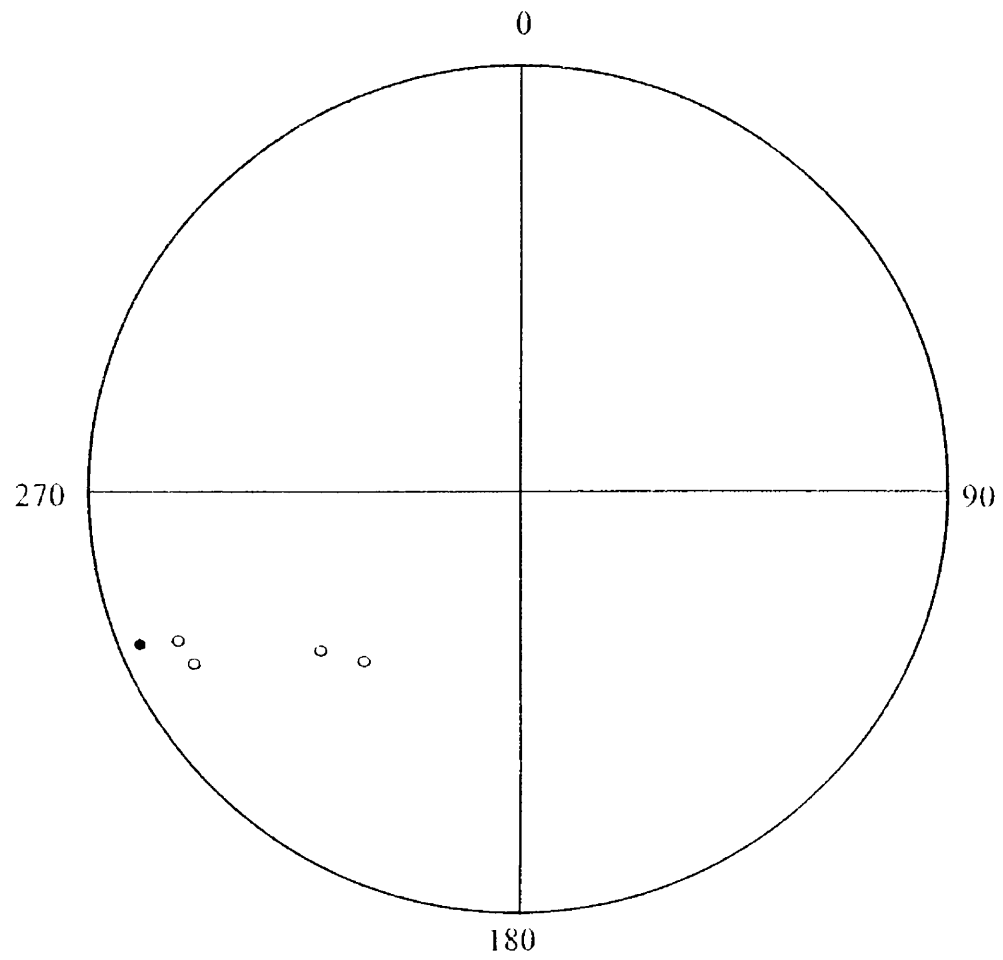equal-area

9-D7-99
stratigraphic coordinates
equal-area

Lith: Trachyandesite Sill   Samples: 5/6

Specimens	J_o	NRM		J_o	ChRM Stratigraphic	
		Dec.	Inc.		Dec.	Inc.
10A	1.68E-05	248.1	4.6	1.38E-05	249.7	-45.7
10B	7.30E-06	231.4	-39.9	6.62E-06	173.9	-59.0
10C	2.73E-04	222.2	-45.2	2.10E-04	156.2	-51.9
10D	2.38E-05	242.4	-14.9	1.97E-05	206.7	-54.8
10E	2.29E-04	245.8	-14.0	1.90E-04	190.6	-64.1
10F	-	-	-	-	-	-

R   4.1735
k   13.9632
α_{95} 21.21
s_{63} 21.75
Dec.   197.0
Inc.   -59.9
VGP   -76/-179.3

10-E4-99
NRM
equal-area

61

10-E4-99
geographic coordinates
equal-area

10-E4-99
stratigraphic coordinates
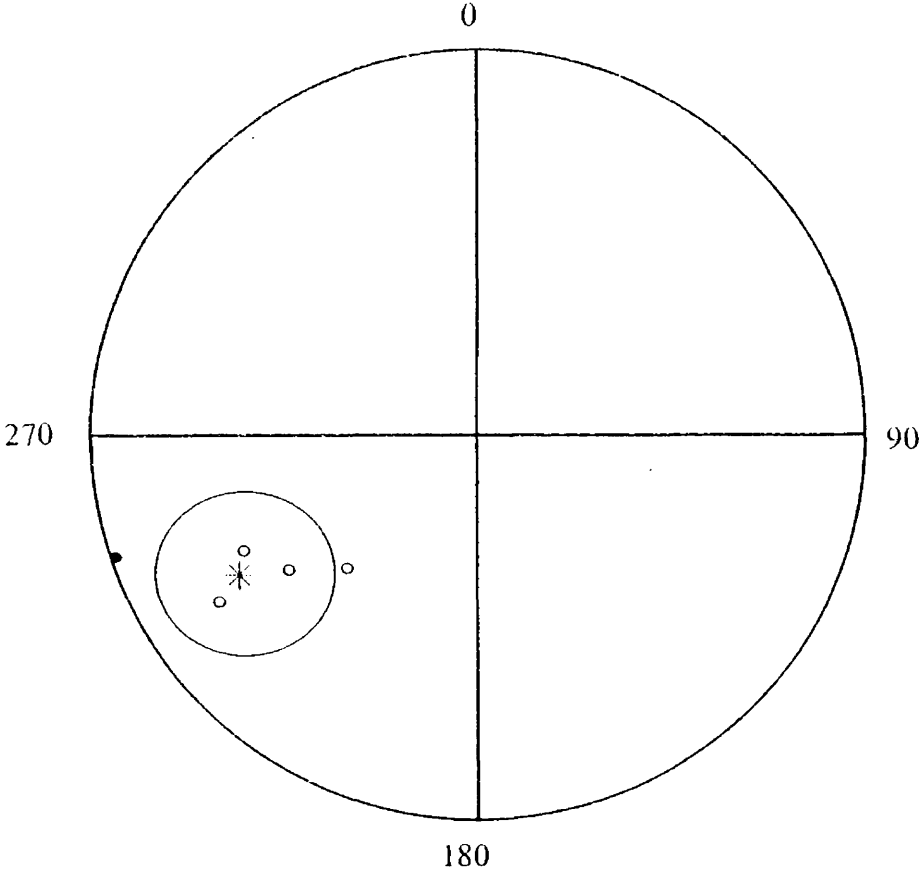equal-area

Lith: Trachyandesite Sill   Samples: 1/2

| Specimens | J_o | NRM | | ChRM Stratigraphic | | |
		Dec.	Inc.	J_o	Dec.	Inc.
11A	-	-	-	-	-	-
11B	1.29E-05	261.5	-8.5	7.65E-06	173.5	-66.0

R   1.00
k   -
α_{95} -
s_{63} -
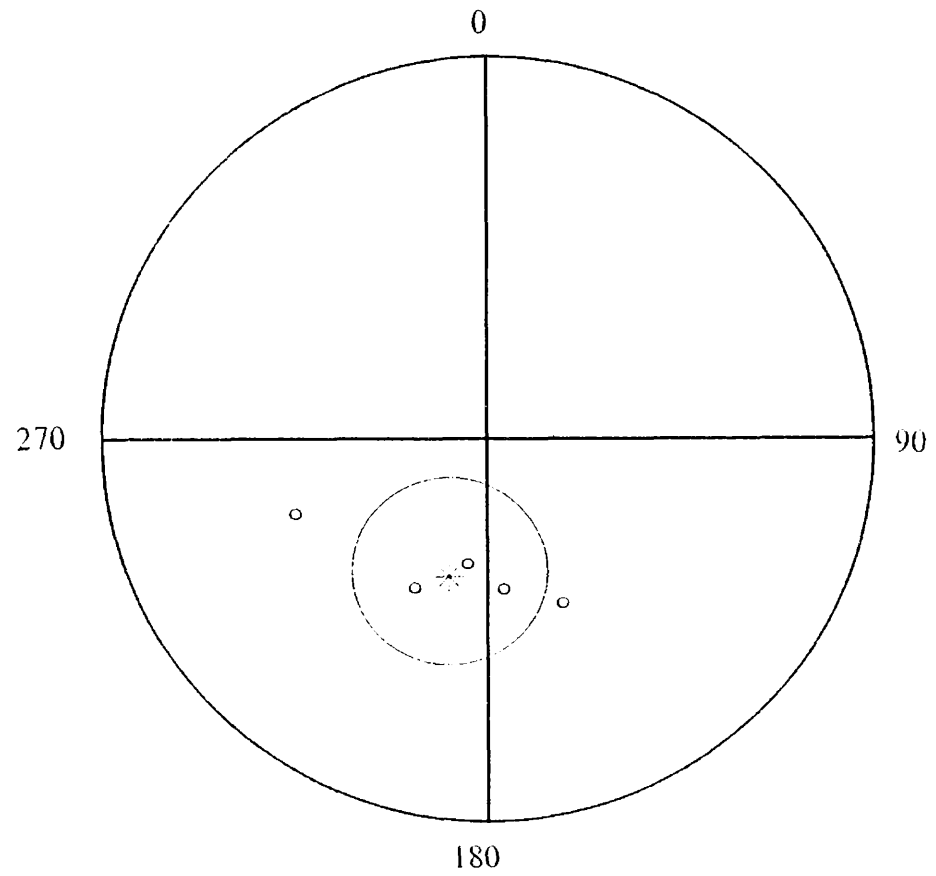Dec.   173.5
Inc.   -12.1
VGP   -85.6/-012.1

11-E4-99
NRM
equal-area

65

11-E4-99
geographic coordinates
equal-area

11-E4-99
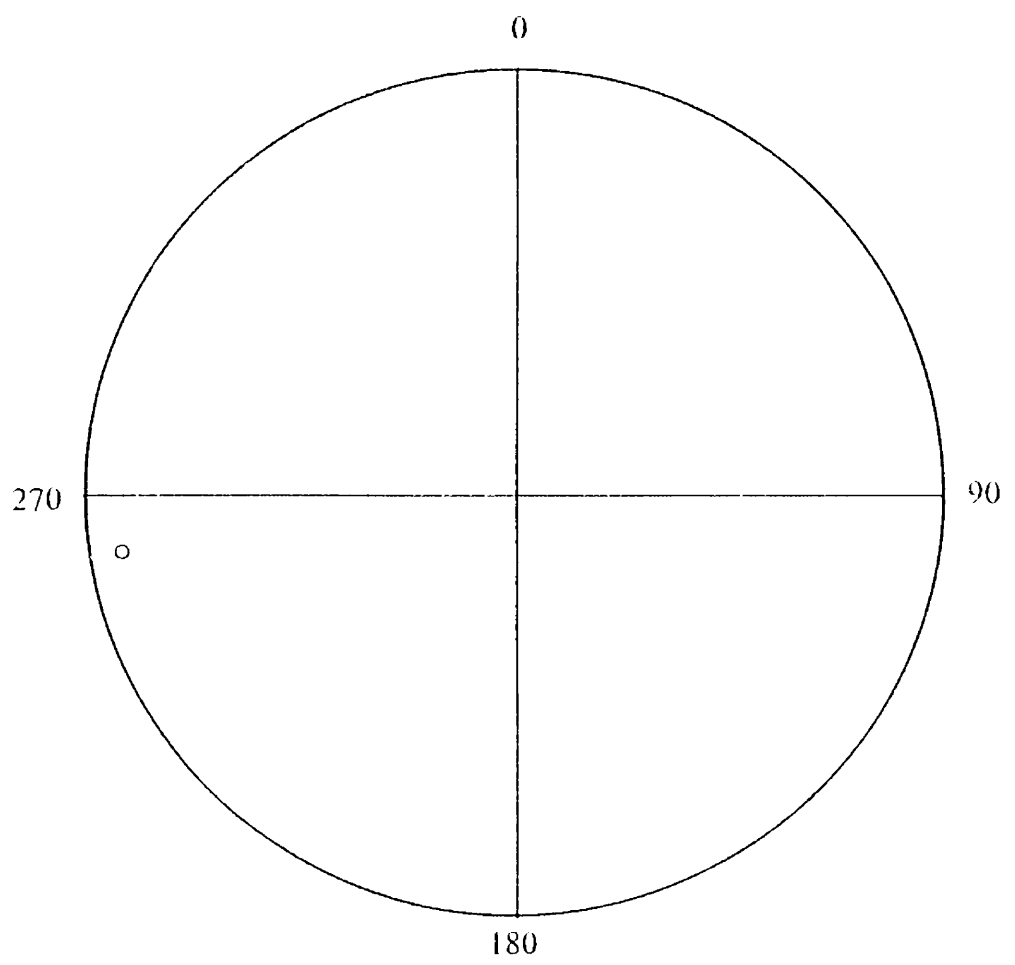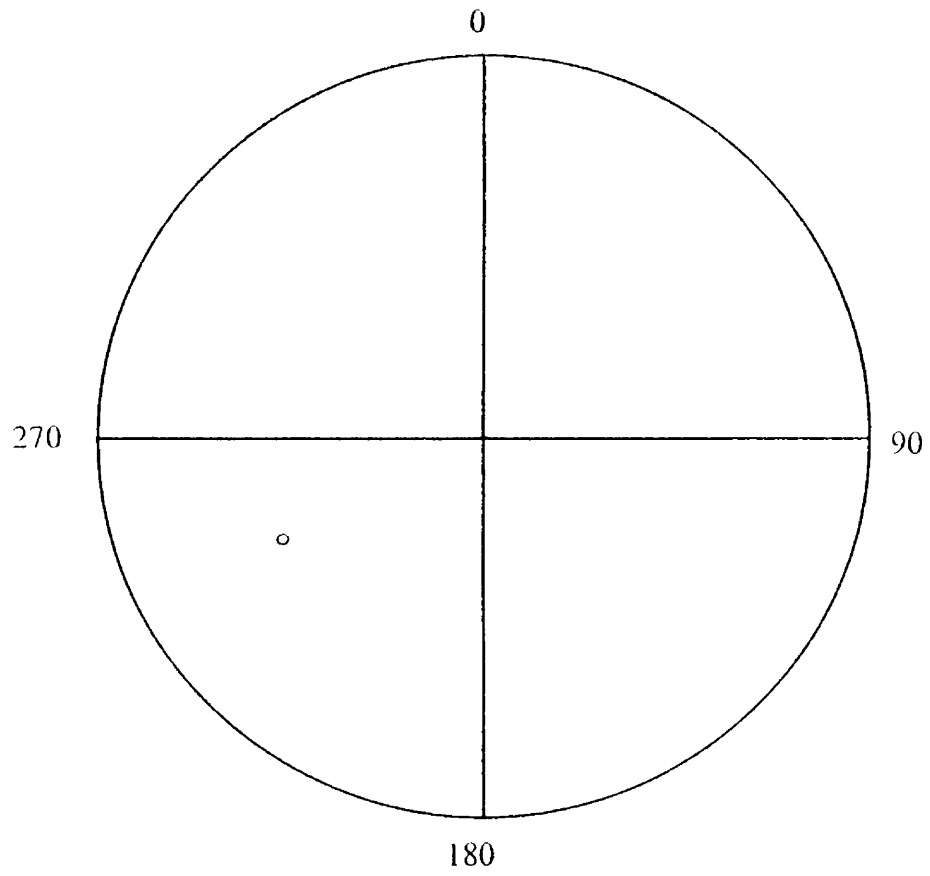stratigraphic coordinates
equal-area

Site: 12-E3-99
Lith: Trachyandesite Sill   Samples: 4/5

Specimens	J_0	NRM Dec.	Inc.	ChRM Stratigraphic J_0	Dec.	Inc.
12A	-	-	-	-	-	-
12B	6.49E-04	176.7	-62.8	3.17E-04	304.8	34.5
12C	2.41E-03	007.2	24.2	2.43E-03	351.4	21.5
12D	3.75E-05	315.7	-11.6	1.48E-05	001.3	-28.2
12E	7.06E-04	159.2	39.7	2.89E-04	266.2	53.0

R   2.9179
k   2.7725
α_{95} 68.64
s_{63} 49.93
Dec.   328.0
Inc.   25.6
VGP   46.6/115.9

12-E3-99
NRM
equal-area

0

270

90

180

69

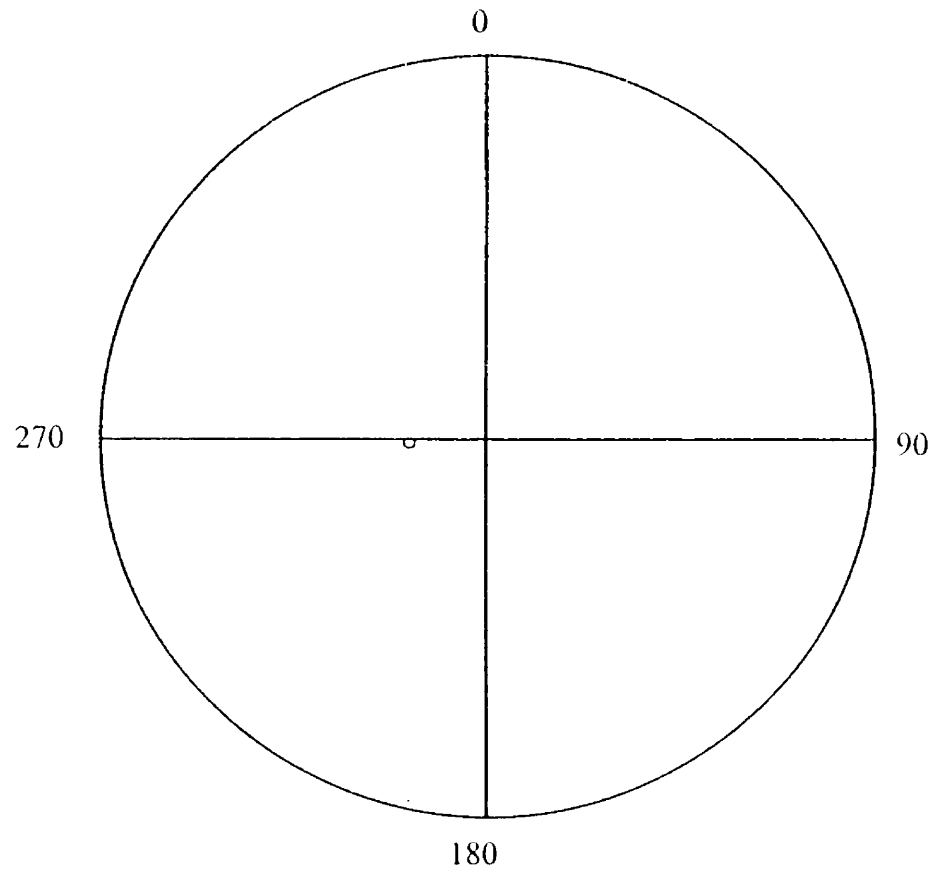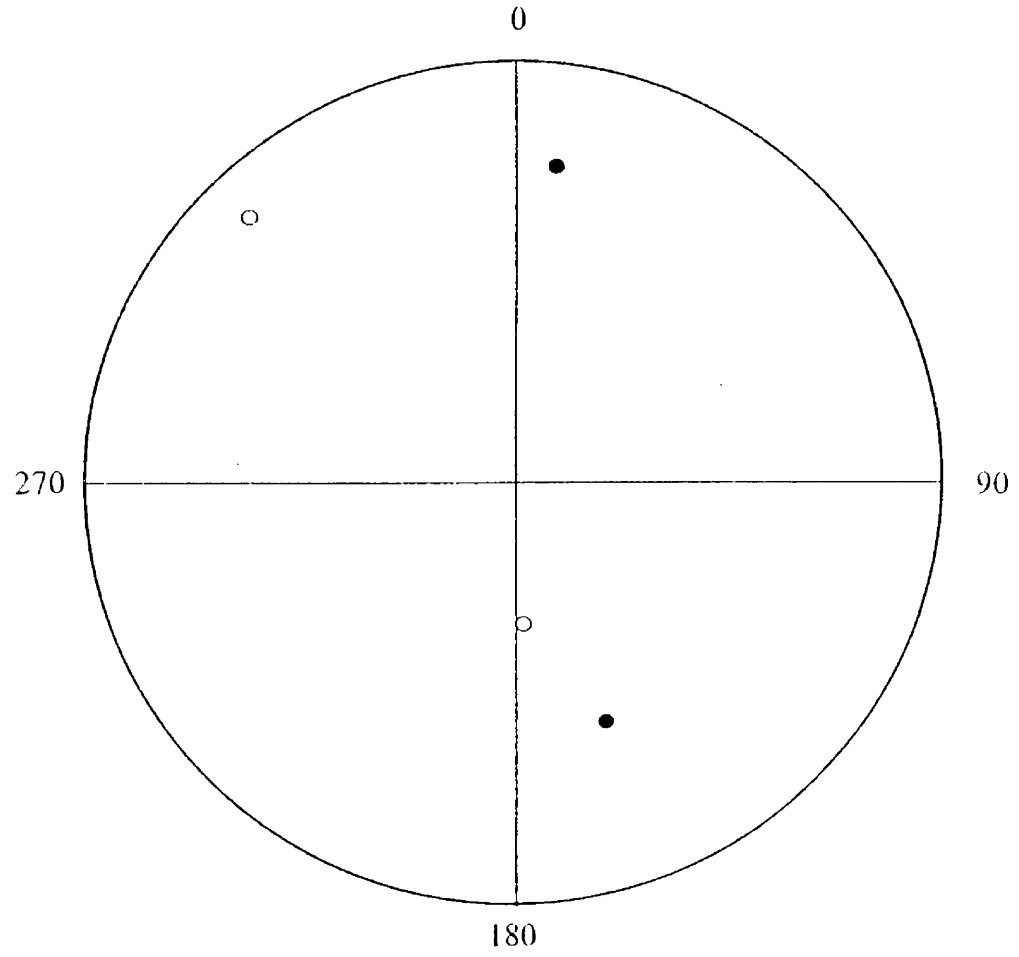12-E3-99
geographic coordinates
equal-area

0

270

90

180

70

12-E3-99
stratigraphic coordinates
equal-area

71

Site: 13-E6-99

Lith: Trachyandesite Sill   Samples: 5/6

Specimens	J_o	NRM			ChRM Stratigraphic		
		Dec.	Inc.	J_o		Dec.	Inc.
13A	4.60E-06	258.2	-23.0	2.36E-06		141.2	-83.1
13B	5.04E-06	245.3	-40.3	4.86E-06		152.8	-77.5
13C	3.84E-06	254.2	-22.7	1.32E-06		026.6	-89.4
13D	2.64E-06	244.4	-14.5	1.03E-06		169.9	-69.4
13E	-	-	-	-		-	-
13F	2.70E-06	257.1	-30.2	1.57E-06		247.5	-80.3

R	4.9396
k	66.2205
α_{95}	9.47
S_{63}	9.94
Dec.	173.0
Inc.	-81.9
VGP	-63.3/062.9

13-E6-99
NRM
equal-area
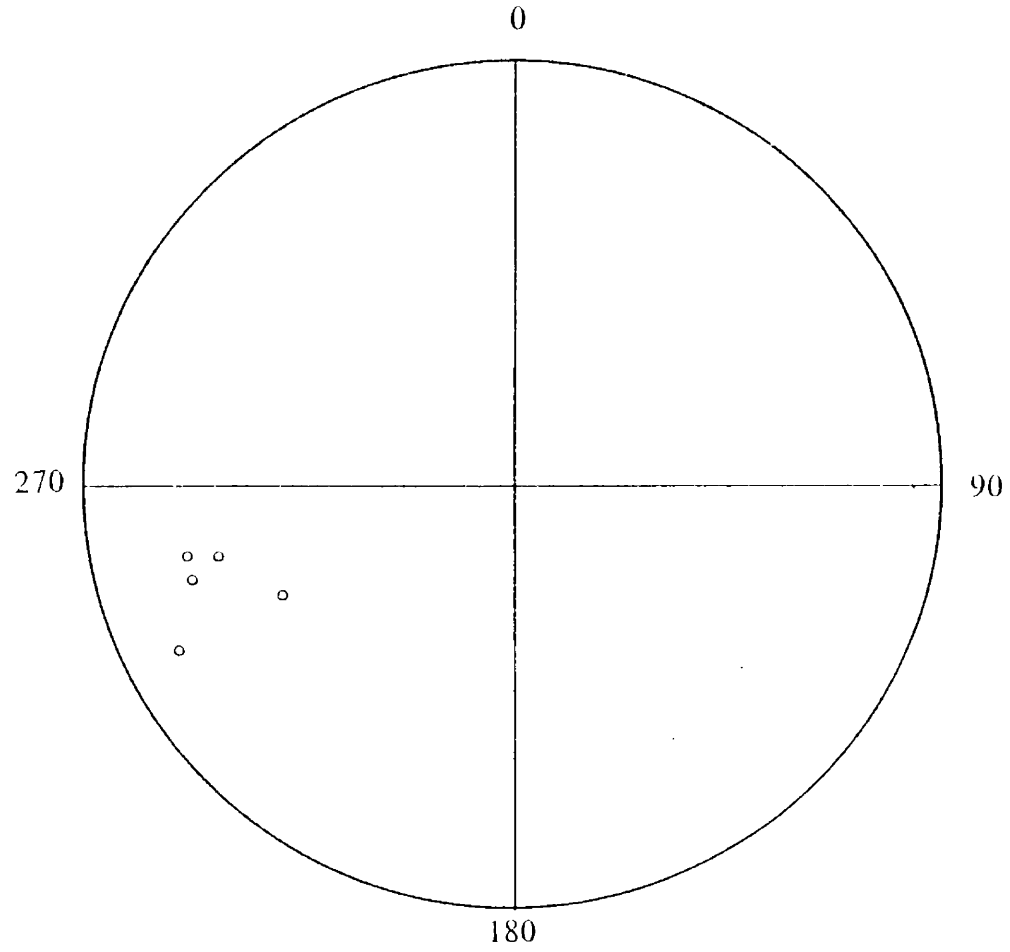
13-E6-99
geographic coordinates
equal-area

74

13-E6-99
stratigraphic coordinates
equal-area
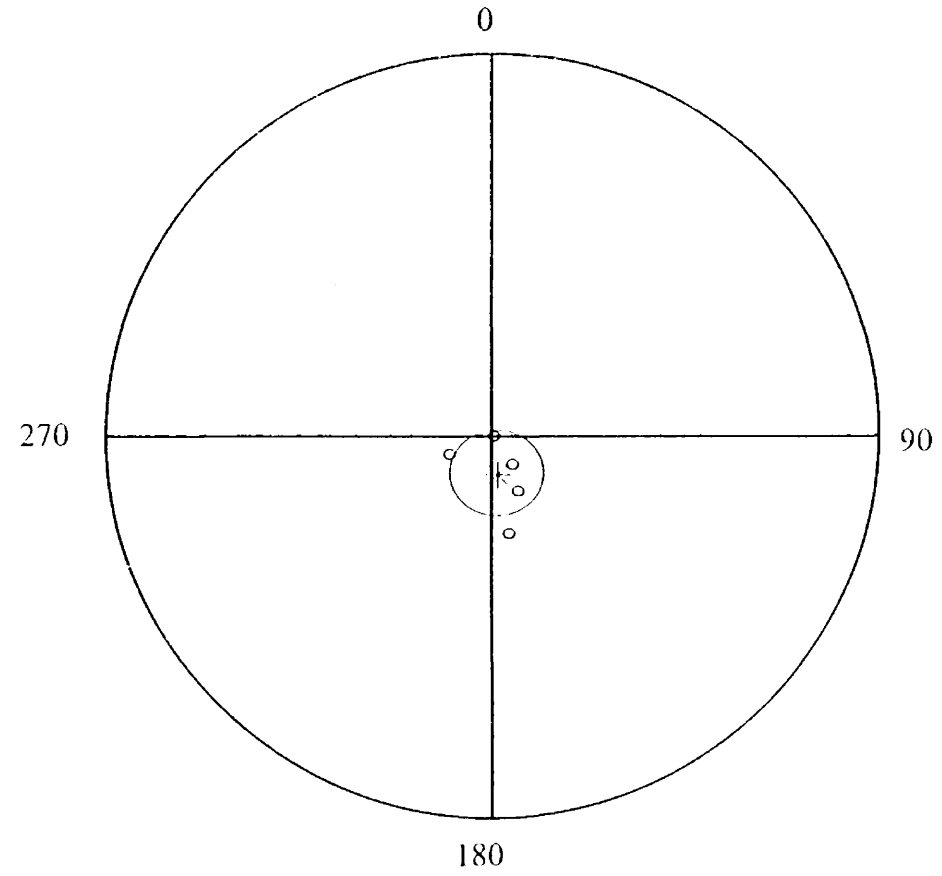
Site: 14-D6-99
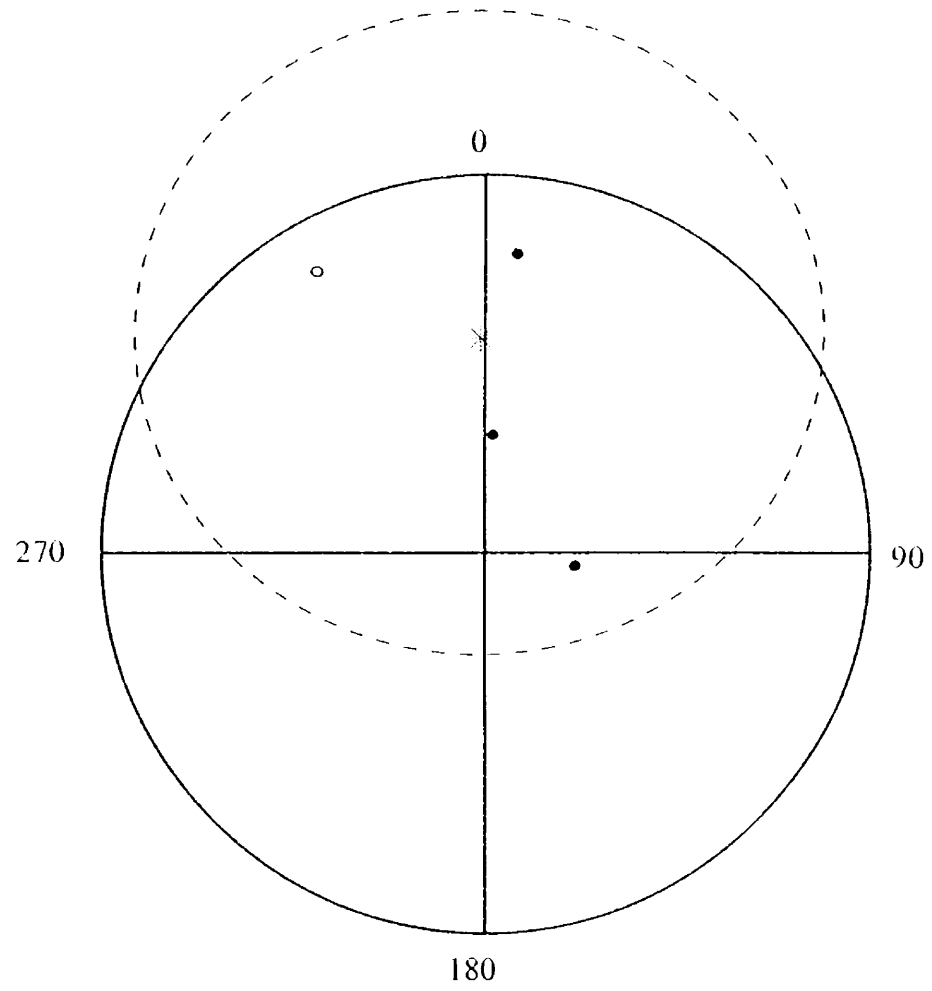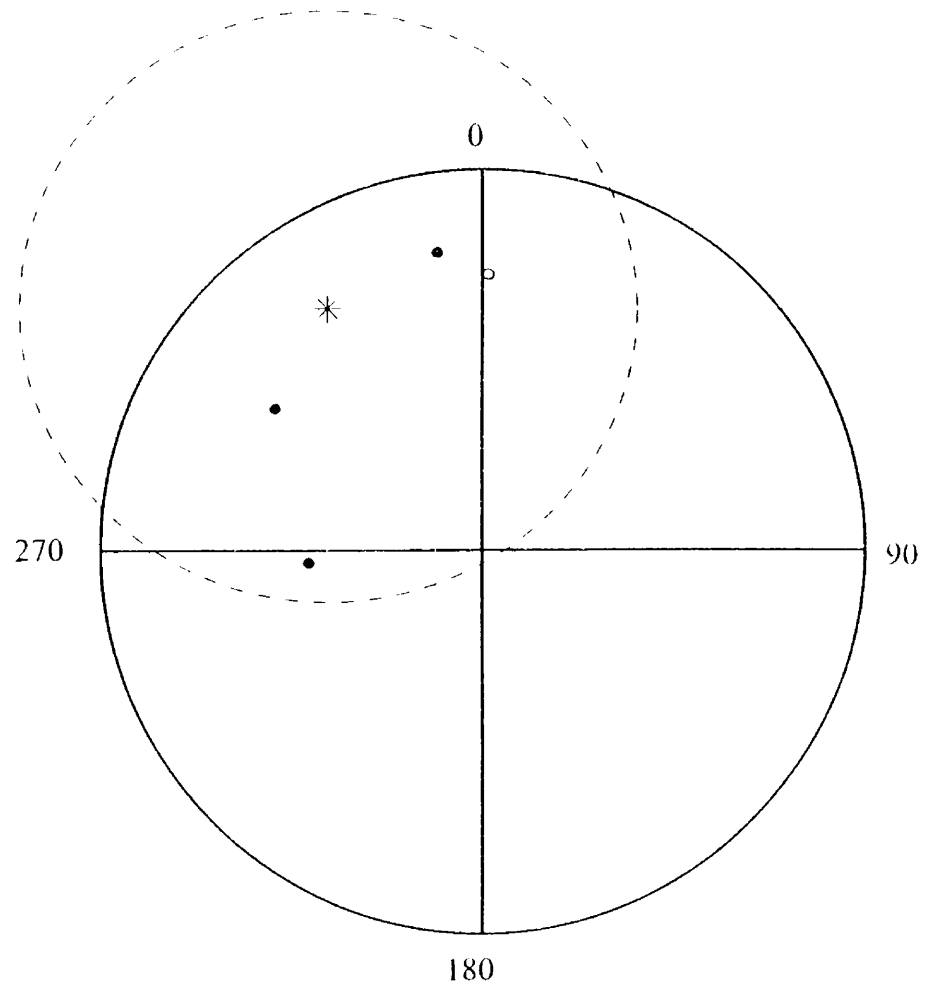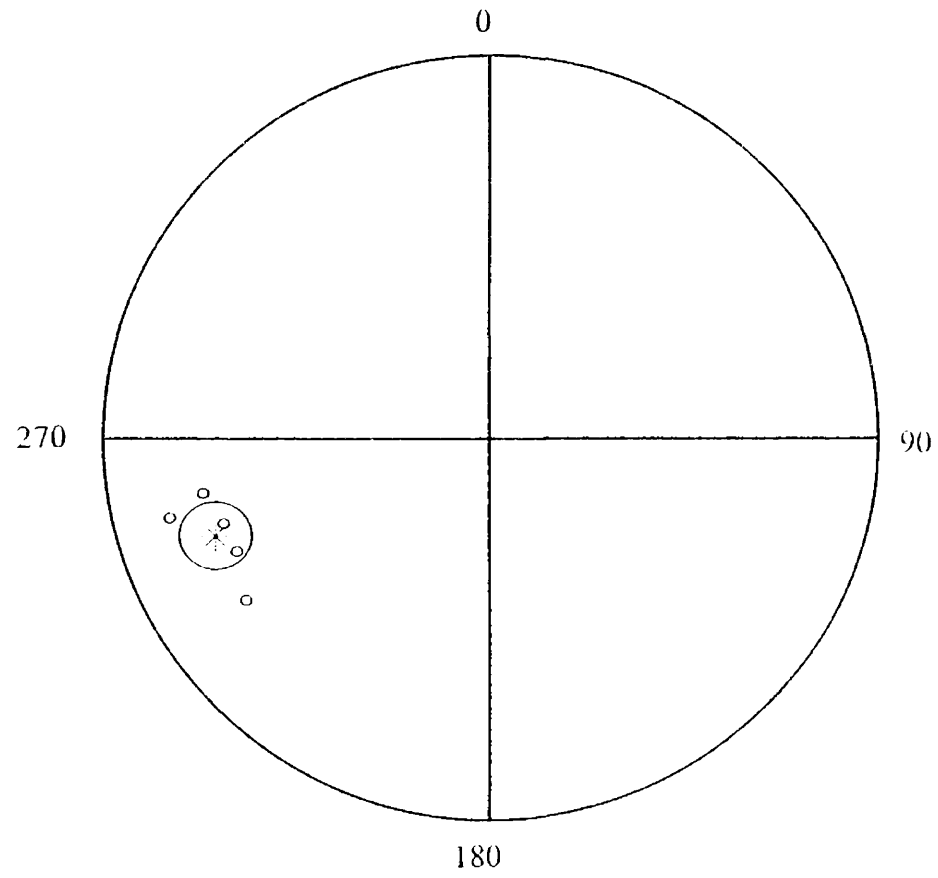Lith: Trachyandesite Sill   Samples: 5/5

Specimens	J_0	NRM Dec.	Inc.	ChRM Stratigraphic J_0	Dec.	Inc.
14A	2.87E-05	100.7	-45.2	2.44E-05	228.4	-46.0
14B	2.33E-05	239.3	-28.7	2.34E-05	254.9	-38.8
14C	2.06E-05	080.3	-60.0	2.02E-05	238.3	-44.8
14D	1.82E-05	082.2	-83.7	4.03E-06	240.3	-22.6
14E	1.29E-05	212.1	-62.1	9.65E-06	228.6	-19.2

R   4.8573
k   28.023
α_{95} 14.71
s_{63} 15.31
Dec.   238.0
Inc.   -34.7
VGP   -35.4/167.8

14-D6-99
NRM
equal-area

0

270

90

180

77
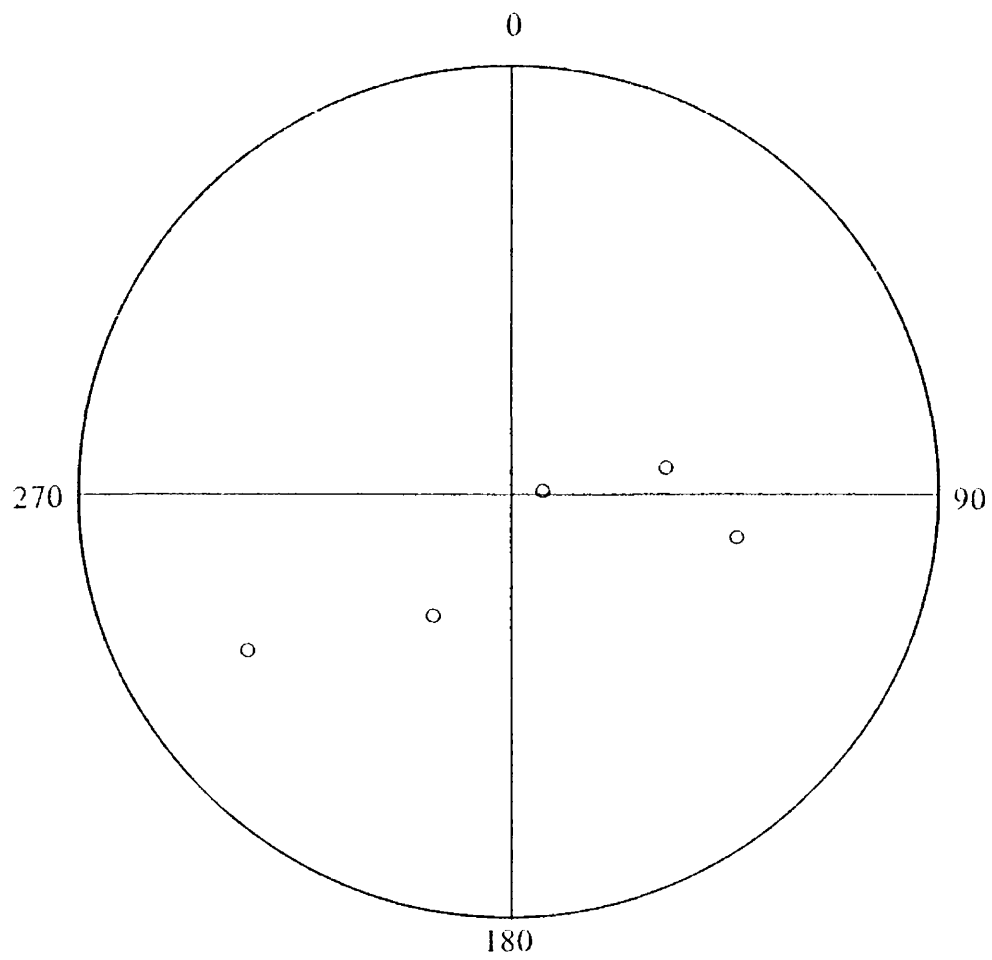
14-D6-99
geographic coordinates
equal-area

78
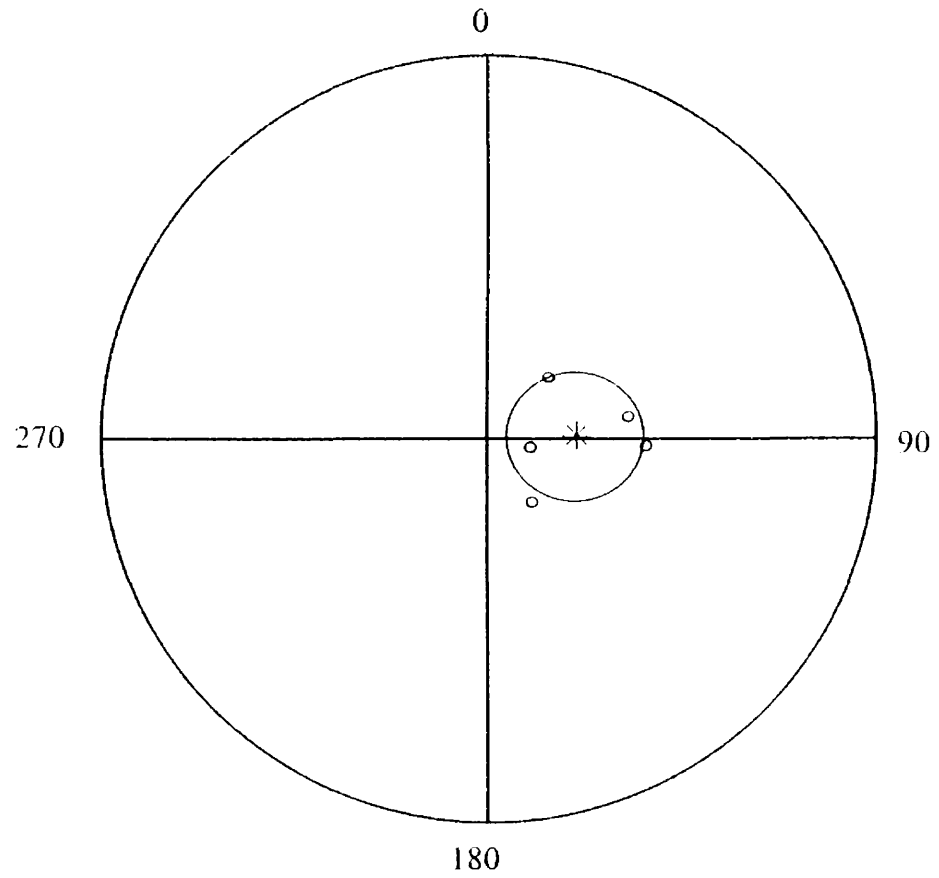
14-D6-99
stratigraphic coordinates
equal-area
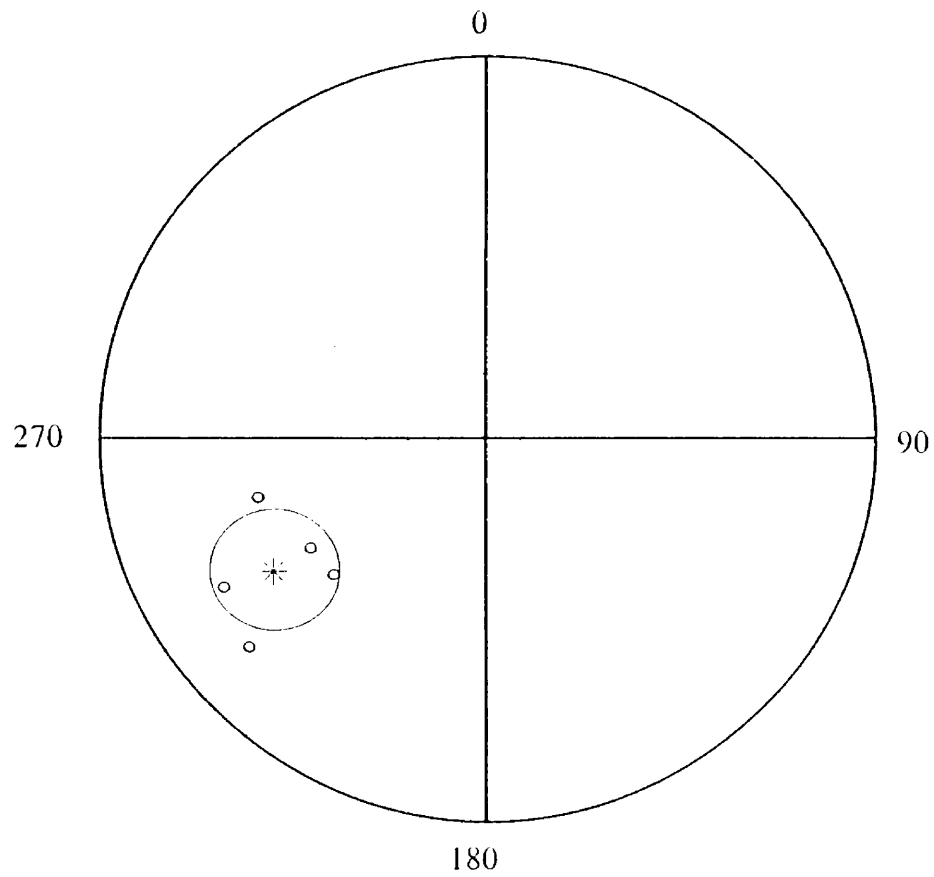
Site: 16-D10-99
Lith: Trachyandesite Sill   Samples: 2/6

Specimens	J_o	NRM			ChRM Stratigraphic		
		Dec.	Inc.	J_o		Dec.	Inc.
16A	-	-	-	-		-	-
16B	-	-	-	-		-	-
16C	8.56E-06	240.9	-8.6	8.17E-06		240.0	-43.0
16D	2.74E-06	006.7	24.9	8.01E-07		342.4	0.8
16E	-	-	-	-		-	-
16F	-	-	-	-		-	-

R   1.2911
k   1.4106
α_{95} 180.0
S_{63} 68.68
Dec.   302.1
Inc.   -31.2
VGP   7.4/122.0

16-D10-99
NRM
equal-area

0

270

90

180

81
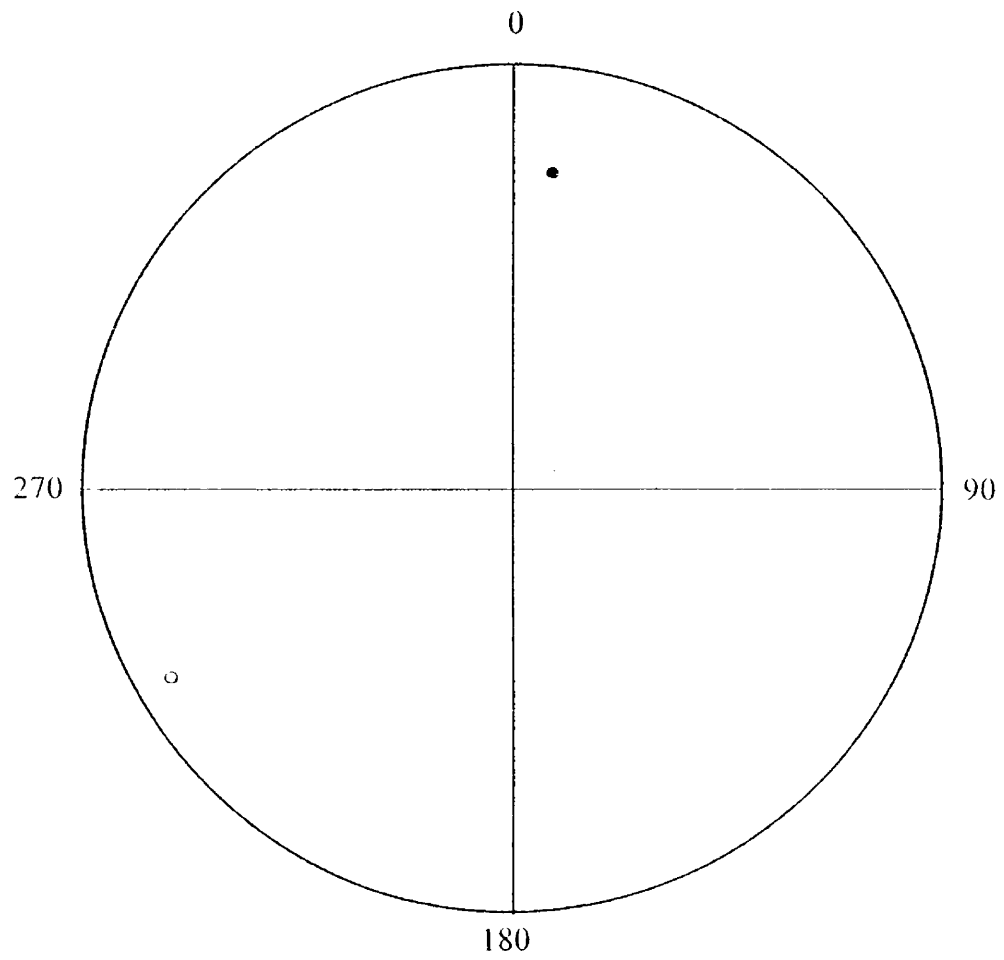
16-D10-99
geographic coordinates
equal-area

16-D10-99
stratigraphic coordinates
equal-area
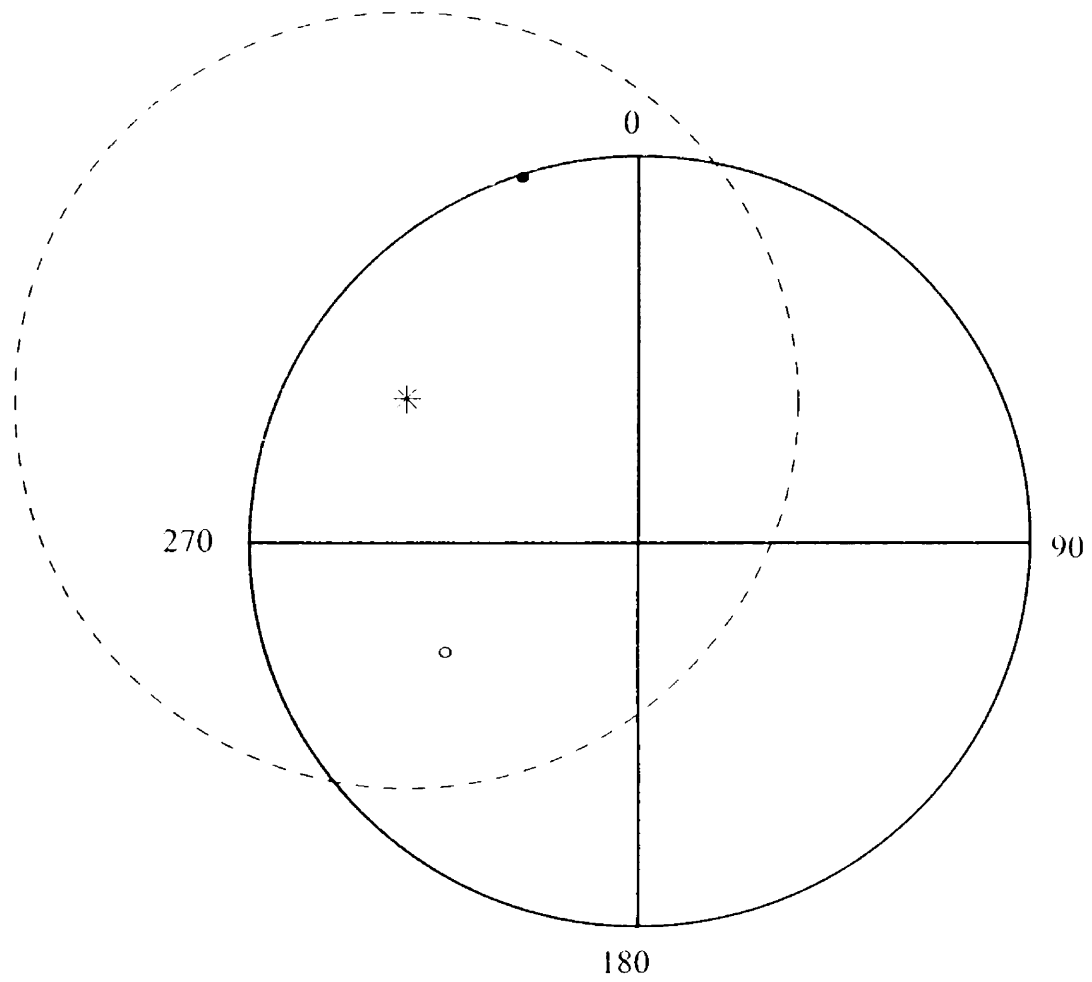
Lith: Trachyandesite Sill   Samples: 4/6

Specimens	J_o	NRM Dec.	Inc.	ChRM Stratigraphic J_o	Dec.	Inc.
17A	-	-	-	-	-	-
17B	6.29E-04	217.5	-40.3	6.54E-04	141.9	-59.2
17C	5.11E-04	001.1	41.0	7.98E-05	216.0	-62.0
17D	3.60E-04	173.3	38.1	2.06E-04	133.3	-49.7
17E	-	-	-	-	-	-
17F	1.09E-03	139.9	-16.8	1.15E-04	208.7	-72.1

R   3.7835
k   13.8560
α_{95} 25.59
s_{63} 21.84
Dec.   166.4
Inc.   -66.0
VGP   -80.9/-013.9

17-E6-99
NRM
equal-area
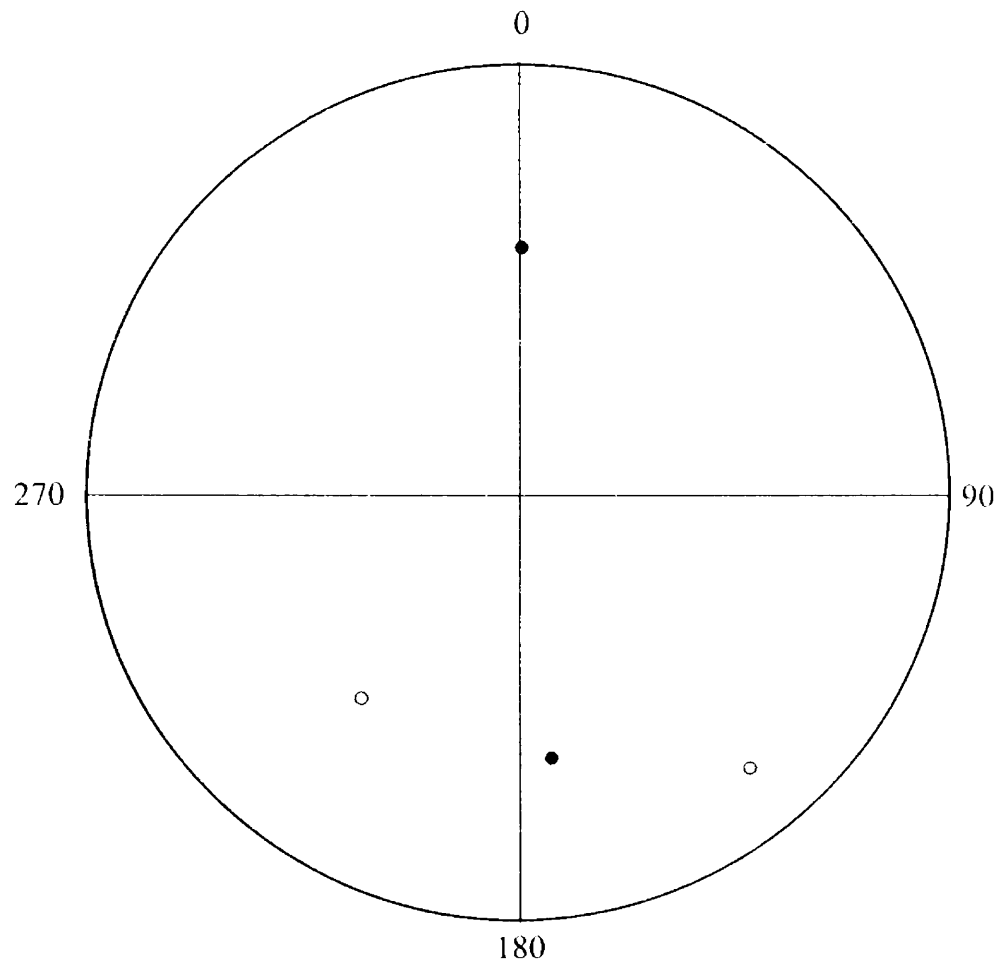
17-E6-99
geographic coordinates
equal-area
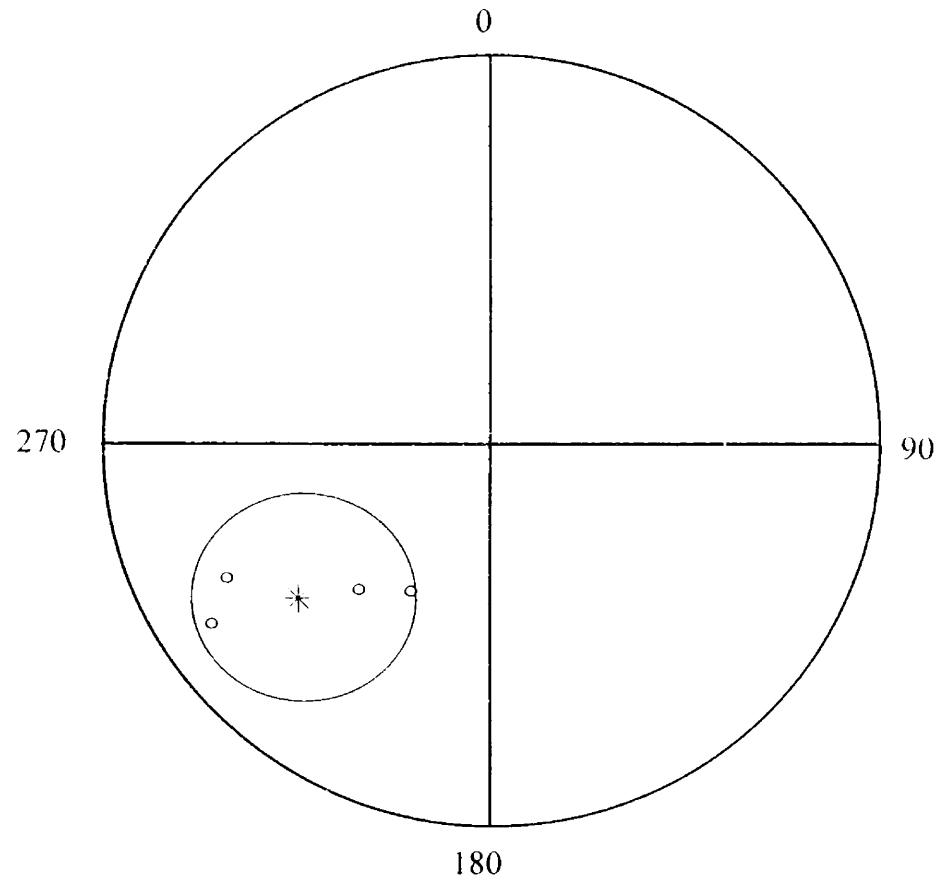
17-E6-99
stratigraphic coordinates
equal-area
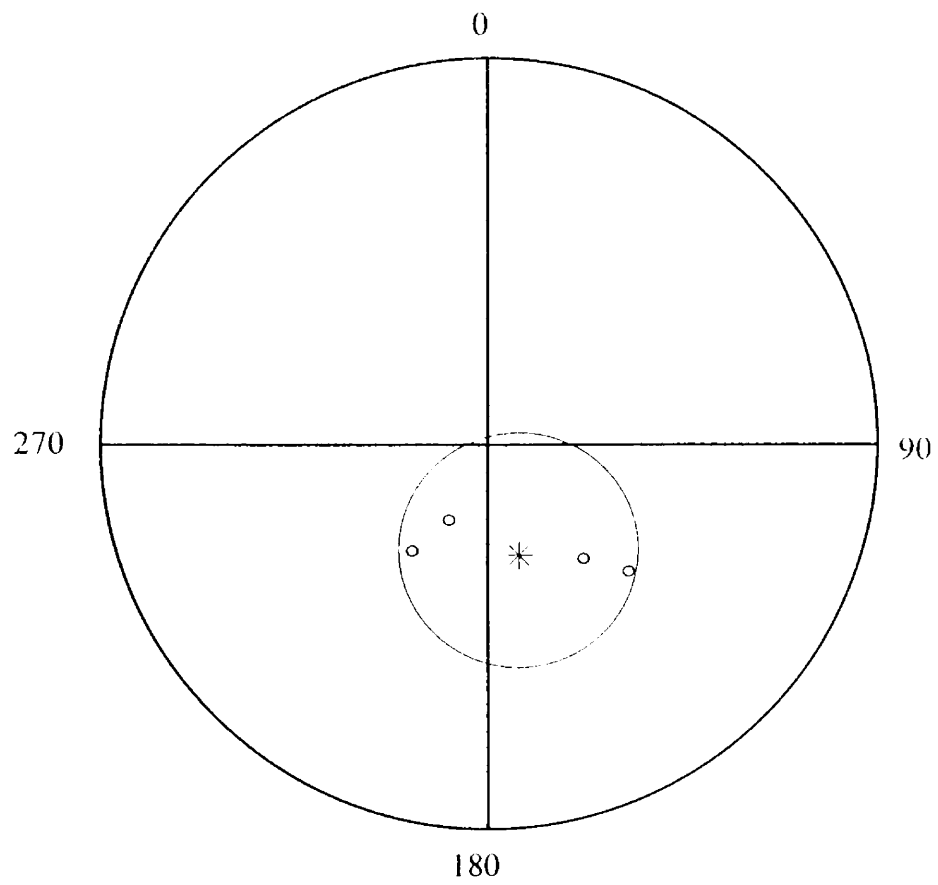
Site: 18-F7-99
Lith: Trachyandesite Sill   Samples: 0/2

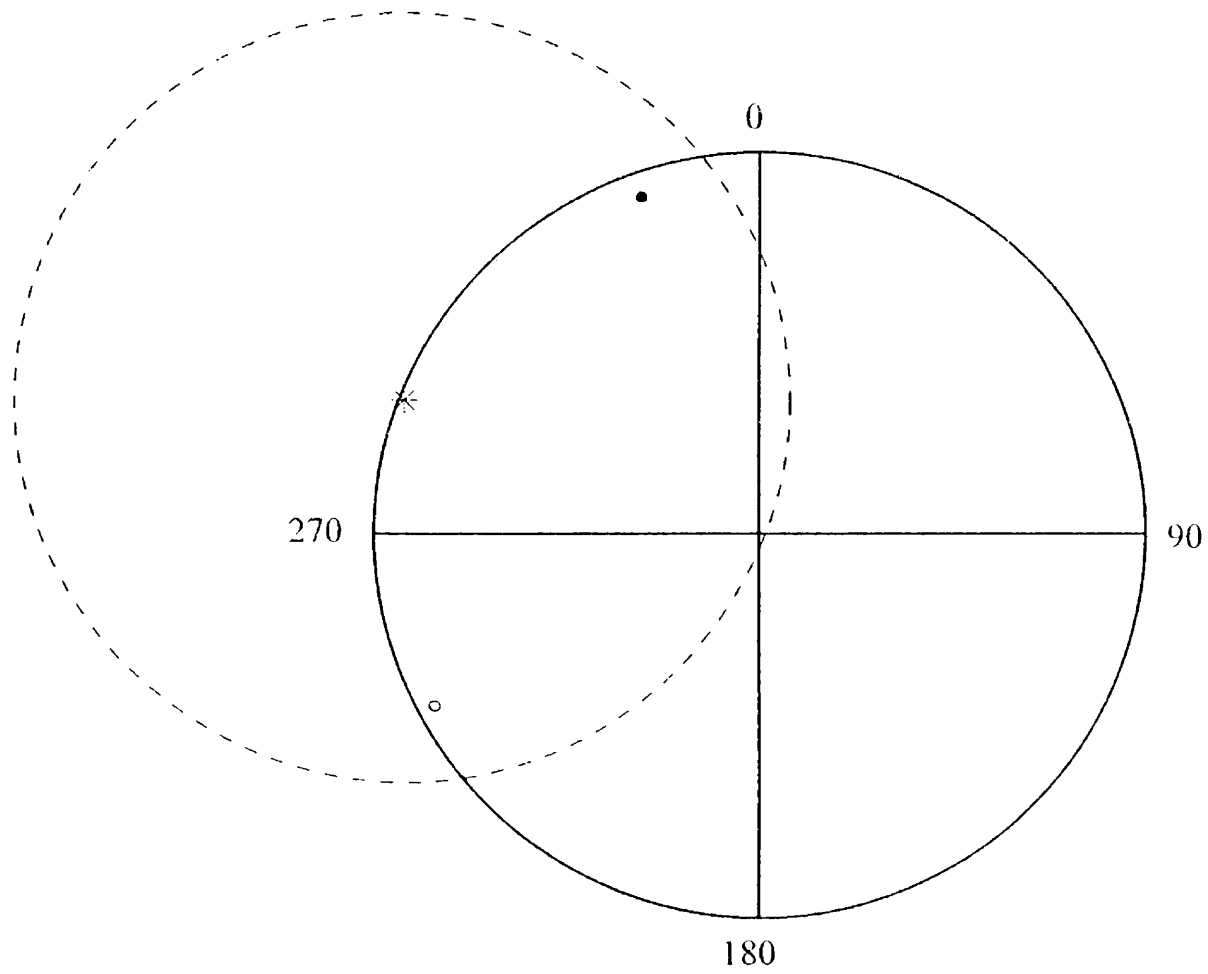| Specimens	J_o	NRM Dec.	Inc.	ChRM Stratigraphic J_o	Dec.	Inc.
18A	-	-	-	-	-	-
18B	-	-	-	-	-	-

R   -
k   -
α_{95} -
S_{63} -
Dec.   -
Inc.   -
VGP   -

Site: 19-D7-00
Lith: Trachyandesite Sill   Samples: 4/4

| Specimens | J_0 | NRM | | ChRM Stratigraphic | | |
		Dec.	Inc.	J_0	Dec.	Inc.
19A	2.08E-04	304.7	-41.3	1.82E-04	198.5	-40.1
19B	1.84E-04	050.2	5.6	6.45E-05	199.3	-36.9
19C	2.48E-04	143.3	24.7	1.29E-04	230.8	-42.2
19D	5.18E-04	319.7	-58.1	4.73E-04	214.6	-45.3

R   3.9346
k   45.8499
α_{95} 13.71
S_{63} 11.95
Dec.   210.4
Inc.   -41.9
VGP   -56.4/-169.2

19-D7-00
NRM
equal-area
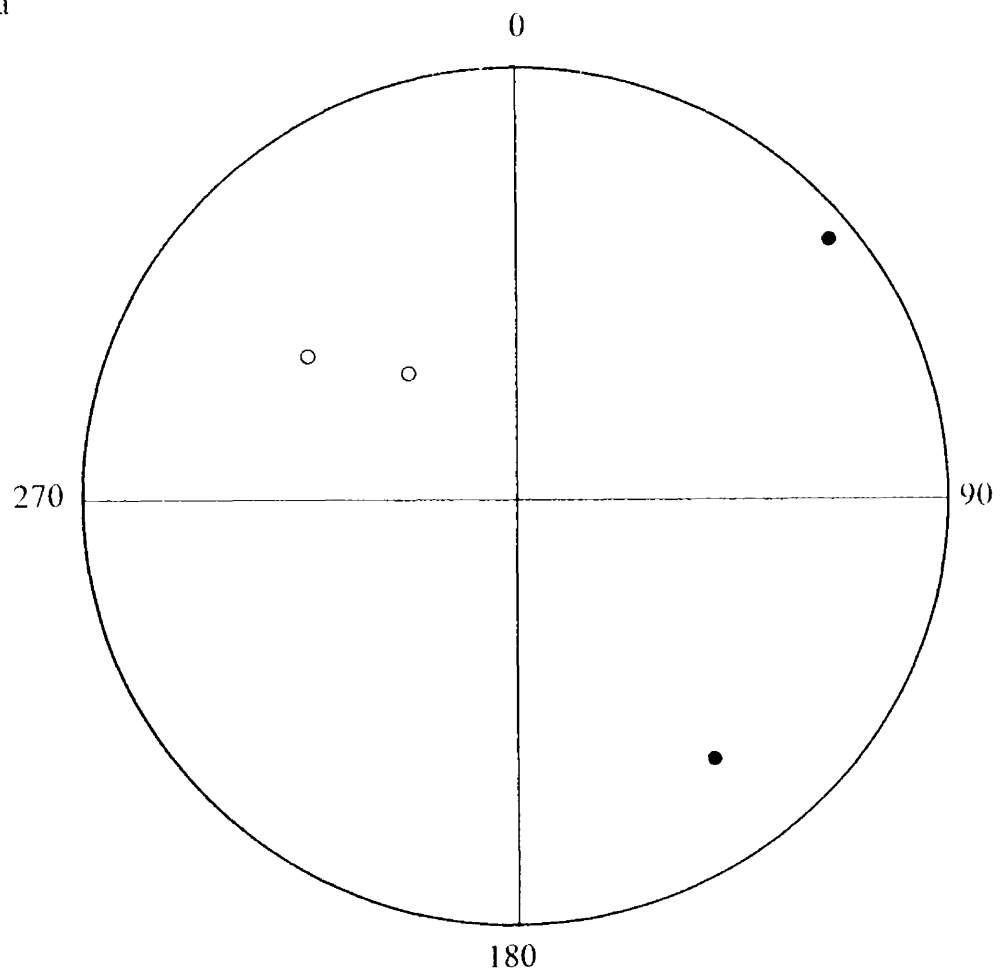
19-D7-00
geographic coordinates
equal-area

0

270

90

180
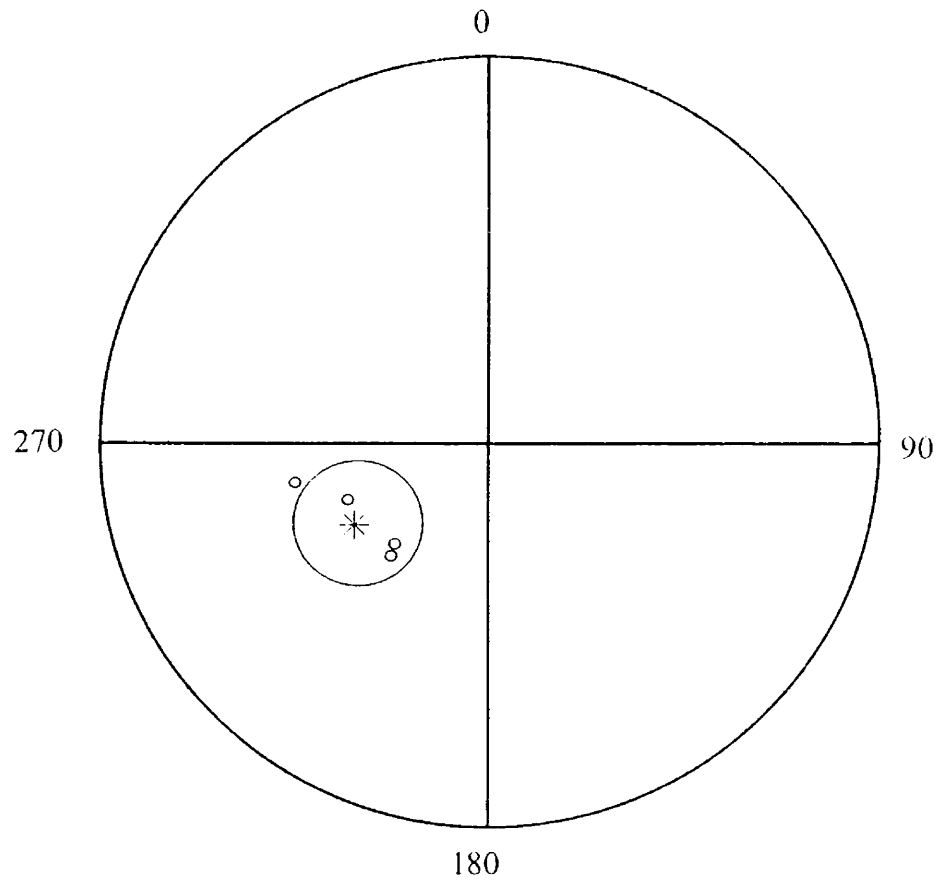
19-D7-00
stratigraphic coordinates
equal-area
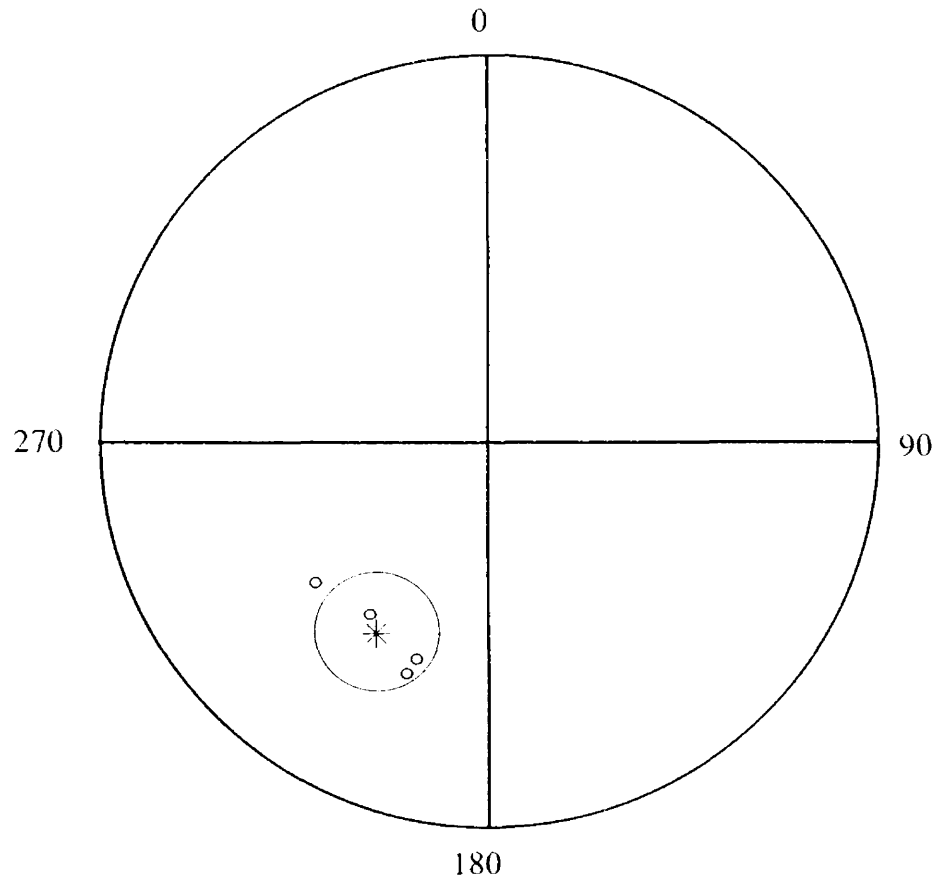
Site: 20-E7-00
Lith: Trachyandesite Sill   Samples: 4/4

| Specimens | J_o | NRM | | ChRM Stratigraphic | | |
		Dec.	Inc.	J_o	Dec.	Inc.
20A	7.86E-04	064.2	-29.8	6.48E-04	170.4	-69.9
20B	4.47E-04	107.1	-27.1	4.09E-04	148.3	-46.2
20C	1.18E-03	087.5	-21.2	5.96E-04	158.3	-68.1
20D	8.91E-04	-98.4	-70.7	6.30E-04	211.2	-52.9

R   3.8383
k   18.5534
α_{95} 21.91
s_{63} 18.84
Dec.   172.2
Inc.   -61.9
VGP   -82.9/-059.7

20-E7-00
NRM
equal-area

20-E7-00
geographic coordinates
equal-area
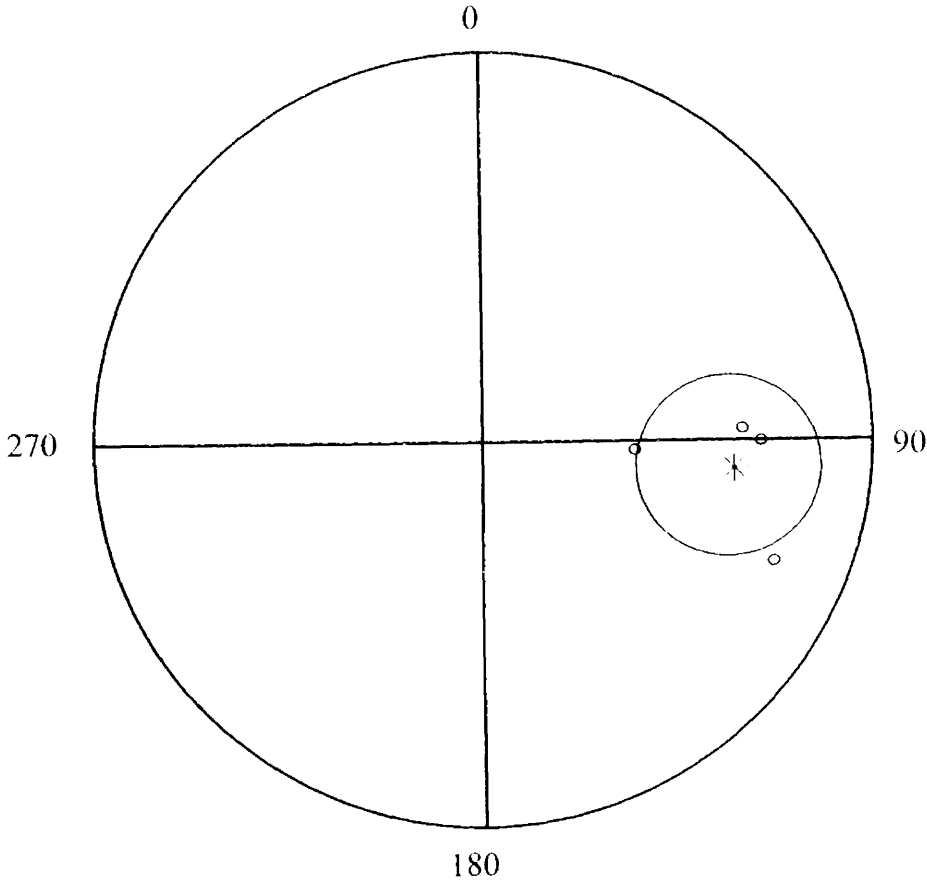
20-E7-00
stratigraphic coordinates
equal-area

SPECIMEN SUMMARY

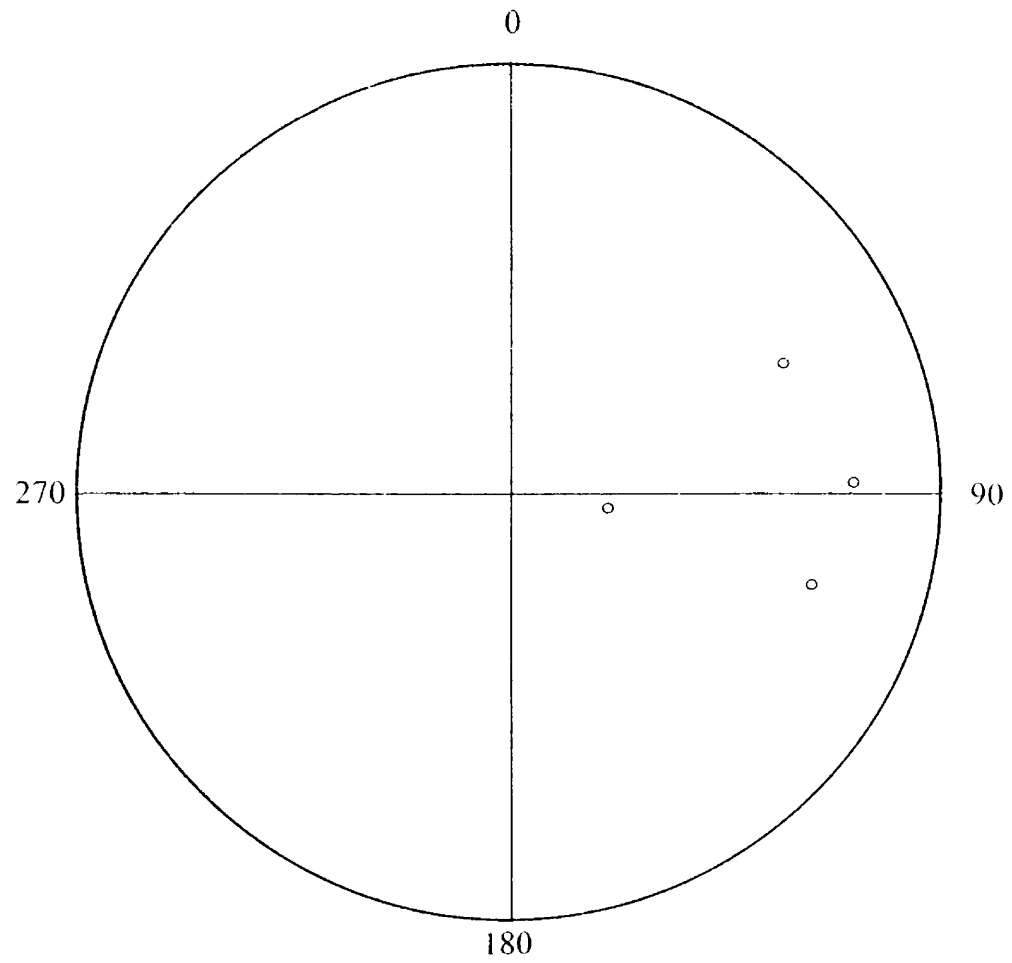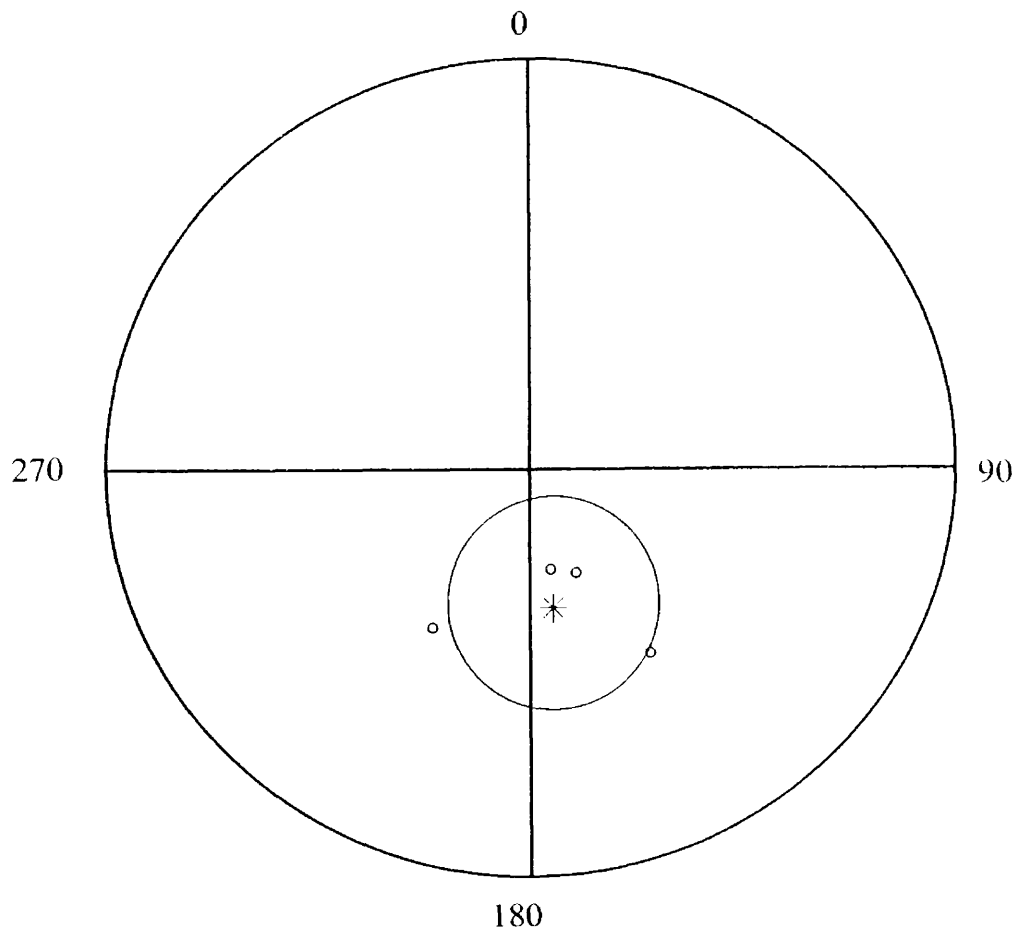| Specimen	NRM		Geographic		Stratigraphic		Unfolding									
							90%		80%		70%		60%		50%	
	Dec	Inc	Dec	Inc	Dec	Inc	Dec	Inc	Dec	Inc	Dec	Inc	Dec	Inc	Dec	Inc
6A	20.4	29.0	229.2	-14.7	181.9	-54.4	191.8	-52.4	200.4	-49.3	207.4	-45.3	213.0	-40.6	217.3	-35.4
6B	261.7	16.9	237.5	-13.3	185.4	-62.4	198.4	-59.7	208.7	-55.8	216.4	-50.8	222.2	-45.2	226.4	-39.2
6D	260.9	0.0	259.1	-5.7	236.6	-79.7	247.2	-72.6	251.5	-65.7	253.8	-57.6	255.2	-50.1	256.0	-42.6
6E	243.3	3.7	237.7	-13.1	185.8	-62.5	198.8	-59.9	209.1	-55.8	216.8	-50.8	222.5	-45.2	226.7	-39.2
7A	257.3	-2.0	240.0	-27.4	212.6	-62.9	216.4	-59.2	219.4	-55.5	221.8	-51.7	223.7	-47.8	225.2	-43.8
7B	247.3	-7.1	242.6	-28.1	214.8	-65.0	218.8	-61.3	221.9	-57.5	224.2	-53.6	226.0	-49.7	227.4	-45.7
8A	218.9	-35.7	226.8	-33.4	189.4	-57.0	194.4	-54.5	198.6	-51.7	202.1	-48.7	205.1	-45.6	207.6	-42.3
8B	233.1	-29.6	238.2	-22.3	217.3	-58.1	220.3	-54.3	222.5	-50.5	224.2	-46.6	225.6	-42.6	226.8	-38.7
9A	175.0	-4.5	224.1	-45.5	188.5	-42.5	191.9	-42.0	195.1	-41.3	198.2	-40.3	201.1	-39.2	203.9	-37.9
10A	248.1	4.6	251.5	1.9	249.7	-45.7	250.3	-41.0	250.8	-36.3	251.2	-31.5	251.5	-26.7	251.7	-22.0
10B	231.4	-39.9	234.3	-40.7	173.9	-59.0	181.6	-58.2	188.8	-56.8	195.3	-54.8	200.9	-52.4	205.8	-49.6
10C	222.2	-45.2	223.5	-50.4	156.2	-51.9	162.4	-52.6	168.7	-52.8	174.9	-52.5	181.0	-51.6	186.7	-50.3
10D	242.4	-14.9	236.8	-22.6	206.7	-54.8	211.6	-51.7	215.6	-48.2	218.9	-44.6	221.6	-40.8	223.8	-36.9
10E	245.8	-14.0	242.5	-33.9	190.6	-64.1	199.0	-61.9	206.1	-59.2	211.8	-56.1	216.4	-52.6	220.2	-48.9
11B	261.5	-8.5	243.6	-41.3	173.5	-66.0	183.7	-65.1	193.1	-63.5	201.1	-61.1	207.7	-58.3	213.1	-55.0
12B	176.7	-62.8	1.4	64.4	304.8	34.5	307.9	37.3	311.5	39.9	308.4	36.4	305.9	32.7	303.8	28.9
12C	7.2	24.2	5.7	21.7	351.4	21.5	353.5	20.3	355.3	19.0	353.5	19.2	251.6	19.3	349.8	19.2
12D	315.7	-11.6	329.4	-14.2	1.3	-28.2	358.5	-30.0	355.6	-31.5	358.7	-31.1	1.8	-30.3	4.7	-29.3
12E	159.2	39.7	98.3	71.6	266.2	53.0	268.4	57.8	271.5	62.7	270.1	57.6	269.1	52.4	268.4	47.3
13A	258.2	-23.0	252.7	-28.3	141.2	-83.1	195.5	-82.8	223.5	-78.1	234.3	-72.2	239.6	-66.0	242.6	-59.7
13B	245.3	-40.3	246.0	-28.8	152.8	-77.5	182.2	-77.2	204.7	-74.1	218.3	-69.3	226.4	-63.8	231.5	-58.0
13C	254.2	-22.7	259.7	-25.0	26.6	-89.4	258.4	-83.9	256.7	-77.4	256.1	-70.9	255.8	-64.4	255.7	-57.9
13D	244.4	-14.5	236.4	-24.7	169.9	-69.4	186.2	-67.9	197.3	-64.8	209.1	-60.7	216.2	-55.9	221.4	-50.6
13F	257.1	-30.2	256.2	-15.4	247.5	-80.3	250.5	-73.8	251.8	-67.3	252.4	-60.8	252.9	-54.3	253.1	-47.8
14A	100.7	-45.2	92.2	-56.8	228.4	-46.0	224.4	-52.5	218.6	-58.8	209.8	-64.5	196.3	-69.2	176.8	-72.1
14B	239.3	-28.7	41.4	-72.2	254.9	-38.8	255.0	-38.2	255.1	-45.6	255.3	-53.0	255.6	-60.4	256.1	-67.8
14C	80.3	-60.0	80.6	-60.4	238.3	-44.8	235.8	-51.9	232.2	-58.5	226.3	-65.6	215.9	-71.8	196.3	-76.8
14D	82.2	-83.7	100.9	-81.9	240.3	-22.6	239.4	-29.8	238.2	-37.0	236.3	-44.1	233.7	-51.1	229.8	-57.9
14E	212.1	-62.1	146.1	-74.3	228.6	-19.2	227.2	-25.8	225.3	-32.4	222.7	-38.8	219.0	-45.0	214.0	-50.9
16C	240.9	-8.6	241.7	-5.2	240.0	-43.0	240.1	-39.2	240.2	-35.4	240.2	-31.6	240.3	-27.8	240.4	-24.0
16D	6.7	24.9	340.7	7.2	342.4	0.8	342.3	0.2	342.3	-0.5	342.3	-1.1	342.2	-1.8	342.0	-2.5
17B	217.5	-40.3	222.7	-47.4	141.9	-59.2	151.0	-60.3	160.5	-60.5	169.9	-59.8	178.5	-58.3	186.2	-56.1
17C	1.1	41.0	237.3	-15.2	216.0	-62.0	220.5	-57.4	223.8	-52.6	226.4	-47.6	228.3	-42.5	229.7	-37.4
17D	173.3	38.1	209.2	-54.0	133.3	-49.7	139.6	-51.6	146.4	-53.0	153.6	-53.8	161.0	-53.8	168.3	-53.2
17F	139.9	-16.8	243.0	-24.1	208.7	-72.1	217.2	-67.6	222.7	-62.9	226.5	-57.9	229.2	-52.8	231.2	-47.7
19A	304.7	-41.3	223.1	-61.1	198.5	-40.1	198.8	-39.8	199.2	-39.3	199.5	-39.3	199.9	-39.0	200.2	-38.8
19B	50.2	5.6	221.0	-58.1	199.3	-36.9	199.6	-36.7	200.0	-36.5	200.3	-36.2	200.6	-36.0	200.9	-35.7
19C	143.3	24.7	258.9	-47.7	230.8	-42.2	231.0	-41.7	231.3	-41.2	231.5	-40.8	231.7	-40.4	231.9	-39.9
19D	319.7	-58.1	247.9	-57.9	214.6	-45.3	214.9	-45.0	215.2	-44.6	215.6	-44.2	215.9	-43.9	216.2	-43.5
20A	64.2	-29.8	87.1	-33.7	170.4	-69.9	150.1	-69.7	136.1	-67.6	125.2	-64.4	117.0	-60.5	111.0	-56.0
20B	107.1	-27.1	112.7	-20.8	148.3	-46.2	141.2	-44.1	136.3	-41.6	132.1	-38.7	128.4	-35.5	125.3	-32.0
20C	87.5	-21.2	89.7	-29.6	158.3	-68.1	140.8	-66.6	129.8	-63.8	121.2	-60.1	114.8	-56.0	109.9	-51.4
20D	98.4	-70.7	93.4	-58.3	211.2	-52.9	203.8	-58.4	195.6	-61.8	185.3	-64.4	173.2	-65.9	160.2	-66.2

APPENDIX C.

EFFECTS OF AF DEMAGNETIZATION

Graph 8A

1.80E-05
1.60E-05
1.40E-05
1.20E-05
1.00E-05
8.00E-06
6.00E-06
4.00E-06
2.00E-06
0.00E+00

J (A/m)

8A

0   20   40   60   80   100   120

B(mT)

Graph 8B

2.50E-05
2.00E-05
1.50E-05
1.00E-05
5.00E-06
0.00E+00

J (A/m)

8B

0   20   40   60   80   100   120

B(mT)

11B

3.50E-05

3.00E-05

2.50E-05

2.00E-05

J (A/m)

1.50E-05

1.00E-05

5.00E-06

0.00E+00

0   20   40   60   80   100   120

B(mT)

14A

3.00E-05

2.50E-05

2.00E-05

J (A/m)

1.50E-05

1.00E-05

5.00E-06

0.00E+00

0   20   40   60   80   100   120

B(mT)

14B

116